

การพัฒนาโครงเนื้อเยื่อกระดูกจากไฮโดรเจลก่อตัวได้ของไฟโบรอินไหมไทยและคอลลาเจน



นายจรินทร์ อภินันท์

จุฬาลงกรณ์มหาวิทยาลัย

CHULALONGKORN UNIVERSITY

บทคัดย่อและแฟ้มข้อมูลฉบับเต็มของวิทยานิพนธ์ตั้งแต่ปีการศึกษา 2554 ที่ให้บริการในคลังปัญญาจุฬาฯ (CUIR)

เป็นแฟ้มข้อมูลของนิสิตเจ้าของวิทยานิพนธ์ ที่ส่งผ่านทางบัณฑิตวิทยาลัย

The abstract and full text of theses from the academic year 2011 in Chulalongkorn University Intellectual Repository (CUIR) are the thesis authors' files submitted through the University Graduate School.

วิทยานิพนธ์นี้เป็นส่วนหนึ่งของการศึกษาตามหลักสูตรปริญญาวิทยาศาสตรดุษฎีบัณฑิต

สาขาวิชาวิศวกรรมชีวเวช (สหสาขาวิชา)

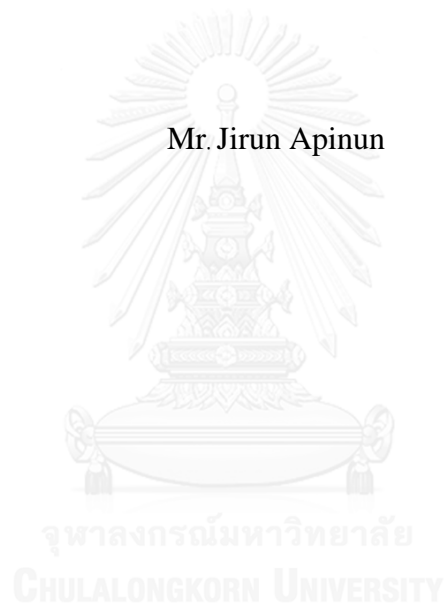
คณะวิศวกรรมศาสตร์ จุฬาลงกรณ์มหาวิทยาลัย

ปีการศึกษา 2559

ลิขสิทธิ์ของจุฬาลงกรณ์มหาวิทยาลัย

Development of Bone Scaffold from In Situ-
Forming Hydrogel of Thai Silk Fibroin and Collagen

Mr. Jirun Apinun



A Dissertation Submitted in Partial Fulfillment of the Requirements
for the Degree of Doctor of Philosophy Program in Biomedical Engineering
Faculty of Engineering
Chulalongkorn University
Academic Year 2016
Copyright of Chulalongkorn University

Thesis Title	Development of Bone Scaffold from In Situ- Forming Hydrogel of Thai Silk Fibroin and Collagen
By	Mr. Jirun Apinun
Field of Study	Biomedical Engineering
Thesis Advisor	Assistant Professor Sorada Kanokpanont, Ph.D.
Thesis Co-Advisor	Associate Professor Somsak Kuptniratsaikul, M.D.

Accepted by the Faculty of Engineering, Chulalongkorn University in Partial Fulfillment of the Requirements for the Doctoral Degree

..... Dean of the Faculty of Engineering
(Associate Professor Supot Teachavorasinskun, D.Eng.)

THESIS COMMITTEE

..... Chairman
(Professor Siriporn Damrongsakkul, Ph.D.)

..... Thesis Advisor
(Assistant Professor Sorada Kanokpanont, Ph.D.)

..... Thesis Co-Advisor
(Associate Professor Somsak Kuptniratsaikul, M.D.)

..... Examiner
(Professor Sittisak Honsawek, M.D., Ph.D.)

..... External Examiner
(Associate Professor Norased Nasongkla, Ph.D.)

จิรันคร์ อภินันท์ : การพัฒนาโครงเนื้อเยื่อกระดูกจากไฮโดรเจลก่อตัวได้ของไฟโบรอินไหมไทยและคอลลาเจน (Development of Bone Scaffold from In Situ-Forming Hydrogel of Thai Silk Fibroin and Collagen) อ.ที่ปริกษาวิทยานิพนธ์หลัก: ผศ. ดร. โสธดา กนกพานนท์, อ.ที่ปริกษาวิทยานิพนธ์ร่วม: รศ. นพ.สมศักดิ์ คุปต์นิริติศัยกุล, 108 หน้า.

การศึกษานี้มีเป้าหมายเพื่อพัฒนาโครงเนื้อเยื่อกระดูกจากไฮโดรเจลก่อตัวได้ของไฟโบรอินไหมไทยและคอลลาเจน สารละลายไฟโบรอินไหมถูกเตรียมขึ้นด้วยกระบวนการผลิตที่ปลอดภัยแล้วนำมากระตุ้นให้เกิดเจลโดยสารลดแรงตึงผิวจากการผสมกรดโอเลอิกและโพลีเอซอเมอร์-188 ที่มีค่าสมดุลไฮโดรฟิลิกและไลโปฟิลิก (เอชแอลบี) ต่าง ๆ แล้วทำการศึกษาผลของค่าเอชแอลบีที่แตกต่างกันของสารลดแรงตึงผิวที่มีต่อเวลาในการเกิดเจลและสมบัติทางกายภาพและเคมีของสารละลายไฟโบรอินไหมความเข้มข้น 4 เปอร์เซ็นต์ ที่ผสมหรือไม่ผสมคอลลาเจนความเข้มข้น 1 เปอร์เซ็นต์ สารลดแรงตึงผิวที่มีค่าเอชแอลบีต่ำกว่าสามารถกระตุ้นให้เกิดเจลได้เร็วขึ้น ค่าประจุของสารละลายไฟโบรอินไหมที่ผสมหรือไม่ผสมคอลลาเจนและเติมสารลดแรงตึงผิวที่มีค่าเอชแอลบีในช่วง 1-20 เข้าไปมีค่าเป็นลบ การวัดค่าสัดส่วนของเจลแสดงให้เห็นความสัมพันธ์แบบผกผันระหว่างค่าเอชแอลบีของสารลดแรงตึงผิวกับเสถียรภาพของไฮโดรเจลของไฟโบรอินไหม ความสามารถในการดูดซึมน้ำมีค่าเพิ่มขึ้นในกลุ่มไฮโดรเจลไหมที่ผสมคอลลาเจนที่ถูกกระตุ้นให้เจลด้วยสารลดแรงตึงผิวที่มีค่าเอชแอลบีสูง การศึกษาคุณสมบัติการไหลเผยให้เห็นถึงค่าเอชแอลบีของสารลดแรงตึงผิวที่จะทำให้เจลมีความแข็งแรงมากที่สุด และผลของคอลลาเจนต่อค่าโมดูลัสของไฮโดรเจล การตรวจด้วยกล้องจุลทรรศน์อิเล็กตรอนพบลักษณะที่เป็นรูพรุนขนาดเล็กต่อกันในไฮโดรเจลทุกกลุ่ม ค่าเอชแอลบีของสารลดแรงตึงผิวที่สูงขึ้นและการที่มีคอลลาเจนผสมอยู่มีผลให้ไฮโดรเจลมีขนาดรูพรุนที่ใหญ่ขึ้นแต่การติดต่อกันระหว่างรูพรุนลดลงและมีเครือข่ายเชื่อมขวางที่หนาขึ้น การศึกษาด้วยดีฟเฟอเรนเชียลสแกนนิ่งคาลอริเมตรีแสดงให้เห็นว่าไฮโดรเจลที่ถูกกระตุ้นด้วยสารลดแรงตึงผิวมีการตกผลึกที่สมบูรณ์กว่าไฮโดรเจลที่ไม่ได้ถูกกระตุ้น และยังพบแนวโน้มที่บ่งชี้ถึงการมีเสถียรภาพทางอุณหภูมิของไฮโดรเจลที่สูงขึ้นจากค่าเอชแอลบีที่สูงขึ้นของสารลดแรงตึงผิว การตรวจอินฟราเรดสเปกโตรสโคปีแสดงให้เห็นปริมาณโครงสร้างแบบเบตาชีทที่เพิ่มขึ้นในไฮโดรเจลที่ถูกกระตุ้นด้วยสารลดแรงตึงผิวที่มีค่าเอชแอลบีที่สูงขึ้น ซึ่งผลนี้ถูกขัดขวางได้โดยการมีคอลลาเจนผสมอยู่ในไฮโดรเจล การเกิดเจลของไฮโดรเจลไฟโบรอินไหมจากการกระตุ้นสารลดแรงตึงผิวที่มีค่าเอชแอลบีต่ำเป็นผลมาจากปฏิสัมพันธ์ระหว่างไฟโบรอินไหมกับสารลดแรงตึงผิวมากกว่าเป็นผลจากการเปลี่ยนแปลงโครงสร้างไปเป็นเบตาชีท การเพาะเลี้ยงเซลล์ในห้องปฏิบัติการยืนยันความเข้ากันได้ของไฮโดรเจลไหมที่ผสมและไม่ผสมคอลลาเจนและศึกษาในการเหนี่ยวนำให้เซลล์ต้นกำเนิดของหนูสามารถสร้างกระดูกขึ้นได้ การทดสอบภายในสิ่งมีชีวิตในหนูแสดงให้เห็นศักยภาพของไฮโดรเจลของไฟโบรอินไหมและคอลลาเจนในการเป็นโครงเนื้อเยื่อและพาหะสำหรับเซลล์และปัจจัยการเจริญเติบโตสำหรับการสร้างเนื้อเยื่อกระดูกขึ้นใหม่

สาขาวิชา วิศวกรรมชีวเวช (สหสาขาวิชา)

ปีการศึกษา 2559

ลายมือชื่อนิติ
.....

ลายมือชื่อ อ.ที่ปริกษาหลัก
.....

ลายมือชื่อ อ.ที่ปริกษาร่วม
.....

5387763221 : MAJOR BIOMEDICAL ENGINEERING

KEYWORDS:

JIRUN APINUN: Development of Bone Scaffold from In Situ-Forming Hydrogel of Thai Silk Fibroin and Collagen. ADVISOR: ASST. PROF. SORADA KANOKPANONT, Ph.D., CO-ADVISOR: ASSOC. PROF. SOMSAK KUPTNIRATSAIKUL, M.D., 108 pp.

This study aimed to develop bone scaffold from in situ-forming hydrogel of Thai silk fibroin (SF) and collagen. SF solution was sterilely produced and induced to form gel by oleic acid and poloxamer-188 surfactant combinations with different HLB values. Effect of different HLB values of surfactants on gelation time and physicochemical properties of induced 4 wt% SF with/without 0.1 wt% collagen was studied. Shorter gelation time could be achieved by induction with lower HLB surfactants. SF and SF blended with collagen solution displayed negative charge with added surfactant between HLB1-20. Gel fraction measurement demonstrated inverse relationship between HLB value of surfactants and SF hydrogel stability. There was a trend showing an increase in water absorption capacity of SF with collagen hydrogel induced by surfactants with higher HLB values. Rheological studies revealed an optimum HLB value of surfactants to achieve maximum gel strength. Effect of collagen on modulus of hydrogels was also demonstrated. SEM micrographs showed typical interconnected microporous morphology of all hydrogels. An increase in HLB value of surfactants and addition of collagen resulted in larger pore size with less interporous connectivity and thicker cross-linking networks. DSC study demonstrated more complete crystallization in hydrogels induced by surfactants compared with non-induced hydrogels. There was a trend indicating higher thermal stability of hydrogels with increased HLB value of surfactants. FTIR results demonstrated higher beta-sheet structure in SF hydrogel induced by higher HLB value of surfactants. The presence of collagen precluded this effect. The gelation of SF hydrogels induced by lower HLB surfactant was resulted from interaction between SF and surfactants rather than conformational change to beta-sheet. *In vitro* cell culture verified the biocompatibility of SF and SF blended with collagen hydrogels with a potential to induce osteogenic differentiation of encapsulated rat's MSC. However, added collagen promoted proliferation more than differentiation and induced matrix formation. *In vivo* study in rat demonstrated the biocompatibility and potential of SF/collagen hydrogel as a scaffold and carrier for cell and growth factor for bone regeneration.

Field of Study: Biomedical Engineering

Academic Year: 2016

Student's Signature

Advisor's Signature

Co-Advisor's Signature

ACKNOWLEDGEMENTS

Firstly, I would like to acknowledge the National Research University Project, Office of Higher Education Commission, Chulalongkorn University, Thailand for supportive funding for this project (NRU59-005HR).

Secondly, I would like to express my heartfelt gratitude to my thesis advisor, Assistant Professor Sorada Konokpanont, for her advice, encouragement, inspiration, patience, and understanding in helping me doing this project. This project would have not been made without her efforts.

I would like to express my thanks to my thesis co-advisor, Associate Professor Dr.Somsak Kuptniratsaikul, for giving me this opportunity and all mercy he gave to me, and Professor Siriporn Damrongsakkul for her valuable advice and constructive suggestions. And I would like to extend my appreciation to Professor Pibul Itiravivong for suggesting and encouraging me to study in this program, Associate Professor Risa Chaisuparat for her insightful histological analyses for in vivo experiment, Assistant Professor Chalika Wangdee for her magnificent skills in animal surgery, and also extend my gratitude to Mr.Somchai Yodsanga for his support in histology techniques.

I gratefully thank, and all my colleagues in the Biomedical Material Laboratory, especially Ms.Runganapa Yamdech and Mr.Supawich Chankow, for their assistance, insightful discussion, encouragement, and friendship. And I would like to extend my sincerely gratitude to Mr.Niphon Teeranon for all his wonderful support during this project.

I sincerely thank Professor Siriporn Damrongsakkul, Professor Sittisak Honsawek, and Associate Professor Norased Nasongkla for serving as the chairman and the thesis committee, respectively, and for their valuable insightful suggestions.

I would like to express my thankfulness for The Queen Sirikit Sericulture Center, Sisaket, Thailand for provide me the supply of Nangnoi Sisaket 1 silk cocoons.

Finally, I would like to express my deepest thanks to my family for their unconditional love and support throughout their lives.

CONTENTS

	Page
THAI ABSTRACT	iv
ENGLISH ABSTRACT.....	v
ACKNOWLEDGEMENTS	vi
CONTENTS.....	vii
LIST OF TABLES	xii
LIST OF FIGURES	xiv
CHAPTER 1 INTRODUCTION	1
1.1 Background.....	1
1.2 Objectives	3
1.3 Scope of Research.....	3
1.3.1 Development of an in situ forming hydrogel scaffold	3
1.3.2 Physicochemical characterization of SF solution, SF/Collagen solution, and hydrogel	3
1.3.3 Biocompatibility of SF/Collagen hydrogel with rat's MSC.....	3
CHAPTER 2 RELEVANT THEORIES AND LITERATURES REVIEW	4
2.1 Structure and component of bone tissue	4
2.2 Bone formation and healing of injured bone	5
2.3 Bone defect	7
2.4 Bone tissue engineering	9
2.5 Hydrogel	10
2.5.1 Hydrogel structure and formation	10
2.5.2 Swelling of hydrogel	14
2.5.3 Hydrogel degradation	15
2.5.4 Physical characteristic of hydrogel.....	16
2.5.5 Hydrogel related bone tissue engineering	16
2.6 Silk.....	17
2.6.1 Structure and property of silk.....	17
2.6.2 Hydrogel of silk fibroin.....	21

	Page
2.6.2.1 Chemical methods.....	21
2.6.2.2 Physical methods	23
2.7 Collagen	24
2.8 Osteogenic differentiation of mesenchymal stem cells	27
2.9 Poloxamer	29
2.10 Oleic acid	30
2.11 Hydrophilic-lipophilic balance (HLB)	31
CHAPTER 3 MATERIALS AND METHODS	33
3.1 Materials	33
3.2 Equipments	34
3.3 Research framework	36
3.4 Methodology	37
3.4.1 Preparation of silk fibroin solution.....	37
3.4.2 Obtaining of sterile silk fibroin solution	38
3.4.2.1 Sterilization of silk fibroin solution.....	38
3.4.2.2 Sterile production of silk fibroin solution	38
3.4.3 Induction of gelation Thai silk fibroin solution.....	39
3.4.3.1 Mechanical stimulation	39
3.4.3.2 Surfactants	40
3.4.4 Induction of gelation Thai silk fibroin/collagen solution with surfactants.....	41
3.4.5 Physicochemical characterization of solutions and hydrogels	42
3.4.5.1 Zeta potential of the solution.....	42
3.4.5.2 Gel fraction of the hydrogel	42
3.4.5.3 Water absorption of the hydrogel	43
3.4.5.4 Rheological property of the hydrogel.....	43
3.4.5.5 Morphology of the hydrogel.....	43
3.4.5.6 Thermal property of the hydrogel	43

	Page
3.4.5.7 Secondary structure of the hydrogel	44
3.4.6 <i>In vitro</i> cell culture	44
3.4.6.1 Isolation of rat bone marrow-derived mesenchymal stem cells (rat's MSC)	44
3.4.6.2 Preparation of silk fibroin and silk fibroin/collagen hydrogels....	45
3.4.6.3 Viability and proliferation	45
3.4.6.4 Osteogenic differentiation	46
3.4.7 <i>In vivo</i> osteogenesis in critical size bone defect induced by in situ- forming silk fibroin/collagen hydrogel.....	47
3.4.7.1 Preparation of Wistar rats	47
3.4.7.2 Preparation of in situ-forming silk fibroin with collagen hydrogel \pm rat's MSC \pm PRP	48
3.4.7.3 Surgical procedure.....	48
3.4.7.4 Evaluation of in vivo bone formation.....	50
3.4.8 Statistical analysis	52
CHAPTER 4 RESULTS AND DISCUSSION.....	53
4.1 Sterilization of SF solution	53
4.1.1 Autoclaving	53
4.1.2 Gamma radiation	53
4.1.3 Sterile filtration.....	54
4.2 Sterile production of silk fibroin solution.....	55
4.3 Induction of gelation of SF solution	56
4.3.1 Mechanical stimulation by vortex and homogenization.....	56
4.3.2 Surfactant-induced gelation.....	57
4.4 Physicochemical characterization.....	58
4.4.1 Zeta potential of the solution.....	58
4.4.2 Gel fraction of the hydrogel	60
4.4.3 Water absorption of the hydrogel	61
4.4.4 Rheological property of the hydrogel.....	62

	Page
4.4.5 Morphology of the hydrogel.....	68
4.4.6 Thermal property of the hydrogel	70
4.4.7 Secondary structure of the hydrogel.....	74
4.5 <i>In vitro</i> cell culture.....	78
4.5.1 Viability and proliferation	78
4.5.2 Osteogenic differentiation	80
4.6 <i>In vivo</i> osteogenesis in critical size bone defect induced by in situ-forming SF with collagen hydrogel.....	85
4.6.1 Gross observation	85
4.6.2 Plain radiograph	86
4.6.3 Micro CT imaging	87
4.6.4 Histological evaluation.....	89
CHAPTER 5 CONCLUSIONS	94
REFERENCES	98
APPENDIX A THE APPROVED OF ANIMAL USE PROTOCOL	106
APPENDIX B SERIAL PLAIN RADIOGRAPHS IN <i>IN VIVO</i> STUDY	107
VITA.....	108

LIST OF TABLES

Table 2.1 Amino acid composition of silk fibroin from various domestic races.....	17
Table 2.2 The structures of silk thread.....	19
Table 2.3 Mechanical characteristics of Bombyx mori silk compare with others compound and human's tissues	20
Table 2.4 Collagen: Types, compositions, and tissues distribution.....	26
Table 3.1 weight percent in total, weight percent of silk fibroin and surfactants, and HLB value of surfactants composed in each silk fibroin hydrogel sample.....	41
Table 3.2 weight percent in total, weight percent of silk fibroin, collagen, and surfactants, and HLB value of surfactants composed in each silk fibroin/collagen hydrogel sample	42
Table 3.3 weight percent in total, weight percent of silk fibroin, collagen, and surfactants, and HLB value of surfactants composed in hydrogel for in vitro cell culture	45
Table 4.1 Microbiological attribution test results of sterilely produced SF solution...55	
Table 4.2 Results of 4 wt% SF solution gelation induced by mechanical stimulation.....	56
Table 4.3 Gelation time of 4 wt% SF hydrogels with and without 0.1 wt% collagen induced by oleic acid-ploxamer surfactants with different HLB values at 37°C	58
Table 4.4 Zeta potentials of oleic acid-ploxamer surfactants with different HLB values at pH 4.0, 5.5, and 7.5 at 37°C.....	59
Table 4.5 Zeta potentials of 1 wt% SF with and without 0.1 wt% collagen mixed with oleic acid-ploxamer surfactants with HLB values and 0.05 wt% collagen at pH 5.5 and 7.5 at 37°C.....	60
Table 4.6 Summary of thermal peaks from DSC of 4 wt% SF hydrogels without 0.1 wt% collagen induced by oleic acid-ploxamer surfactants with different HLB values	72
Table 4.7 Summary of thermal peaks from DSC of 4 wt% SF hydrogels with 0.1 wt% collagen induced by oleic acid-ploxamer surfactants with different HLB values	73
Table 4.8 Summary of peak intensities from FTIR spectra of 4 wt% SF hydrogels with and without 0.1 wt% collagen induced by oleic acid-ploxamer surfactants with different HLB values	75

Table 4.9 Weight percent of C, O, Ca, and P, and Ca/P ratio of SF, SF/0.05C, and SF/0.1C hydrogels cultured with rat's MSC from elemental analysis results (without blank deduction).....	83
Table 4.10 Morphometric parameters on newly formed bone in the segmental bone defect at 4 and 12 weeks in control and experiment groups	88



LIST OF FIGURES

Figure 2.1 The compartment of long bone.....	5
Figure 2.2 The healing of bone across the fracture site in primary bone healing.....	6
Figure 2.3 Callus formation around the fracture site in secondary bone healing	7
Figure 2.4 Treatment of bone defect by distraction osteogenesis.....	8
Figure 2.5 Ionic interaction.....	10
Figure 2.6 Hydrophobic association	11
Figure 2.7 Chain aggregation.....	11
Figure 2.8 Complex coacervation	11
Figure 2.9 Hydrogen bonding	12
Figure 2.10 Crystallizing segment	12
Figure 2.11 Stereocomplexation	12
Figure 2.12 Radical polymerization.....	13
Figure 2.13 Functional group crosslinking by addition of glutaraldehyde.....	13
Figure 2.14 Enzymatic reaction	14
Figure 2.15 Swelling of hydrogel	14
Figure 2.16 Types of water in hydrogel.....	15
Figure 2.17 Load-deformation curve of hydrogel.....	16
Figure 2.18 Preformed vs In situ-forming hydrogel	17
Figure 2.19 SEM images of silk fibroin (A) silk fibroin without sericin removed, (B) silk fibroin with sericin removed, (C) Bombyx mori Nangnoi Srisaket 1 Thai silk thread.....	19
Figure 2.20 The arrangement of fibroin as antiparallel β -sheet.....	20
Figure 2.21 Structure of collagen.....	25
Figure 2.22 The differentiation of mesenchymal stem cell into other tissues	28
Figure 2.23 Cellular expression in osteogenic differentiation of mesenchymal stem cells	29
Figure 2.24 Structure of poloxamer	30
Figure 2.25 Structure of oleic acid	31
Figure 2.26 Demonstrates HLB numbers of some commonly used surfactants.....	32

Figure 3.1 Diagram of experimental procedures	36
Figure 3.2 Process of silk fibroin solution preparation using LiBr.....	37
Figure 3.3 Dialysis of sterile dissolved silk fibroin/ LiBr solution under sterile condition	39
Figure 3.4 A vial of silk fibroin solution attached with a holder being vortexed	39
Figure 3.5 Homogenization of silk fibroin solution.....	40
Figure 3.6 Hydrogel sample for in vitro cell culture (A) Before culture, (B) During culture	46
Figure 3.7 Anesthesia of Wistar rat: Induction chamber (left), Under mask (right) ...	49
Figure 3.8 Creation of critical size defect in the ulnar bone	49
Figure 3.9 Injection of in situ-forming hydrogel into the bone defect.....	50
Figure 3.10 Positions of Wistar rat during x-ray : Lateral view (left) , Anteroposterior view (right)	51
Figure 4.1 Sterilization of 1-5 wt% SF solution by autoclaving. (A) SF solution before autoclaving, (B) SF solution after autoclaving.....	53
Figure 4.2 Sterilization of 1-5 wt% SF solution by gamma radiation. (A) SF solution before irradiation, (B) SF solution after irradiation	53
Figure 4.3 Sterilization of 1 wt% SF solution by sterile filtration. The appearance of resultant filtrate demonstrated mixed solution and white gel strips	54
Figure 4.4 Mechanical stimulation for SF gelation induction. (A) 4 wt% SF solution being vortexed for 5 min. The solution became more turbid but no gel formation, (B, C and D) 4 wt% SF solution being homogenized for 60 min. Massive bubble formation occurred but no gel formation.....	56
Figure 4.5 Appearance of hydrogel of 4 wt% SF induced by oleic acid-ploxamer surfactants	58
Figure 4.6 Gel fractions of 4 wt% lyophilized SF hydrogels with and without 0.1 wt% collagen induced by oleic acid-ploxamer surfactants with different HLB values after incubation in DI water at 37°C for 24 h.....	61
Figure 4.7 Water absorption capacity of 4 wt% SF hydrogels with and without 0.1 wt% collagen induced by oleic acid-ploxamer surfactants with different HLB values after incubation in DI water at 37°C for 24 h.....	62
Figure 4.8 Stress and strain wave relationships for a purely elastic (ideal solid), purely viscous (ideal liquid) and a viscoelastic material	63
Figure 4.9 Geometric relationship between G^* and its components G' and G''	63

Figure 4.10 Amplitude sweep at 0.01 – 10% strain, 1 Hz of 4 wt% SF hydrogels (top) and SF hydrogels with collagen (bottom).....	65
Figure 4.11 The ratio of loss modulus/storage modulus (G''/G') of 4 wt% SF hydrogels without 0.1 wt% collagen induced by oleic acid-poloxamer surfactants with different HLB values	66
Figure 4.12 The ratio of loss modulus/storage modulus (G''/G') of 4 wt% SF hydrogels with 0.1 wt% collagen induced by oleic acid-poloxamer surfactants with different HLB values.....	66
Figure 4.13 Frequency sweep at 1 – 10 Hz, 0.03% strain, 1 Hz of 4 wt% SF hydrogels (top) and SF hydrogels with collagen (bottom).....	67
Figure 4.14 SEM images of 4 wt% SF hydrogels with and without 0.1 wt% collagen induced by oleic acid-poloxamer surfactants with HLB 3, 10, and 20.....	70
Figure 4.15 DSC curves of 4 wt% SF hydrogels without 0.1 wt% collagen induced by oleic acid-poloxamer surfactants with different HLB values	72
Figure 4.16 DSC curves of 4 wt% SF hydrogels with 0.1 wt% collagen induced by oleic acid-poloxamer surfactants with different HLB values	73
Figure 4.17 FTIR spectra of 4 wt% SF hydrogels induced by oleic acid-poloxamer surfactants with different HLB values	74
Figure 4.18 FTIR spectra of 4 wt% SF hydrogels with 0.1 wt% collagen induced by oleic acid-poloxamer surfactants with different HLB values	74
Figure 4.19 Relative contents of secondary structures of 4 wt% SF hydrogels without 0.1 wt% collagen induced by oleic acid-poloxamer surfactants with different HLB values.....	77
Figure 4.20 Relative contents of secondary structures of 4 wt% SF hydrogels with 0.1 wt% collagen induced by oleic acid-poloxamer surfactants with different HLB values	77
Figure 4.21 Growth kinetics of rat's MSC cultured on SF, SF/0.05C, and SF/0.1C hydrogels for 14 days.....	78
Figure 4.22 DNA assay (A), ALP activity (B), and calcium content (C) of rat's MSC cultured on SF, SF/0.05C, and SF/0.1C hydrogels in osteogenic induction medium for 14 days	80
Figure 4.23 SEM images of rat's MSC cultured on SF, SF/0.05C, and SF/0.1C hydrogels under different magnifications	82
Figure 4.24 Elemental analysis of SF, SF/0.05C, and SF/0.1C hydrogels cultured with rat's MSC by EDS	83

Figure 4.25 In situ gelling of the hydrogel injected into the segmental bone defect of ulnar bone of Wistar rat.....	86
Figure 4.26 Plain radiographic images obtained at 12 weeks. (A) Control group showed no signs of bone regeneration. (B) SF gel + MSC + PRP group showed radiopaque shadow with focal calcification in the bone defect.	87
Figure 4.27 Image in axial view from micro-CT scan of SF gel + MSC group at 12 weeks revealed new bone formation in the ulnar bone defect.	88
Figure 4.28 H&E staining of decalcified sections at 4 weeks, (A) an empty defect surrounded by fibrosis in the control group, (B) Collection of hydrogel appeared as eosinophilic irregular-shaped material surrounded by inflammatory cells in SF gel group, (C) Higher amount of inflammatory cells surrounding gel material in SF gel + PRP group compared with hydrogel without PRP groups, (D) New vessel formation in SF gel group showed in high power view.....	91
Figure 4.29 Histological section at 12 weeks of SF gel + MSC group, (A) H&E staining showed new bone formation and residual hydrogel fragments in SF gel + MSC group, (B) Alizarin Red S staining showed new bone formation appeared as collected reddish orange material in pale green background.....	92
Figure A.1 Certificate approval for animal use protocol number 06/2560 by the ethical committee of animal care and use protocol of Chulalongkorn University.....	106
Figure B.1 Serial radiographs at 0, 4, 8, and 12 wks of the control group, SF/Col hydrogel group, SF/Col hydrogel + MSC group, SF/Col hydrogel + PRP group, and SF/Col hydrogel + MSC + PRP group.....	107

CHAPTER 1

INTRODUCTION

1.1 Background

Bone defect is a common and important problems in orthopedic surgery. The causes of bone defect include high energy trauma, disease, and iatrogenic causes such as revision surgery or tumor resection [1]. Available treatment options currently are bone shortening, distraction osteogenesis, and bone grafting [2]. Bone shortening can be used for defects up to 2-3 inches in acute setting. However, main disadvantage of shortening is loss of the length of the affected limb, especially in lower limbs. Distraction osteogenesis uses an external fixation to distract the osteotomized bone to completely fill the defect. Nevertheless, this approach needs long treatment time with patient inconvenience and discomfort. Recurrent pin tract infections and pin loosening are also possible complications. Bone graft used for transplantation can be acquired from autologous or allogenic sources. Nonetheless, considerable shortcomings are donor site morbidity and insufficient amount of graft in autologous bone graft and risks of infection and immunologic reaction in allogenic bone graft. Synthetic bone substitutes have thereafter been developed to be used in place of the transplanted bone graft to avoid drawbacks from bone graft. Many types of bone substitutes are available in the market, for example, calcium phosphate, calcium phosphate-collagen composites, and calcium sulfate. However, limited osteogenic efficacy, local reaction, and time required for transformation and incorporation are concerned [3].

To overcome limitations of current treatment options, bone tissue engineering has recently emerged as an alternative approach for management of bone defect. The concept involves three essential elements, including cells, scaffold, and growth factors to regenerate new bone tissue for reconstruction of the defect [4].

Generally, an ideal scaffold should be designed to facilitate cell attachment, proliferation, and differentiation which bone tissue can be

generated. It should be biocompatible and biodegradable with appropriate degradation rate corresponded with rate of bone tissue regeneration [5].

Hydrogel is a crosslinked hydrophilic polymer network that exhibit high water content [6]. Its hydrated network architecture provides a place for cell to adhere, proliferate, and differentiate. It is generally nontoxic and biocompatible [7]. In tissue engineering, it can be utilized for encapsulation of living cells as a cell delivery system and scaffold for tissue regeneration. Moreover, it can be delivered into target site in a minimally invasive manner. Anyway, gelling process must be friendly for cell survival without damaging to loaded cells [8].

Silk fibroin, the self-assembling structural protein in natural silkworm fibers, is a naturally-derived polymer available in Thailand. It attributes good biocompatibility and slow biodegradability. In tissue engineering, it has been widely studied in designing various forms of scaffolds in regeneration of different tissues [9, 10]. Silk fibroin solution can be processed into hydrogel in controlled time using chemical and physical methods, which makes it appropriate for development into in situ-forming hydrogel for tissue engineering of the bone.

Collagen is a major protein in the extracellular matrix (ECM). It plays a significant role in supporting and strengthening the structural integrity of connective tissue, especially vessel, skin, tendon, cartilage, tooth, and bone. Due to its properties of biocompatibility, non-immunogenicity, non-toxicity, and promotion of cell adhesion; it is a promising biomaterial for tissue engineering.

Scaffold made of combined silk fibroin and collagen has been developed aimed to attain benefits from bioactivity of collagen and mechanical properties with porous structure of silk fibroin. Various designs of silk fibroin/collagen scaffold have been manufactured for potential tissue engineering of nerve, vessel, airway, ear, cornea, urethra, cartilage, and bone [11-18]. *In vitro* proliferation of vascular smooth muscle cell culture in pre-formed hydrogel prepared by crosslinking of blended collagen and silk solution revealed favorable biocompatibility results [19].

Marelli et al. demonstrated enhanced biomineralization in co-existence of collagen and silk fibroin derived polypeptide [20]. Thus, hydrogel developed from a combination of collagen and silk fibroin could

be beneficial in bone tissue engineering strategy. According to the existing literature, production and application of in situ-forming hydrogel from Thai silk fibroin and collagen as a delivery system for cells and growth factor for bone tissue engineering has never been studied before. Therefore, this study was conducted in order to develop an in situ-forming hydrogel from Thai silk fibroin and collagen and to investigate its properties and potential in induction of bone regeneration.

1.2 Objectives

- 1.2.1 To develop an in situ-forming hydrogel scaffold composed of Thai silk fibroin and collagen
- 1.2.2 To study the physicochemical properties of the developed hydrogel scaffold
- 1.2.3 To study the biological properties of the developed scaffold *in vitro* cell culture and *in vivo* animal model

1.3 Scope of Research

- 1.3.1 Development of an in situ forming hydrogel scaffold
 - 1.3.1.1 Preparation of silk fibroin solution using LiBr
 - 1.3.1.2 Sterile production of silk fibroin solution
 - 1.3.1.3 Induction of gelation of silk fibroin solution using mechanical stimulation and surfactants
 - 1.3.1.4 Induction of gelation of silk fibroin/collagen solution using surfactants
- 1.3.2 Physicochemical characterization of SF solution, SF/Collagen solution, and hydrogel
- 1.3.3 Biocompatibility of SF/Collagen hydrogel with rat's MSC
 - 1.3.3.1 *In vitro* cell culture
 - a) Viability and proliferation
 - b) Osteogenic differentiation
 - 1.3.3.2 *In vivo* animal model (Wistar rat)
 - a) Biological response at the implantation site
 - b) General health of the host
 - c) Bone formation compared to non-treatment group

CHAPTER 2

RELEVANT THEORIES AND LITERATURES REVIEW

2.1 Structure and component of bone tissue

Bone tissues consist of various types of cells such as osteoblasts, osteocytes, osteoclasts and the extracellular matrix (ECM) (organic 30% and inorganic 70%). The osteoblasts have an important role in bone formation through mineralization of bone in ECM. The osteocytes are the mature form of osteoblasts and common cells found in bone tissues. The osteocytes are essential to support bone metabolism, regulate calcium levels, and regulate bone absorption and bone formation which affect bone remodeling. The osteoclasts play a role in bone reabsorption to break down the bone tissues and to regenerate new bone tissues. The organic matrix consists of collagen type 1 (90%) and other components such as proteoglycans and other proteins (10%). The inorganic matrix consists of calcium and phosphate in the form of hydroxyapatite which promotes strength of the bone [21].

Classification of bone by structure:

- a) Woven bone is the immature bone found in fetal development and proliferation of bone which is replaced by cortical or cancellous bone later on.
- b) Cortical bone (compact bone or lamellar bone) is the exterior part bone that mainly supports the whole body and also has higher density than cancellous bone.
- c) Cancellous bone (trabecular bone or spongy bone) is the porous bone which is weaker than cortical bone but more flexible, mostly found in the enlarged ends of the long bones, the ribs and shoulder blades, the flat bones of the skull and skeleton.

Extremity bone has cortical bone as its outer part and cancellous bone as its inner part. The medullary cavity in the middle of the bone contains bone marrow. There are connective tissues covering cortical bone called periosteum and surrounding the medullary cavity called endosteum.

Both periosteum and endosteum contain cells that play roles in the remodeling of fractured or injured bone (Figure 2.1)

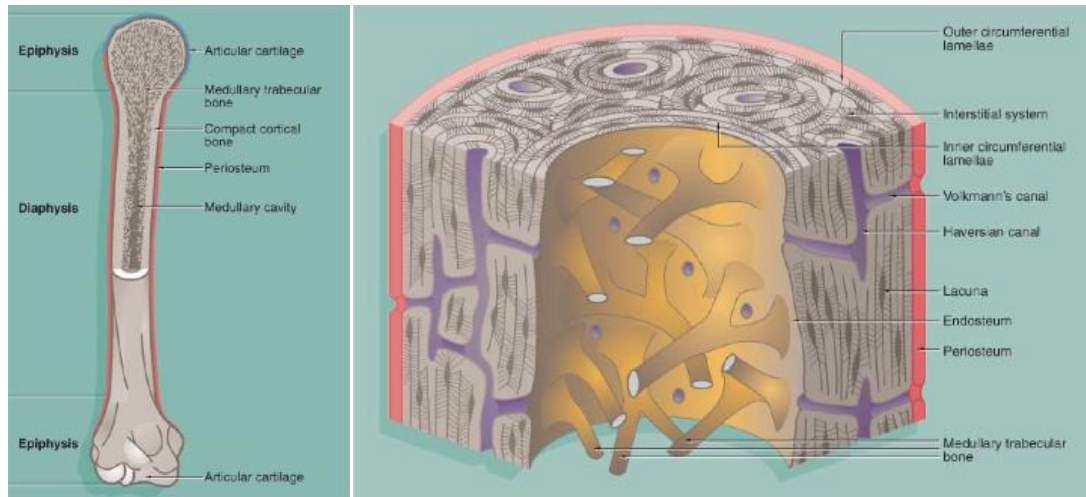


Figure 2.1 The compartment of long bone (Young et al, 2006)

2.2 Bone formation and healing of injured bone

Bone formation involves the following two processes [21]:

1) Endochondral ossification is the formation of bone by osteogenic cells to create cartilage which undergoes hypertrophy with deposition of calcium. The osteoprogenitor cells differentiate into osteoblasts and osteocytes and generate the bone. This process is found in long bone formation and primary ossification.

2) Intramembranous ossification is the formation of bone by osteogenic cells which develop into osteoblast and then directly generate bone without undergoing the process of cartilage generation as in the case of endochondral ossification.

Bone healing involves the following two patterns [3]:

1. Primary bone healing occurs when the ends of fracture site are completely contacted and well-stabilized. The bridging bone forms across from each bone end (gap healing) (Figure 2.2). The type of connective bone depends on the length of gap. The lamellar bone will form at the gap when the gap space is less than 200 μm . If the gap space is more than 200 μm , woven bone will form first and then develops into lamellar bone. This type

of healing is found in the fixation of long bone and impacted fracture of cancellous bone.

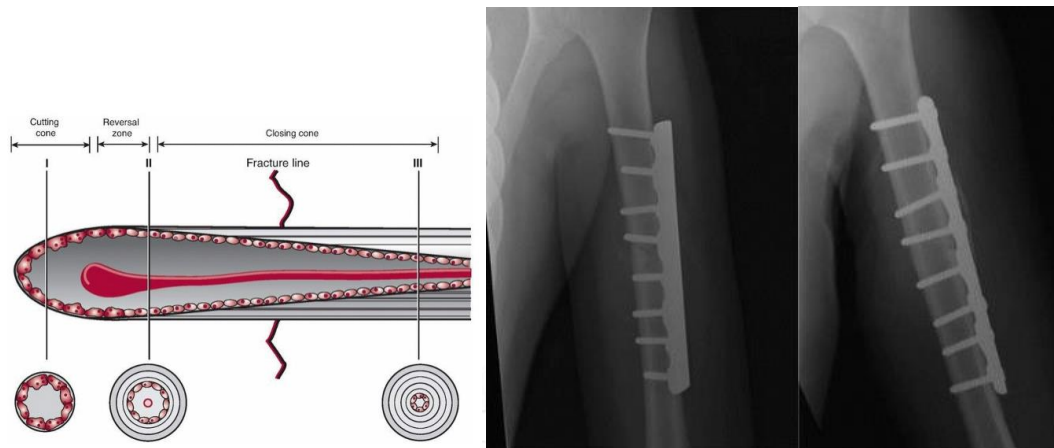


Figure 2.2 The healing of bone across the fracture site in primary bone healing (Buckwalter et al., 2010)

2. Secondary bone healing occurs when the fracture site is displaced without fixation. The callus forms and accumulates around to stabilize the fracture (Figure 2.3). The process of secondary bone healing is as follows:

2.1. Formation of hematoma occurs due to rupture of blood vessels. Hematoma acts as a fibrin scaffold to support adhesion and proliferation of osteogenic cells.

2.2. Platelets and osteogenic cells release growth factor and other signaling protein resulting in inflammation and cells migration. Mesenchymal stem cells from periosteum, medullary cavity, and nearby muscles will form matrix around the fracture site to regenerate the damaged vessels (angiogenesis).

2.3. Mesenchymal stem cells differentiate into bone and cartilage. Initial soft tissue callus (woven bone) consolidates and turns into hard callus (lamellar bone) resulting in more strength and stability of the fracture site. These stages continue until the fracture site is completely healed.

2.4. The bone continues its remodeling process to improve its structure and properties. This process takes several months to years.

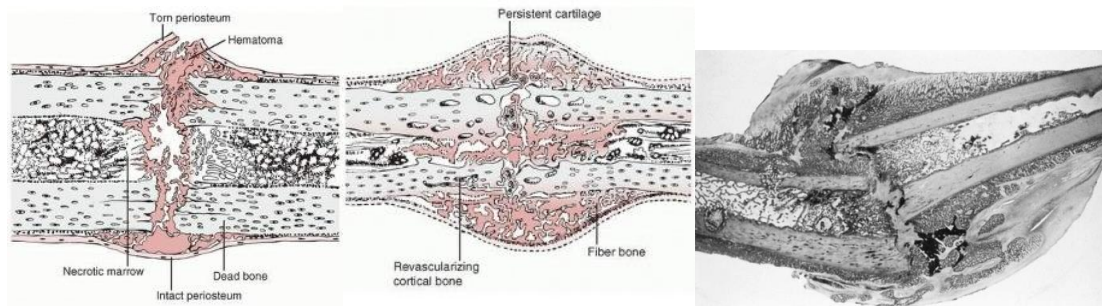


Figure 2.3 Callus formation around the fracture site in secondary bone healing (Buckwalter et al., 2010)

2.3 Bone defect

Bone defect is the loss of some part of bone. The primary cause of bone defect is bone injury from trauma, weaponry, infection, and tumor. The removal of bone because of infection, tumor, or nonunion after fracture are the secondary causes of bone defect. Bone defect is an important problem in orthopedics causing inferior result of treatment, complications, prolonged treatment period and increased financial burden.

Size of the deficit bone plays an important role in the prognosis of prediction. The smallest size of bone that cannot heal spontaneously or grows lower than 10% in lifetimes are called critical-sized bone defect. The approximate length of critical-sized bone defect is higher than 2-2.5 folds of diameter [22], however critical-sized bone defect is varied by species and location of defect. Furthermore, the surrounding tissue, vascular, age, metabolic, and other systematic disease have an effect to progression of bone healing [23].

There are several treatments for bone defect [2]:

1. Direct approximation of each bone ends leads to bone shortening. The advantages of this technique are: easily performed, less treatment time, and no donor site is necessary. However, this method has the following compromises: the activities of surgical site, less cosmetic, occurrence of deep vein thrombosis, limitation of the size of treatment, and wound complications.
2. Distraction osteogenesis is the facilitation of gradual bone growth through external fixation of the bone (figure 2.4). This procedure can

provide immediate weight bearing and treatment of large defect size (2-10 cm). The disadvantages of the procedure are prolonged fixation, slow bone healing, instruments infection, scar adhesion, and limp function deficit.



Figure 2.4 Treatment of bone defect by distraction osteogenesis (Aronson, 2007)

3. Bone graft from donor are used to replace the loss of bone. The donor bone can be autograft or allograft. The autograft has the advantages of fast healing and high reunion rate but the major drawbacks are increase the injury at harvested sites, prolong surgical time, need for protected weight bearing during healing, and limited amount. The allograft provides less injuries or complications the donor site but it has slower healing rate, price, high risk of infection, immunologic complications, and risk for long term fracture if allograft is not completely incorporated.
4. Bone graft substitutes are used to replace bone defect. There are many types of substitutes [3] such as slow degradation calcium phosphate ceramics (hydroxyapatite), fast degradation calcium phosphate ceramics (tricalcium phosphate), calcium phosphate-collagen composites manufactured from calcium phosphate and bovine collagen (Collagraft), calcium sulfate, injected-calcium phosphate cements (Norian SRS). The advantage of bone graft substitutes is no donor site morbidity, however there are some limitations such as efficacy, bone transformation times, and higher cost than bone graft.
5. Bone tissue engineering to replace the loss bone which will be described further in the next section.

2.4 Bone tissue engineering

Tissue engineering is a new interdisciplinary science which combines molecular biotechnology, molecular biology, chemistry, physics, material science, engineering, and medicine to recreate tissues or new organs for the replacement and/or promotion of tissue and old organ healing of patients. Tissue engineering has the following 3 main strategies:

1. Cell-based strategy (Osteogenesis) which involves cell implants which differentiate as bone tissue in specific bone. The cells used for implantation can be mesenchymal stem cells, osteoprogenitor cells, or differentiated osteoblasts.
2. Growth factor-based strategy (Osteoinduction) is the signaling of polypeptide to control the growth, development, and gene expression for stimulation of bone tissue growth. However, the growth factor has short half-life, expensive, and limited amount of receiving to increase the efficiency of growth factor by use growth factors controlled release system. The involvement growth factor induces bone tissue included bone morphogenic protein (BMP), vascular endothelial growth factor (VEGF), fibroblast growth factor (FGF), insulin-like growth factor (IGF), platelet-derived growth factor (PDGF), and epidermal growth factor (EGF).
3. Scaffold-based strategy (Osteoconduction) is the use of scaffolds as the foundation for cells attachment, differentiation, and regeneration to bone tissue. The proper characteristics of a scaffold are biocompatibility, biodegradation, balance of decay rate and growth rate, good mechanical integrity, tissue integration and vascularization facilitation, easy fabrication and sterilizability. The important factors that affect the characteristic of scaffold are the materials of scaffold, appearance, and surface.

Nowadays, the research and treatment with bone tissue engineering is using a combination of strategies to improve the potentials of bone regeneration.

2.5 Hydrogel

2.5.1 Hydrogel structure and formation

Hydrogels are crosslinked polymers with hydrophilic nature. They have ability to swell but not soluble in aqueous medium. The water content in hydrogel is more than 30% of the weight of hydrogel. The strength of hydrogel depends on the crosslink of polymer chains [6].

Synthetic hydrogels, such as hydrogel of aliphatic biodegradable polyesters (PEG-PLA and PEG-PGA copolymers), fumaric acid-based macromers (poly (propylene fumarate-co-ethylene glycol) (P(PF-co-EG))), and oligo (poly (ethylene glycol) fumarate) (OPF), has their advantages of controllable chemical and physical properties (by hydrogel composition and crosslink); and mass production. While hydrogels from natural polymers, mostly protein, such as collagen, gelatin, fibrin, and polysaccharide i.e. hyaluronic acid, alginate, chitosan, and dextran are more difficult in property control but they usually presents higher biocompatibility and better cellular stimulation [7].

Hydrogel forms when chemical or physical crosslinking of polymer occurs resulting in network chain. Inducers can be chemical or physical factor such as pH or temperature. There are two types of crosslinking in hydrogel formation [7, 24, 25] as following:

2.5.1.1 Physical crosslinking

a) *Ionic interaction* is the crosslinking of ionic polymers by addition of di- or tri-valent counterions, for example, calcium induced gelation of alginate (Figure 2.5).

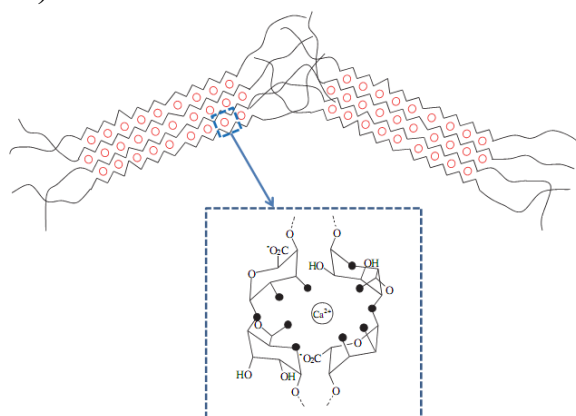


Figure 2.5 Ionic interaction (Gulrez et al., 2011)

b) *Hydrophobic association* is the crosslinking of amphiphilic polymers by rearrangement of hydrophobic and hydrophilic segments in solution (Figure 2.6), such as the rearrangement of fibroin to β -sheet assembly.



Figure 2.6 Hydrophobic association (Omidian et al., 2012)

c) *Chain aggregation* is rearrangement of polymers into new conformation, for example, helix-formation when there is physical alteration (Figure 2.7) such as heat-induced gelation of carrageenan or gelatin.

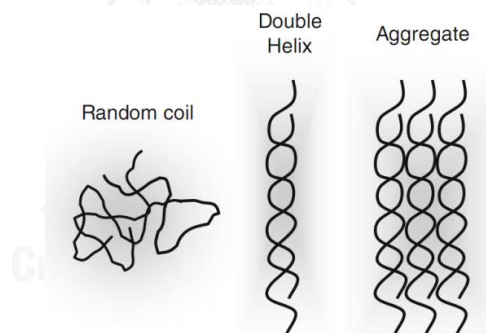


Figure 2.7 Chain aggregation (Omidian & Park, 2012)

d) *Complex coacervation* occurs when anionic polymers mix with cationic polymers (Figure 2.8) such as mixture of xanthan and chitosan.

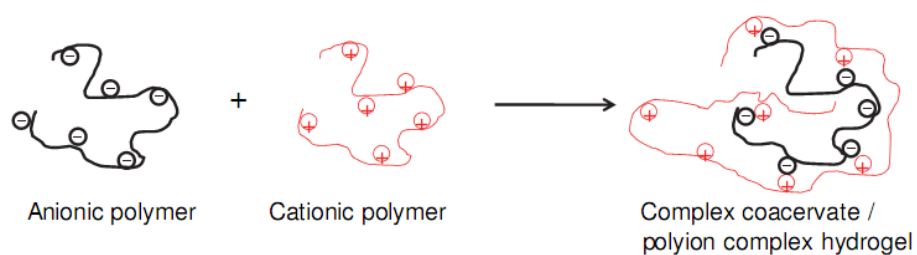


Figure 2.8 Complex coacervation (Gulrez et al., 2011)

e) *Hydrogen bonding* is the crosslinking with network chains of hydrogen bonding (Figure 2.9) such as the gelation of polymers containing carboxy group (e.g. carboxymethyl cellulose, carboxymethylated chitosan) when pH decreases.

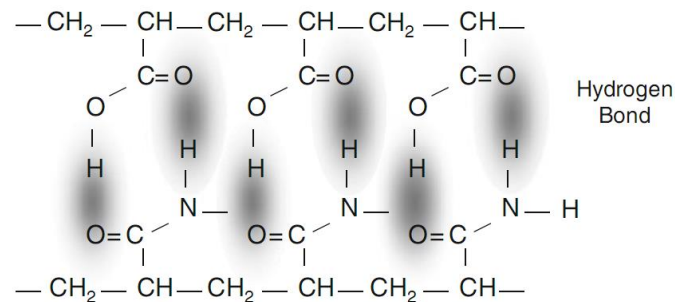


Figure 2.9 Hydrogen bonding (Omidian & Park, 2012)

f) *Crystallizing segment* is the gelation by production of crystallites in the structure (Figure 2.10) such as hydrogel from freeze-thawing cycles of polyvinyl alcohol and xanthan.

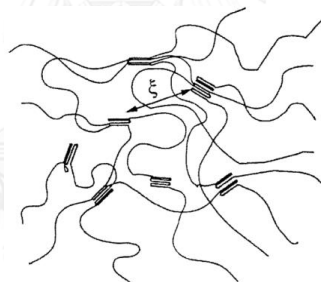


Figure 2.10 Crystallizing segment (Hassan & Peppas, 2000)

g) *Stereocomplexation* Co-crystallization occurs when 2 stereoisomers of polymers are mixed in stereocomplex, such as hydrogel of PLLA and PDLA blocks (Figure 2.11).

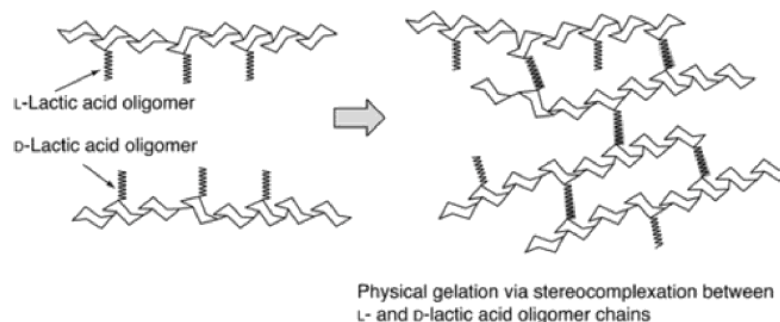


Figure 2.11 Stereocomplexation of PLLD and PDLA (Ebara, 2011)

2.5.1.2 Chemical crosslinking

is crosslink by chemical bonding in the network chains, mostly covalent bonding.

a) *Radical polymerization* by induction of free radicals in the polymer with radiation, ultraviolet ray, temperature, or redox reaction (Figure 2.12).

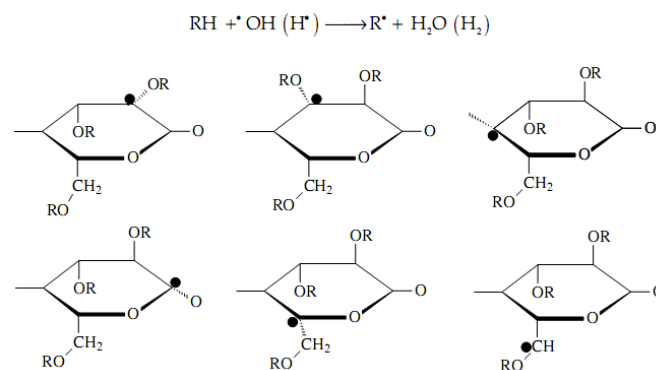


Figure 2.12 Radical polymerization. Formation of primary radicals in irradiated anhydroglucose (Gulrez et al., 2011)

b) *Functional group crosslinking* is the reaction between functional groups of polymers by chemical crosslinker such as glutaraldehyde or epichlorohydrin (Figure 2.13).

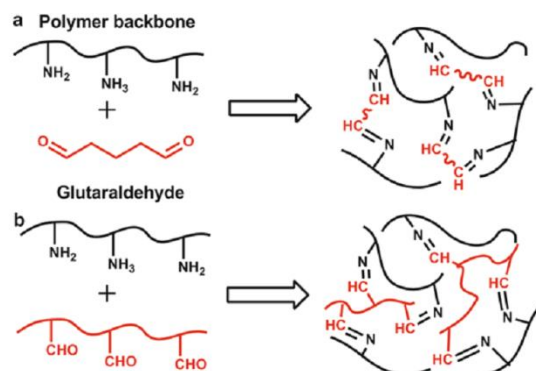


Figure 2.13 Functional group crosslinking by addition of glutaraldehyde (Jin & Dijkstra, 2010)

c) *Enzymatic reaction* is enzyme induction of crosslinking (Figure 2.14).

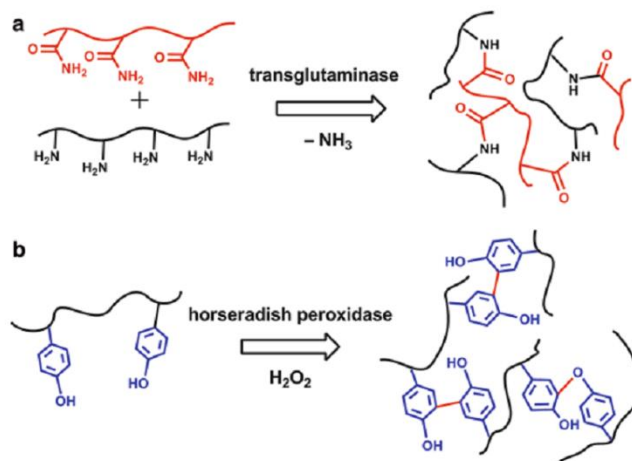


Figure 2.14 Enzymatic reaction (Jin & Dijkstra, 2010)

2.5.2 Swelling of hydrogel

Swelling is the important characteristics of hydrogel. The potential of swelling depends on ultimate capacity that water can be absorbed into the space between crosslinked networks of hydrogel. This water absorption capacity is related to polymer solubility, electric charge, and osmotic pressure. The resistance to swelling is elastic force from crosslinked bonds in hydrogel. Balance of water absorption and resistance determines the equilibrium hydrogel swelling which is affected by polymer properties, crosslinked networks, and porosity of hydrogel (Figure 2.15).

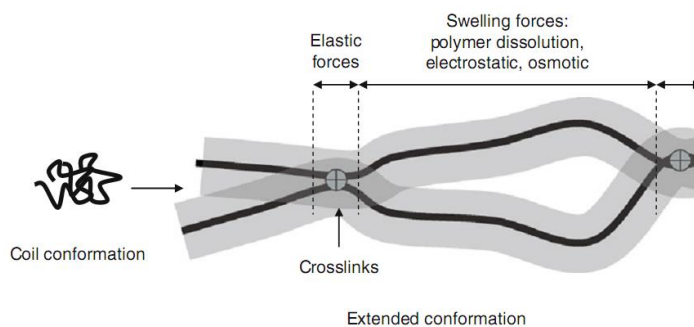


Figure 2.15 Swelling of hydrogel (Omidian & Park, 2010)

Water in hydrogel can be classified into 4 types including primary bound water, secondary bound water, interstitial water, and free water. The primary bound water is the water bound to polar hydrophilic groups which

is the first area of binding when exposed with water. Then hydrogel becomes swollen and the hydrophobic groups are exposed and interacted with water. The water bound to the hydrophobic groups is secondary bound water (semi-bound water). Total bound water is the summation of primary and secondary bound water. After this, hydrogel is still able to absorb water the crosslink network chains of hydrogel can absorb in 2 patterns including interstitial water which is absorbed by osmotic pressure and free water (bulk water) which is loosely bound at the outer surface of hydrogel (Figure 2.16).

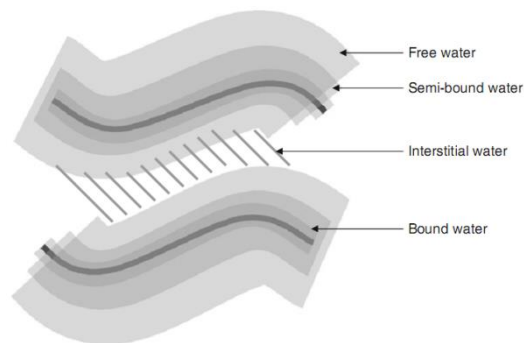


Figure 2.16 Types of water in hydrogel (Omidian & Park, 2010)

2.5.3 Hydrogel degradation

There are 3 basic mechanisms of hydrogel degradation [26] as following:

2.5.3.1 *Hydrolysis reaction* such as ester linkage in PEG-PLA copolymers. The degradation rate depends on composition of hydrogel but not the environment.

2.5.3.2 *Enzymatic degradation* such as hydrogel of collagen, chitosan, or hyaluronic acid. The degradation rate depends on the number of cleavage sites in materials and amount of enzyme in environment.

2.5.3.3 *Dissolution* such as ionically crosslinked alginate. The rate of dissolution depends on ions in environment.

2.5.4 Physical characteristic of hydrogel

Hydrogel is viscoelastic material that response to loading as shown in Figure 2.17. In phase I, hydrogel is elastic and response followed load-deformation curve. At point II, which is the hydrogel maximum strength, hydrogel starts to break. In phase III, hydrogel breaks apart.

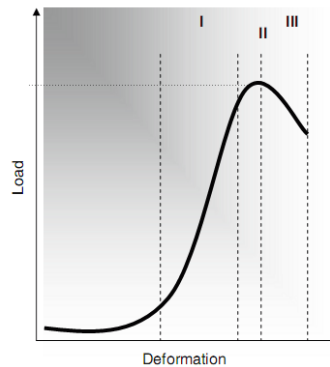


Figure 2.17 Load-deformation curve of hydrogel (Omidian & Park, 2010)

Wet-state stability is the stability of hydrogel to maintain its shape in the swollen state. Low wet-state stability leads to leakage of absorbed water resulting in change in shape and characteristics of hydrogel. Wet-state stability is related to crosslink density. Nevertheless, crosslink density is inversely related to swelling capacity [6].

2.5.5 Hydrogel related bone tissue engineering

Hydrogel has suitable properties to be used in medical engineering including high water content facilitating effective mass transport of biomolecules, tissue-resemble physicochemical characteristics, good biocompatibility, and minimal irritation to tissue. However, the use of hydrogel as scaffold and cell carrier in bone tissue engineering, the gel formation should be in a short time and cell-friendly. The gel strength must be sufficient and has proper degradation rate [8, 26].

There are 2 ways to use hydrogel: preformed vs in situ-forming hydrogel (Figure 2.18)

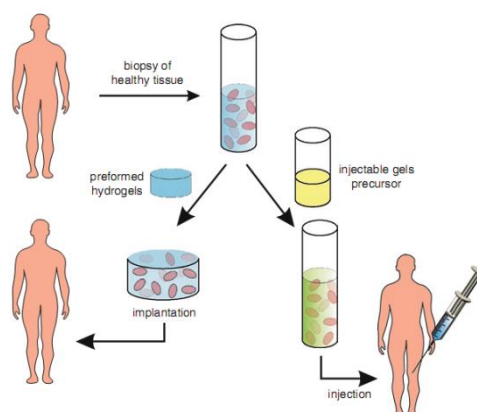


Figure 2.18 Preformed vs In situ-forming hydrogel (Jin & Dijkstra, 2010)

2.6 Silk

2.6.1 Structure and property of silk

Silk is protein polymers spun into fiber by *Lepidoptera* larva such as silkworms, spiders, scorpions, ticks, and flies. The composition, structure, and property of silk are varied according to the source of silk (Table 2.1). In the present study, we focus only on *Bombyx mori* silk that has been researched and widely used in Thailand.

Table 2.1 Amino acid composition of silk fibroin from various domestic races (http://www.chulapedia.chula.ac.th/index.php/ไหมไทย:_การประยุกต์ใช้เป็นชีววัสดุเพื่อการแพทย์)

Domestic race	Thai Nangnoi Srisaket 1	Japanese	Chinese
Hydrophilic amino acid			
Negative side chain			
Aspartic acid	1.63	2.08	2.18
Glutamic acid	1.15	1.52	1.51
Positive side chain			
Arginine	0.30	0.31	0.44
Lysine	0.20	0.26	0.30
Histidine	0.83	0.81	1.02
Polar side chain			
Serine	13.42	16.87	16.30
Threonine	0.80	1.08	1.08
Cysteine	0.00	0.00	0.00
Total	18.33	22.93	22.83

Hydrophobic amino acid			
Aliphatic side chain			
Glycine	38.32	33.00	35.76
Alanine	34.29	31.26	29.39
Proline	0.42	0.64	0.64
Valine	1.15	1.67	1.53
Leucine	0.27	0.38	0.43
Isoleucine	0.20	0.31	0.32
Methionine	0.08	0.13	0.10
Aromatic side chain			
Tyrosine	5.75	7.66	7.16
Phenylalanine	0.98	1.69	1.39
Tryptophan	0.21	0.33	0.45
Total	81.67	77.07	77.17

Structure of Silk contains fibroin protein as a core protein coated by sericin protein that acts like glue to connect the core protein (Figure 2.19). Fibroin protein comprises light chain and heavy chain in 1:1 ratio. The heavy chain fibroin protein (MW 325 kDa) composed of repetition of amino acid sequences of Alanine-Glycine with Serine or Tyrosine. The light chain fibroin protein (MW 25 kDa) contains several amino acids such as Leucine, Isoleucine or Valine. The heavy and light chains were connected together with disulfide bond. Fibroin proteins have two patterns of arrangement (Table 2.2) including 1) random-coil and amorphous regions; 2) antiparallel β -sheet (Figure 2.20) [10, 27, 28].

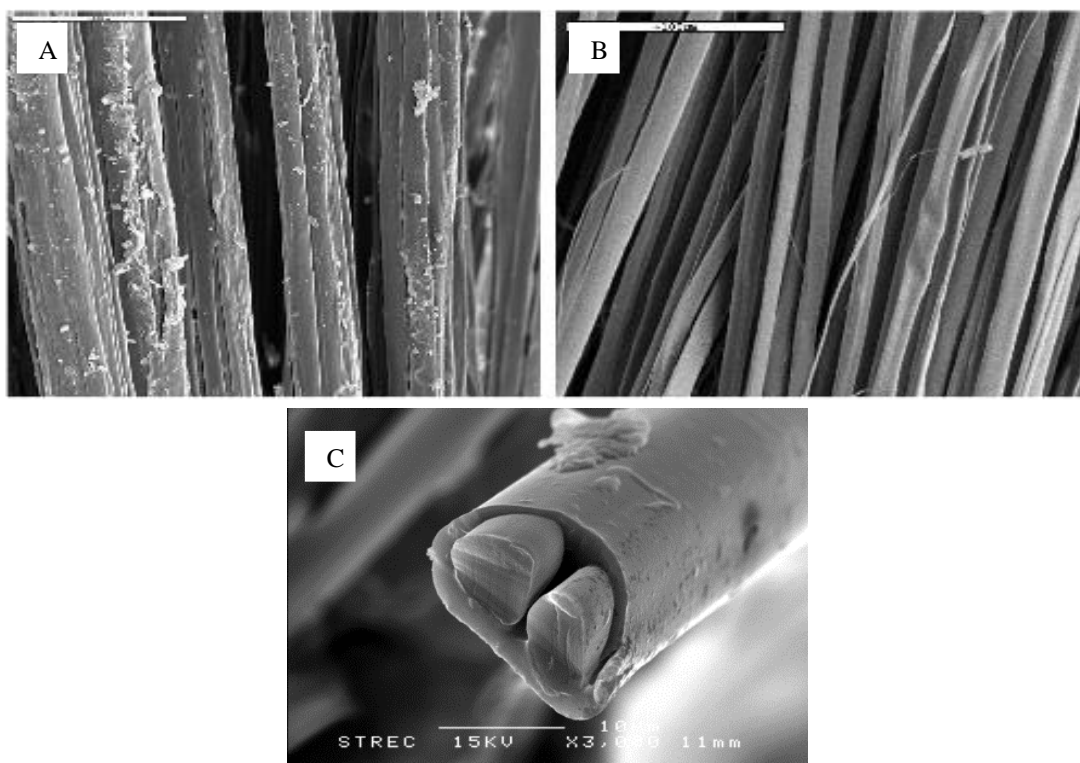


Figure 2.19 SEM images of silk fibroin (A) silk fibroin without sericin removed, (B) silk fibroin with sericin removed, (C) *Bombyx mori* Nangnoi Srisaket 1 Thai silk thread (Altman et al., 2003; http://www.chulapedia.chula.ac.th/index.php/ไหมไทย:_การประยุกต์ใช้เป็นชีววัสดุเพื่อการแพทย์)

Table 2.2 The structures of silk thread (Cao et al., 2009)

Silk fiber	Fibroin (72-81%)		Sericin (19-58%)
	Heavy chain	Light chain	a glue-like protein
Molecular weight	325 kDa	25 kDa	~ 300 kDa
Polarity	Hydrophobic		Hydrophilic
T-Structure	Silk I (random coil or unordered structure) Silk II (crystalline structure)		Non-crystalline structure

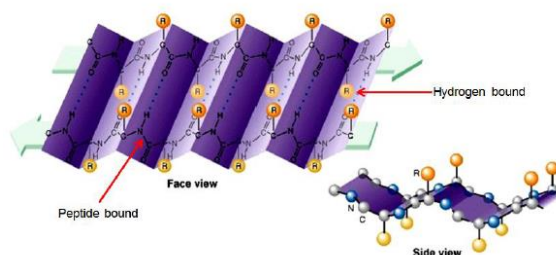


Figure 2.20 The arrangement of fibroin as antiparallel β -sheet
(<http://www.mun.ca/biology/scarr/Gr09-06.html>)

Fibroin protein has hydrophobic nature. It is insoluble in most solvents including water, weak acid, and weak base. The promising properties of fibroin is biocompatibility, slow degradation with proteolysis, light weight, good permeability, and outstanding mechanical characteristics as showing in Table 2.3.

Table 2.3 Mechanical characteristics of *Bombyx mori* silk compare with others compound and human's tissues (Altman et al., 2003)

Material	Ultimate tensile strength (MPa)	Modulus (Gpa)	% Strain at break
<i>Bombyx mori</i> silk (w/sericin)	500	5-12	19
<i>Bombyx mori</i> silk (w/o sericin)	610-690	15-17	4-16
Spider silk	875-972	11-13	17-18
Collagen	0.9-7.4	0.0018-0.046	24-68
Collagen X-linked	47-72	0.4-0.8	12-16
Polylactic acid (PLA)	28-50	1.2-3.0	2-6
Tendon (comprised of mainly collagen)	150	1.5	12
Bone	160	20	3
Kevlar (49 fiber)	3,600	130	2.7
Synthetic rubber	50	0.001	850

2.6.2 Hydrogel of silk fibroin

Silk fibroin solution can spontaneously assemble into β -sheet and form hydrogel but with prolong gelation time. At 0.6-15 wt% of silk fibroin, gelation at room temperature takes several days to weeks. Hydrogel of silk fibroin has proper biocompatibility. Wang et al. (2006) reported proliferation of mesenchymal stem cells for 21 days in sonication-induced silk fibroin hydrogel. Sonication-induced silk fibroin hydrogel also showed superior mechanical properties compared with hydrogels of other materials such as alginate, agarose, fibrinogen or PEG, indicating potential of silk fibroin hydrogel as a cell carrier in tissue engineering [29].

Factors accelerated SF gelation include:

2.6.2.1 Chemical methods

a) Salts

The gelation of SF by salts is widely employed. The salts can induce protein precipitation by the salting out method. The external layers of proteins are dehydrated by the salts leading to protein association [30, 31]. Furthermore, calcium salts significantly decrease the gelation times of SF than potassium salts [32].

b) Organic solvents

Organic solvents such as alcohols (methanol, ethanol) have an effect on protein-protein interaction by inducing dehydration of the α -helix, stimulating the occurrence of β -sheet assembly, and reducing the solvent property of water. Moreover, organic solvents also change the dielectric constant resulting in reduced electric field in the solution and stimulating proteins aggregation [31, 33-35].

c) Surface agents

Surfactants induce gelation through electrostatic effect and increase of hydrophobic force which encourages protein unfolding with rapid gel formation [36, 37]. A good example of surface agents is sodium dodecyl sulfate (SDS).

d) Large polymeric precipitation agents

The addition of large polymers (polyethylene glycols, polyethylene oxide) to SF solutions can stimulate gel formation by the volume exclusion effect and water osmosis. The increase of the SF contents influences the depletion of solvent and protein solution and promotes the osmosis of water in proteins, resulting in dehydration of protein. The aggregation which follows leads to gel formation [31, 32].

e) Low molecular weight polymers (LMWPs)(Poloxamer)

The LMWPs such as polyols, glycerol, and poloxamers encourage gel formation through their ionic strength or specific reaction between small polymer agents and specific proteins. In addition, the LMWPs also increase the hydrophobicity of proteins which greatly reduces gelation [36, 38-40].

f) Decreasing pH

Decreasing the pH has a direct effect on the distribution and total charges of the SF solution. The adjustment of pH to approach the isoelectric point of SF (pH 3.8-4.0) can induce proteins aggregation. The hydrogels are formed due to the reduction of the repulsive force between silk proteins leading to proteins collisions and physical crosslink. Moreover, the acidity of the SF solution favors gel formation through relatively weak interaction such as hydrogen bonding or hydrophobic interaction [32, 41-44].

g) High pressure CO₂ gas

High pressure CO₂ gas plays an important role in aqueous acidification. The SF hydrogel prepared from this procedure has increased porosity and physical properties. The improvement of porosity of the SF hydrogel is the result of the phase inversion process that partitions the solution into a polymer-rich and a polymer-lean phases. When CO₂ is removed, the bubble nucleation stops encouraging and preserving the porosity in the SF hydrogel [45].

h) Chemical modification of SF

The chemical modification of SF performed by addition of diazonium coupling eg. sulfonic acid, carboxylic acid, ketones, or alkanes. These non-natural functional groups (inorganic group) facilitate gel formation through alteration of the hydrophobic and hydrophilic properties of tyrosine which spontaneously assembles into β -sheets. The gelation time depends on the tyrosine volume adjustment or the concentrations of the SF solution [46, 47].

2.6.2.2 Physical methods

a) Temperature

Increased temperature directly causes hydrophobicity thus compromising the free energy state (according to Gibbs free energy law) of proteins resulting in hydrophobic exposure, protein unfolding, and interaction and increasing association of hydrophobic parts [32, 43, 48]. The increase in temperature from room temperature to 37 °C can reduce the gelation time from 12 days to 8 days [43].

b) Vortex

The combination of extension and rotation forces can produce shear force to the SF solution. Both forces change protein arrangement and stretching protein chains which produce a fluctuation of the SF content, boost protein interaction and beta-sheet assembly [49-52]. The gelation time can be reduced by the speed of vortex [53].

c) Sonication

The ultrasound produces cavitation and bubbles. The eruption of the bubbles generates high temperature and pressure in the SF solution. The gel is formed by the hydration of free water which is a consequence of bubbles explosion [54, 55]. The duration of gel formation depends on the parameter setting of sonication (power output, times) [55].

d) Electric field

Electric currents accumulate proteins at the anode, resulting in decreasing the pH in the SF solution and also change the SF structure from random coil to alpha helix. The acidification and structure change by the electric field causes the SF solution finally to become hydrogel [52, 56]. The formation of the hydrogel by this method is reversible by changing the polarity of the applied current [57].

2.7 Collagen

Collagen is the structural protein in ECM providing structural and mechanical support for connective tissues especially tendons, bones, cartilages, teeth, vessel walls, and skin. Collagen monomer, Tropocollagen, is cylinder-shaped protein with 300-kDa weight, 2,800-Å length, and 15-Å diameter approximately. It contains 3 α -chain polypeptides. Each polypeptide has over 1,000 amino acids (Glycine 33%, Proline 12%, and Hydroxyproline 11%, etc.) which are repeatedly linked as –Gly-X-Y (X = Proline and Y = Hydroxyproline, but can also be other amino acids except Tryptophan). Three polypeptides form a right-handed helix, bound with hydrogen bonds, to be a Tropocollagen. Tropocollagens are parallel arranged and connected with van der Waals and hydrophobic force, forming collagen fibers (Figure 2.21).

Collagen can be divided into 29 types according to amino acid sequence, molecular mass, composition of subunit, length of helix change, properties, and size of non-helix portion [58]. Moreover, collagen can be subtypes by sequencing of DNA and/or protein [59] as shown in Table 2.4. Collagen type I is the main collagen in bone tissue providing tensile strength and scaffold for deposition of inorganic bone compound, calcium hydroxyapatite.

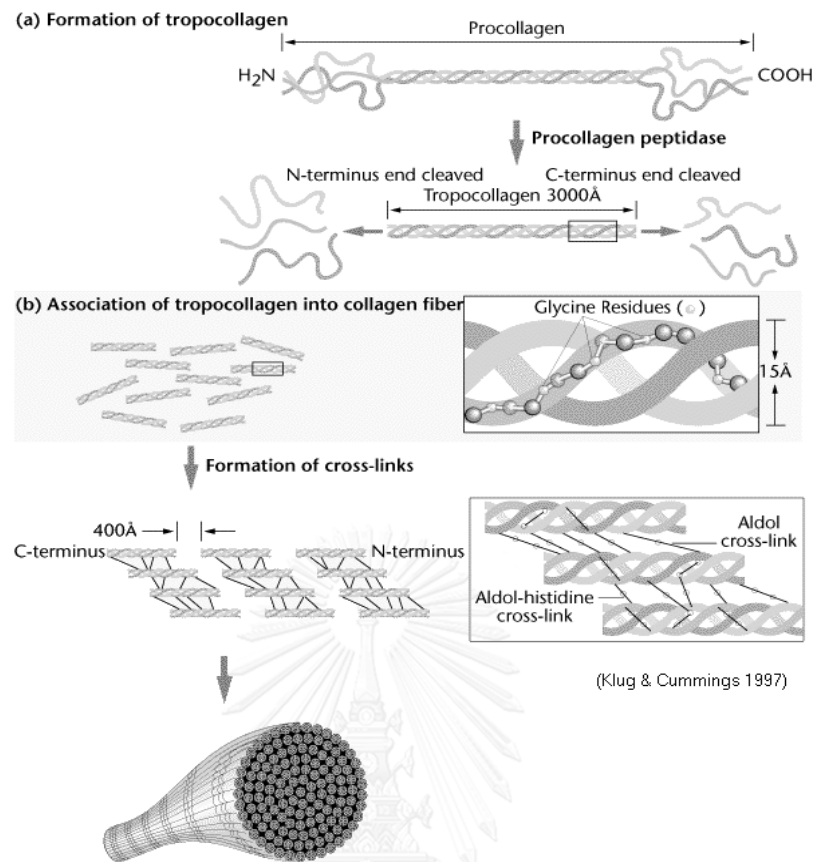


Figure 2.21 Structure of collagen
http://www.mun.ca/biology/scarr/collagen_structure

Table 2.4 Collagen: Types, compositions, and tissues distribution
(Freiss, 1998)

Collagen type	Chain composition	Tissue distribution
I	$(\alpha 1(I))_2\alpha 2(I)$ or trimer $(\alpha 1(I))_3$	Skin, tendon, bone, cornea, dentin, fibrocartilage, large vessels, intestine, uterus, dentin, dermis, tendon
II	$(\alpha 1(II))_3$	Hyaline cartilage, vitreous, nucleus pulposus, notochord
III	$(\alpha 1(III))_3$	Large vessels, uterine wall, dermis, intestine, heart valve, gingiva (usually coexists with type I except in bone, tendon, cornea)
IV	$(\alpha 1(IV))_2\alpha 2(IV)$	Cornea, placental membranes, bone, large vessels, hyaline cartilage, gingiva
V	$\alpha 1(V)\alpha 2(V)\alpha 3(V)$ or $(\alpha 1(V))_2\alpha 2(V)$ or $(\alpha 1(V))_3$	Descemet's membrane, skin, nucleus pulposus, heart muscle
VII	$(\alpha 1(VII))_3$	Skin, placenta, lung, cartilage, cornea
VIII	$\alpha 1(VIII)\alpha 2(VIII)$ chain organization of unknown helix	Produced by endothelial cells, Descemet's membrane
IX	$\alpha 1(IX)\alpha 2(IX)\alpha 3(IX)$	Cartilage
X	$(\alpha 1(X))_3$	Hypertrophic and mineralizing cartilage
XI	$\alpha 1(XI)\alpha 2(XI)\alpha 3(XI)$	Cartilage, intervertebral disc, vitreous humour
	$\alpha 1(XI)\alpha 2(XI)\alpha 3(XI)$	Chicken embryo tendon, bovine periodontal
XII	$(\alpha 1(XII))_3$	Ligament
XIII	Unknown	Cetal skin, bone, intestinal mucosa

Collagen is insoluble in water, weak acid, and weak base. But when concentration of acid or base increases, crosslinking of collagen can be partially damaged resulting in swelling and increased solubility. Heat can denature collagen. The helix chains is denatured at the temperature between 15-65 °C depends on type and source of collagen, and amount of hydroxyproline and proline in polypeptide chain. Collagen can be biologically degraded by collagenase enzyme.

2.8 Osteogenic differentiation of mesenchymal stem cells

Mesenchymal stem cells (MSC) is spontaneous differentiation cells that can develop into other tissues such as fat, bones, cartilages, tendons, and muscles (Figure 2.22). The development of MSC into tissues depends on numerous factors such as cell density, cell arrangement, type of medium, growth factors, and cytokines [60]. International Society for Cellular Therapy (ISCT) proposed criteria for identification of MSC including 1) attachment of the cells on culture plate, 2) cellular expression of CD73, CD 90, and CD105 surface markers, 3) no cellular expression of hematopoietic stem cells surface markers as CD11b, CD14, CD19, CD34, CD45, CD79 α , and HLA-DR [61].

Mesenchymal stem cells can be harvested from bone marrow, adipose tissue, cord blood, periosteum, synovial membrane, and other organs (muscle, skin, and teeth).

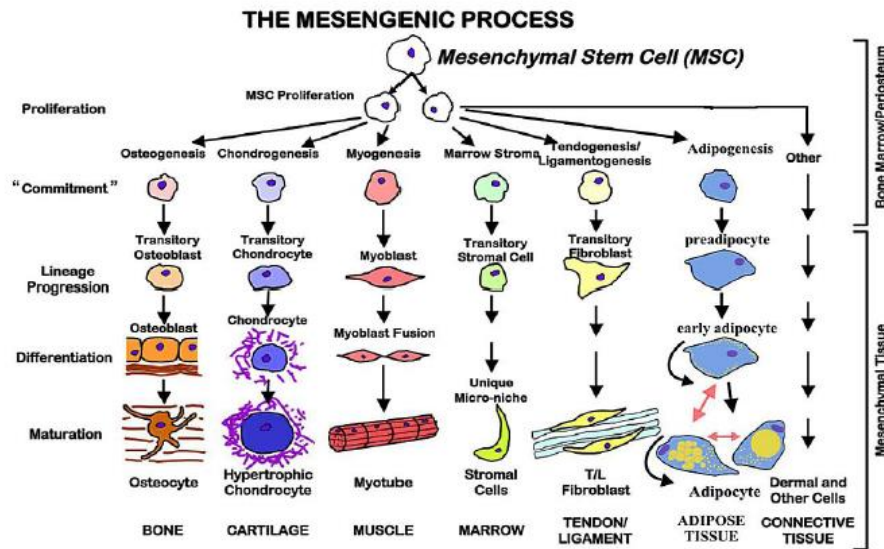


Figure 2.22 The differentiation of mesenchymal stem cell into other tissues. (<http://www.discoverymedicine.com/Tracey-L-Bonfield/2010/04/15/adult-mesenchymal-stem-cells-an-innovative-therapeutic-for-lung-diseases>)

The process of differentiation of mesenchymal stem cell can be divided to 3 phases [62, 63] (Figure 2.23) as following:

1) *Proliferation phase* Cell number increases with expression of histone, fibronectin, collagen, cFos/cJun, TGF- β 1, and osteopontin genes.

2) *Matrix maturation phase* Cell growth decreases and ECM production begins. Early markers of cell differentiation such as alkaline phosphatase (ALP), bone sialoprotein, collagen, and Fra2/JunB can be detected in this phase.

3) *Mineralization phase* Calcium deposition occurs with expression of osteocalcin, osteopontin, and collagenase, which are the late markers of osteogenic differentiation

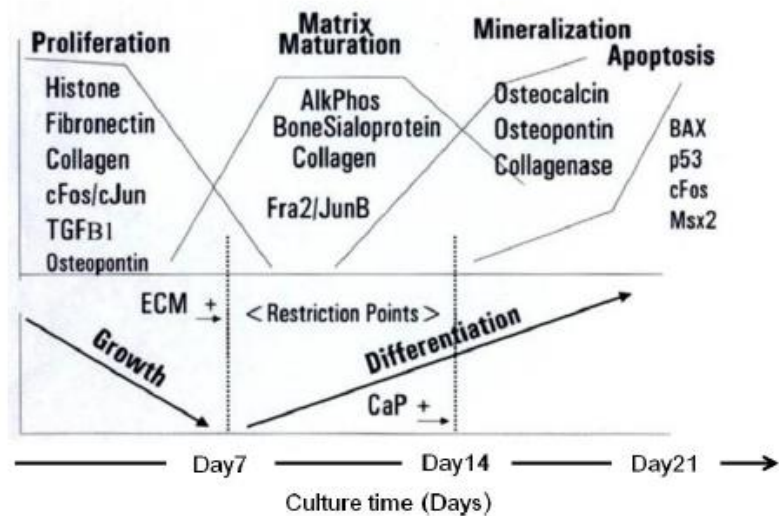


Figure 2.23 Cellular expression in osteogenic differentiation of mesenchymal stem cells (Lian et al., 1992)

2.9 Poloxamer

Poloxamer; with its commercial names as Supronic, Pluronic, Tetronic, Synperonic; is a non-ionic triblock copolymer consisted of 2 hydrophilic chains of polyoxyethylene (POE) linked by a central hydrophobic polyoxypropylene (POP). It is widely used as a surfactant, solubilizer, stabilizer, and gelling agent due to its property and biocompatibility. The POE-POP-POE structure has a chemical formula as $\text{HO}(\text{C}_2\text{H}_4\text{O})_a(\text{C}_3\text{H}_6\text{O})_b(\text{C}_2\text{H}_4\text{O})_a\text{H}$ with varying a and b values. This various length of polymer blocks results in distinct amphiphilic property characterized by hydrophilic-lipophilic balance (HLB) value. Its generic representation uses a letter P following by a three-digit number. The first 2 digits multiplied by 100 represents the molecular mass of the POP block and the last digit multiplied by 10 represents the amount of the POE chain in percentage. For example, poloxamer P188 means a copolymer with 1800 g/mol molecular weight of POP and 80% POE content [64, 65].

With amphiphilic property, poloxamer can aggregate and exhibit micellar structure in aqueous solutions. At a constant temperature, the concentration of poloxamer at which micelles are formed is defined as critical micelle concentration (CMC). The CMC strongly depends on the molecular structure of the poloxamer. An increase in the hydrophilic POE

chain length results in a CMC increase, whereas the CMC decreases as the length of POP block increases [66].

Table 2.5 Physicochemical characteristics of some poloxamers (modified from Torcello-Gómez et al., 2014)

Poloxamer	MW	CMC at 37°C (M)	POE units	POP units	HLB
P181	2000	1.1×10^{-4}	2	30	3
P235	4600	6.5×10^{-5}	26	40	16
P188	8400	4.8×10^{-4}	75	29	29
P407	12600	2.8×10^{-6}	100	65	22

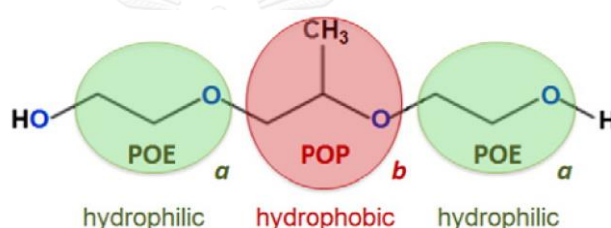


Figure 2.24 Structure of poloxamer (Torcello-Gómez et al., 2014)

Poloxamer was reported to have an effect on acceleration of the gelation of SF solution. The mechanism was the dehydration of SF due to absorption of the water around SF molecules by hydrophilic parts of the poloxamer inducing the conformational change of SF structure from random coil to β -sheet. An increase in the poloxamer concentration resulted in decreased gelation time [39].

2.10 Oleic acid

Oleic acid is classified as a monounsaturated omega-9 fatty acid. It has the formula $\text{CH}_3(\text{CH}_2)_7\text{CH}=\text{CH}(\text{CH}_2)_7\text{COOH}$. It is colorless oily liquid with a relative molecular mass of 282.47, the specific gravity of 0.895 (25°C liquid), freezing point of 4°C, the boiling point of 286°C (13,332 Pa), and the refractive index of 1.463 (18°C). At normal pressure, it is subjected to decomposition at 80-100°C. It is a component of the normal human diet as it exists naturally in the animal and vegetable oil fat, mainly in the form of glyceride. It is insoluble in water but soluble in alcohol,

benzene, chloroform, ether, and other volatile oil or fixed oil. It is used as antifoaming agent, fragrance, binder, lubricant, and flotation agent. It can also be used as an emulsifying or solubilizing agent in aerosol products. With its structure comprises a long hydrocarbon chain and a carboxylate functional group, the surface activity of oleic acid is due to the non-polar hydrocarbon chain. While the polar carboxylate functional group promotes the dissolution of the surfactant in aqueous solution.



Figure 2.25 Structure of oleic acid (Valenzuela & Valenzuela, 2013)

2.11 Hydrophilic-lipophilic balance (HLB)

Hydrophilic-lipophilic balance (HLB) was introduced as a semiempirical scale to classify nonionic surfactants according to their relative affinity for the water and oil phases. Nevertheless, HLB is not a parameter for universal application among all surfactants. The relationship between HLB and solution properties exists merely within a single surfactant category. Two emulsifiers with the same HLB may represent different characteristics of solubility [67]. Moreover, even within the same surfactant category and HLB, other factors such as molecular weight, temperature, electrolyte concentration in the water, oil polarity, and water-to-oil ratio also have influence on features of the formed emulsion [68, 69].

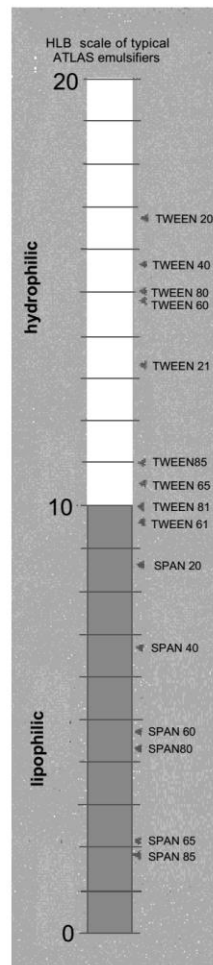


Figure 2.26 Demonstrates HLB numbers of some commonly used surfactants (Tadros, 2013).

It has been found that a combination of one hydrophilic surfactant and the other more hydrophobic surfactant is often more effective than a single intermediate one in making a stable emulsion. And by blending two surfactants together, the ideal surfactant with exactly desired HLB can be achieved [70]. The average HLB number of a surfactant combination can be determined by a calculation as in Equation 2.1.

$$\text{Average HLB} = x_1\text{HLB1} + x_2\text{HLB2} \quad (2.1)$$

(x_1 and x_2 = weight fractions of the surfactants with HLB1 and HLB2)

CHAPTER 3

MATERIALS AND METHODS

3.1 Materials

- Absolute ethanol (Analytical grade, QReC, New Zealand)
- Alpha-modified eagle powder medium (α -MEM(s), Hyclone, USA)
- Bisbenzimidazole H33258 Fluorochrome Trihydrochloride in DMSO solution ($C_{25}H_{24}N_6O \cdot 3HCl$, MW= 533.88, Sigma-Aldrich, USA)
- $CaCO_3$ (Sigma-Aldrich, USA)
- Collagen BM (sterile, Nitta Gelatin Inc, Japan)
- Deionized water (DI water)
- Dexamethasone (Sigma-Aldrich, USA)
- Ethanolamine (Sigma-Aldrich, USA)
- Fetal bovine serum (FBS; HyClone, Thermo Scientific, USA)
- Formaldehyde (Richard-Allan Scientific™ Formaldehyde (37%), USA)
- Hydrochloric acid (HCl, J.T. Baker, NJ, USA)
- Lithium bromide (LiBr, Sigma-Aldrich Laborchemikalien, USA)
- NaCl (Ajax Finechem, Australia)
- O-cresolphthalein complex substrate (OCPC, Sigma-Aldrich, USA)
- Oleic acid ($C_{18}H_{34}O_2$, Merck, Germany)
- Penicillin-Streptomycin Solution (Pen/Strep, Cat.No.: SV30010/ Lot.No.: J090701, Hyclone, USA)
- Phosphate buffered saline (PBS, pH (1%water) 7.3-7.5, Bio Basic Canada Inc., Canada)
- p-nitrophenyl phosphate (Sigma-Aldrich, USA)
- Poloxamer-188 solution ($C_5H_{10}O_2$, 10% sterile-filtered, Sigma-Aldrich, USA)
- SDS lysis buffer (HyClone, Thermo Scientific, USA)
- Sodium bicarbonate (Na_2CO_3 , Ajax Finechem, Australia)
- Sodium hydroxide (NaOH, Ajax Finechem, Australia)

- Sodium lauryl sulphate ($\text{CH}_3(\text{CH}_2)_{11}\text{OSO}_3\text{Na}$ = 288.38, Ajax Finechem, New Zealand)
- Tri-sodium citrate dehydrate ($\text{C}_6\text{H}_5\text{Na}_3\text{O}_7 \cdot 2\text{H}_2\text{O}$ = 294.10, Merck, Germany)
- Trypan blue Stain 0.4% (Gibco, U.S.A.)
- Trypsin-EDTA (0.25% trypsin with EDTA, Hyclone, Thermo Scientific, USA))
- Yellow *Bombyx mori* silk cocoons (Nangnoi Srisaket 1) (Queen Sirikit Sericulture Center, Nakorn Ratchasima and Srisaket Provinces, Thailand)
- β -glycerophosphate (Sigma-Aldrich, USA)

3.2 Equipments

- 48 well, 96-well polystyrene tissue culture plate (Corning, USA)
- Autopipette (Eppendorf, Germany)
- Branson 450 Sonifier (Branson Ultrasonic Co., Danbury, USA)
- Centrifuge (Universal 320R, Hettich, Germany)
- Critical point dryer (K850, Emitech, UK)
- Desiccator (SR Lab, Thailand)
- Dialysis Tube ((MWCO=12,000-16,000, Viskase, Japan)
- Disposable Syringe (1 ml, NIPRO, Japan)
- DSC-204 F1 Phoenix (Netzsch, Germany)
- Fine coater (JFC-1200, Jeol, Japan)
- Fourier Transform Infrared spectrometer (FT-IR, Spectrum One, Perkin Elmer, UK)
- Freeze dryer (CHRIST®, Germany)
- Freezer (-20 °C) (Sanden intercool, Thailand)
- Freezer (-40 °C) (Haier, China)
- Freezer (-80 °C) (New Brunswick scientific, USA)
- FT/IR-6200 Spectrometer (Jasco, Japan)
- Hemacytometer (Boeco, Germany)
- Homogenizer (Ika, Germany)
- Hypodermic needle (27Gx1/2", NIPRO, Japan)
- Laminar Flow (Thermo scientific, USA)
- Lyophilizer (Christ, Germany)

- Magnetic stirrer / Hot plate (RCT Basic, Ikalabortechnik, Germany)
- Micro plate reader (UVM 340, ASYS, Australia)
- Micro-CT scanner (μ CT 35, SCANCO Medical, Switzerland)
- Mini-oscillating saw (Synthes, Switzerland)
- Nonpyrogenic serological pipette (Costar®, Corning, USA)
- Oscillating rheometer (Kinexus Pro, Malvern, UK)
- pH-meter (professional meter PP-50, Germany)
- Polystyrene tissue culture flask (Corning, USA)
- Portable X-ray (SR-130, Source-Ray Inc., USA)
- Scanning electron microscopy (SEM, JSM-5410LV, Jeol, Japan)
- Steri-Cycle CO2 Incubator HEPA class 100, Thermo scientific, USA)
- UV-Vis spectrophotometer (UV -2450, Shimudzu, Japan)
- Vortex mixer (MX-S, Dragon Laboratory Instruments, Beijing, China)
- Water bath (1235 PC, Shel-Lab)
- Weighting scale (METTLER TOLEDO, UK)
- Zeta sizer (Nano ZS, Malvern, UK)

3.3 Research framework

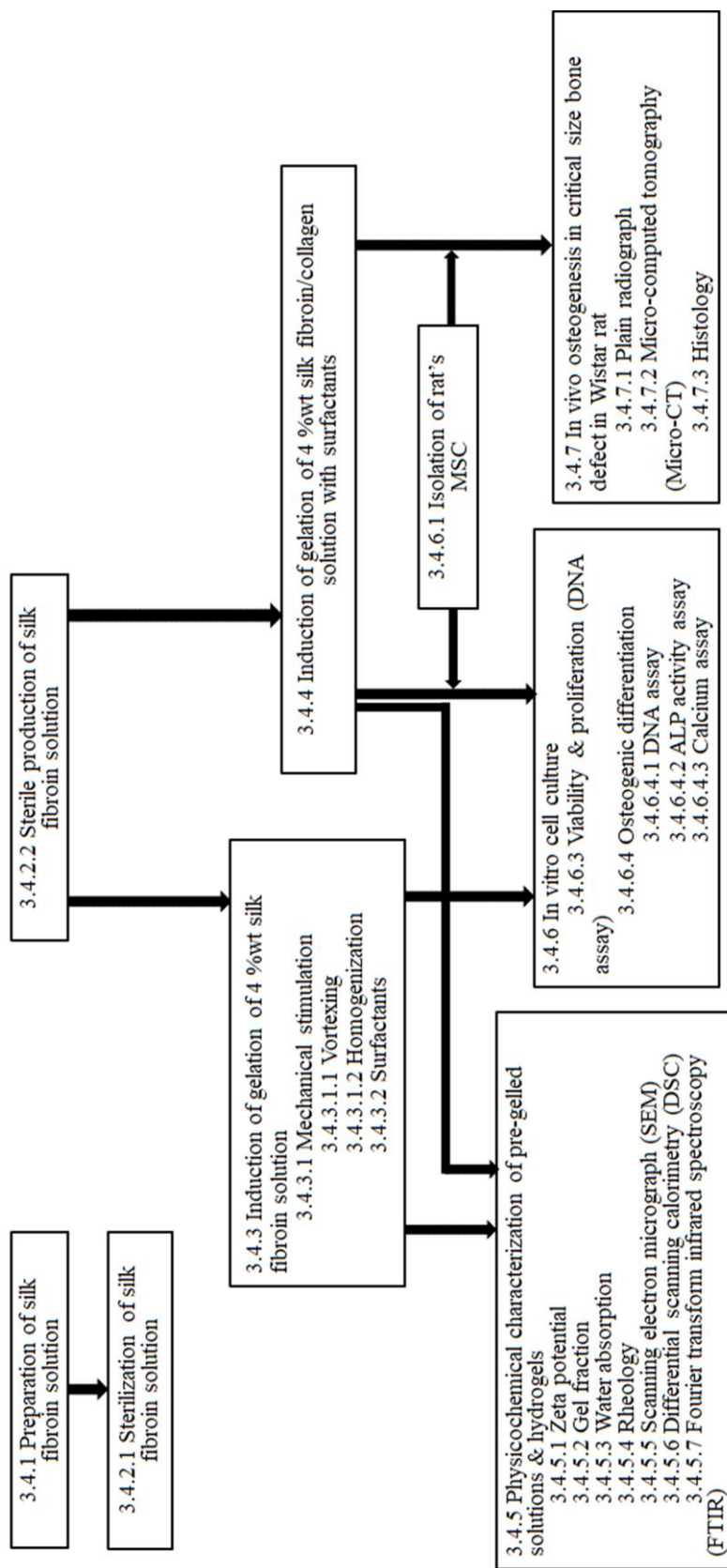


Figure 3.1 Diagram of experimental procedures

3.4 Methodology

3.4.1 Preparation of silk fibroin solution

Thai silk fibroin solution was prepared using a method adapted from Kim and Tungtasana [32, 71]. Forty grams of *Bombyx mori* Thai silk worm cocoons, Nangnoi Srisaket 1, were boiled in 1M Na₂CO₃ for 20 min to clean and remove silk glue, then they were rinsed with deionized water for 4-5 times. The process was repeated for 2 times. After that, the degummed cocoons were air-dried for 2 days followed by torning and fluffing of cocoons into fibers. Eight grams of degummed silk fibers were dissolved in 9.3M 16 mL of LiBr concentration 9.3 M/16 ml at 60°C for 4 h. The silk fibroin solution was then dialyzed against DI water for 3 days using dialysis tubes (MWCO 12,000-16,000 kDa) to remove LiBr solution. The dialyzed silk fibroin solution was centrifuged at 9,000 rpm, 4°C for 20 min to remove residual insoluble parts. The concentration of obtained silk fibroin solution was 6-6.7% (w/w). The solution was kept at 4°C before further use.

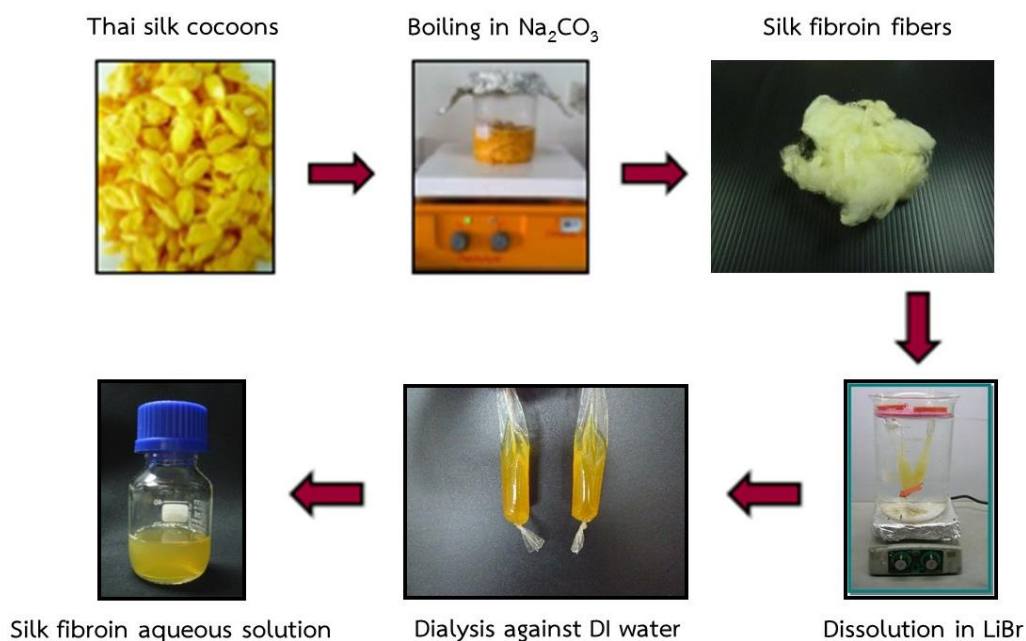


Figure 3.2 Process of silk fibroin solution preparation using LiBr

3.4.2 Obtaining of sterile silk fibroin solution

3.4.2.1 Sterilization of silk fibroin solution

Thai silk fibroin solution were prepared in varied concentrations into 1%, 2%, 3%, 4%, and 5% (w/w). The samples were sterilized with 3 following methods:

- a) Filtration with 0.2 μm -pore size filter paper
- b) Autoclaving at 121°C for 15 min
- c) ^{60}Co Gamma irradiation at 25 kGy, 50°C for 224 min

The characteristics of sterilized samples were observed and sterility of samples was examined by total plate count & total yeast and mold tests.

3.4.2.2 Sterile production of silk fibroin solution

Forty grams of *Bombyx mori* Thai silk worm cocoons, Nangnoi Srisaket 1, were boiled in Na_2CO_3 concentration 1M/1000 ml for 20 min to clean and remove silk glue, then they were rinsed with deionized water for 4-5 times. The process was repeated for 2 times. After that, the degummed cocoons were air-dried for 2 days followed by torning and fluffing of cocoons into fibers. The dried silk fibers were sterilized by autoclaving at 121°C for 15 min, then dried in a desiccator to remove steam. Eight grams of sterilized silk fibers were dissolved in LiBr concentration 9.3 M/16 ml at 60°C for 4 h. The solution was dialyzed under sterile condition against sterile DI water for 48 h to remove LiBr. The obtained silk fibroin solution was then centrifuged at 9,000 rpm, 4°C for 20 min to remove residual insoluble parts. The final concentration of regenerated Thai silk fibroin aqueous solution was about 5.5 - 6.0% (w/w). All equipments in this protocol were sterilized.



Figure 3.3 Dialysis of sterile dissolved silk fibroin/LiBr solution under sterile condition

3.4.3 Induction of gelation Thai silk fibroin solution

3.4.3.1 Mechanical stimulation

a) *Vortex*

A 5-ml vial of 4 wt% Thai silk fibroin solution was attached to a holder and vortexed at 2500 rpm for 1, 3, and 5 min. The vials containing the solutions were checked for gelation by tilting at 45° angle at regular intervals. Transition into gel state was considered as no deformation of the meniscus upon 90° angle tilting of the tubes and no falling of the gel with turning the vials upside down [32, 72]. The gelation time was recorded.



Figure 3.4 A vial of silk fibroin solution attached with a holder being vortexed

b) *Homogenization*

Ten milliliters of 4 wt% Thai silk fibroin solution with 7.4 pH-adjusted was being homogenized at 6500 rpm for 30 and 60 sec. Then the homogenized solution was transferred into a vial. Gelation time was observed and recorded.

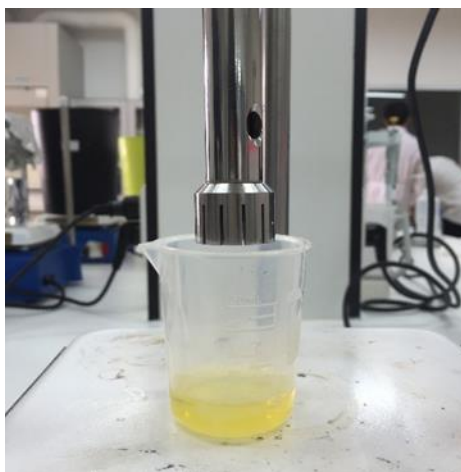


Figure 3.5 Homogenization of silk fibroin solution

3.4.3.2 Surfactants

Thai silk fibroin solution was mixed with DI water and surfactant blended systems of oleic acid and poloxamer-188. The weight ratio of oleic acid to poloxamer-188 was varied to obtain a mixture of surfactants at different HLB values of the surfactants (1, 3, 5, 10, 15 and 20). The SF solution mixed with different HLB-valued surfactants was labeled as shown in Table 3.1. Each sample was vortexed at 2500 rpm for 90s before incubation at 37°C. Gelation time was observed and recorded.

Table 3.1 weight percent in total, weight percent of silk fibroin and surfactants, and HLB value of surfactants composed in each silk fibroin hydrogel sample

Sample	wt% in total	wt% silk	wt% oleic acid	wt% poloxamer	HLB of surfactants
SF	4.00	4.00	0	0	N/A
SF/HLB1	4.00	3.00	1.00	0.00	1
SF/HLB3	4.00	3.00	0.93	0.07	3
SF/HLB5	4.00	3.00	0.86	0.14	5
SF/HLB10	4.00	3.00	0.68	0.32	10
SF/HLB15	4.00	3.00	0.50	0.50	15
SF/HLB20	4.00	3.00	0.32	0.68	20

3.4.4 Induction of gelation Thai silk fibroin/collagen solution with surfactants

Thai silk fibroin solution was mixed with steriled collagen solution, DI water, and oleic acid-poloxamer surfactants with varied HLB (1, 3, 5, 10, 15, and 20) as in Table 3.2. Each sample was vortexed at 2500 rpm for 90 s before incubation at 37°C. Gelation time was observed and recorded.

Table 3.2 weight percent in total, weight percent of silk fibroin, collagen, and surfactants, and HLB value of surfactants composed in each silk fibroin/collagen hydrogel sample

Sample	wt% in total	wt% silk	wt% oleic acid	wt% poloxamer	wt% collagen	HLB of surfactants
SFC	4.10	4.00	0.00	0.00	0.10	N/A
SFC/HLB1	4.10	3.00	1.00	0.00	0.10	1
SFC/HLB3	4.10	3.00	0.93	0.07	0.10	3
SFC/HLB5	4.10	3.00	0.86	0.14	0.10	5
SFC/HLB10	4.10	3.00	0.68	0.32	0.10	10
SFC/HLB15	4.10	3.00	0.50	0.50	0.10	15
SFC/HLB20	4.10	3.00	0.32	0.68	0.10	20

3.4.5 Physicochemical characterization of solutions and hydrogels

3.4.5.1 Zeta potential of the solution

Analysis of zeta potential was performed at 25 °C in 1 wt% solution of silk fibroin, silk added with surfactants, and silk fibroin/collagen added with surfactants as in Table 3.1 and 3.2; 0.05 wt% collagen; 1 wt% oleic acid-poloxamer surfactants with varied HLB (1,3,5,10,15, and 20). Initial pH of the surfactant solutions was at 4.0 while those of the protein solutions were at 5.5. The samples were adjusted with 0.1 M NaOH to obtain pH of 5.5 and 7.5.

3.4.5.2 Gel fraction of the hydrogel

Hydrogels as in Table 3.1 and 3.2 were lyophilized for 72 h. Then, the lyophilized hydrogels were incubated in DI water at 37°C for 24 h. Remained hydrogels were dried in an oven at 60°C. Initial and final weights of the lyophilized hydrogels were obtained. Calculation of insoluble gel fraction of hydrogels was as in Equation 3.1.

$$Gel\ fraction = \left(\frac{Final\ weight}{Initial\ weight} \right) \times 100\% \quad (3.1)$$

3.4.5.3 Water absorption of the hydrogel

Hydrogels as in Table 3.1 and 3.2 were incubated in DI water at 37°C for 24 h. Initial and final weights of hydrogels were obtained. Water absorption capacity of hydrogels was calculated as in Equation 3.2.

$$\text{Water absorption} = \left(\frac{\text{Final weight} - \text{Initial weight}}{\text{Initial weight}} \right) \times 100\% \quad (3.2)$$

3.4.5.4 Rheological property of the hydrogel

Hydrogels were cut into 20 mm x 20 mm-pieced specimens and were kept hydrated in DI water. The rheological study was performed with a 20-mm plate-plate oscillating rheometer at 25°C. Plate-plate gaps were set using a constant force at 0.5 N from the probe pressing onto the specimens. Amplitude sweeps were performed first at 0.01-10% strain and 1 Hz. Frequency sweeps were performed later at 0.1-10 Hz and 0.03% strain. Elastic modulus (G') and viscous modulus (G'') were recorded.

3.4.5.5 Morphology of the hydrogel

Hydrogels were cut into specimens and dehydrated in series of ethanol concentrations. The specimens were submerged in 30 and 50% (v/v) ethanol solutions for an hour each time followed by 70% (v/v) for 12 h. They were then submerged in 90, 95, and 100% (v/v) ethanol solutions for an hour each time before drying by a critical point dryer. The dried specimens were sputtered with gold by a fine coater. They were then examined with scanning electron microscopy (SEM) under different magnifications.

3.4.5.6 Thermal property of the hydrogel

Hydrogels were freeze-dried at -80°C for 72 h. Differential scanning calorimetry (DSC) measurement of freeze-dried hydrogels was performed in the temperature range of -20 - 400°C and with a heating rate of 20°C/min and a N₂ flow of 50 ml/min.

3.4.5.7 Secondary structure of the hydrogel

Hydrogels were freeze-dried at -80°C for 72 h. Fourier transform infrared raman spectroscopy (FTIR) measurement of freeze-dried hydrogels was performed in ATR mode with scanning range $400\text{-}40000\text{ cm}^{-1}$ at 4 cm^{-1} resolution for each sample. The Fourier Self Deconvolution (FSD) was performed using OMNIC Pro9 Software, FSD factors (bandwidth= 25 cm^{-1} , enhancement 2.7), for curve fitting.

3.4.6 *In vitro* cell culture

3.4.6.1 Isolation of rat bone marrow-derived mesenchymal stem cells (rat's MSC)

MSC was isolated from femurs of 3-week old female Wistar rat from Animal research center, Mahidol University by a modification of the method of Takahashi & Tabata [73]. The animal use protocol was approved by the ethical committee of animal care and use protocol of Chulalongkorn University (Approval number 06/2560) (Appendix A). The femurs were dissected and cleaned with PBS before cutting at proximal and distal ends. The bone marrow was flushed out using a 24-gauge needle with 1 ml of alpha-modified eagle medium (α -MEM) supplemented with 15% fetal bovine serum (FBS) and 1% penicillin-streptomycin. The flushing was repeated until all marrow plug was harvested, then the tissue was disrupted by repeated aspiration through a needle. The resulting cell suspension was placed into 75 cm^2 tissue culture bottle containing 10 ml of medium and cultured in an incubator at 37°C , 5% CO_2 . The medium was changed on the 4th day, and every 3 days thereafter.

When large cell colonies developed, the cells were released from the dish by treatment with trypsin-EDTA and subcultured into a new set of culture dish at a density of 5×10^4 cells/ cm^2 as the first passage cells. The first passage cells were again subcultured before they became confluent. And the second passage cells were used for the experiment.

3.4.6.2 Preparation of silk fibroin and silk fibroin/collagen hydrogels

Hydrogels were prepared from a combination of sterile SF solution and oleic acid-poloxamer surfactants (HLB value = 3) with/without collagen solution as in Table 3.3. Then each sample was mixed by a vortex mixer at 2500 rpm for 90 seconds before incubation at 37°C for 30-45 min.

Table 3.3 weight percent in total, weight percent of silk fibroin, collagen, and surfactants, and HLB value of surfactants composed in hydrogel for *in vitro* cell culture

Sample	wt% in total	wt% silk	wt% oleic acid	wt% poloxamer	wt% collagen	HLB of surfactants
SF/HLB3	4.00	3.00	0.93	0.07	0	3
SFc/HLB3	4.05	3.00	0.93	0.07	0.05	3
SFC/HLB3	4.10	3.00	0.93	0.07	0.10	3

3.4.6.3 Viability and proliferation

Before uses, rat's MSC were trypsinized and resuspended in α -MEM to obtain a cell density of 5×10^6 cell/ml. Then 100 μ l of the cell suspension was added and mixed with the vortexed silk fibroin or silk fibroin/collagen solution to reach a final concentration of 5×10^5 cells/ml [55]. A 0.5 ml aliquot of the mixtures was quickly pipetted into each stainless-steel ring placed in 24-well cell culture plates as template for gel setting. All samples were incubated at 37°C, 5% CO₂. After hydrogel formed at approximately 30-45 min, the rings were removed to obtain cylindrical-shaped gels with 12 mm in diameter and 5 mm in thickness. All samples were then cultured at 37°C, 5% CO₂ in 2 ml of growth media containing alpha-modified eagle medium (α -MEM) supplemented with 15% fetal bovine serum (FBS) and 1% penicillin-streptomycin. The medium was refreshed every 2 days.

The number of cells was analyzed by the fluorometric quantification of cellular DNA (as in section 3.4.6.4 a) [74] at 6-h, 1-day, 3-day, 5-day, 7-day, 10-day, and 14-day time.

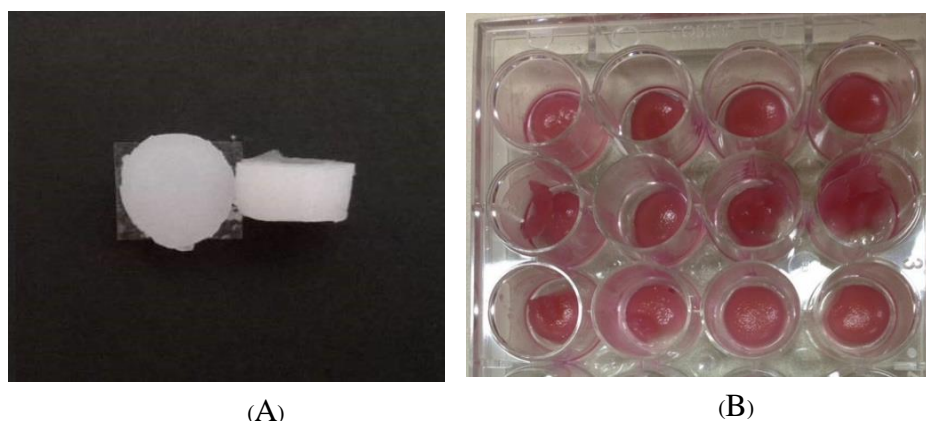


Figure 3.6 Hydrogel sample for *in vitro* cell culture (A) Before culture, (B) During culture

3.4.6.4 Osteogenic differentiation

Rat's MSCs (1,000,000 cells/ml) were stimulated to induced the osteogenic differentiation by culturing in α -MEM supplemented with 10% fetal bovine serum (FBS), 1% penicillin/streptomycin, 50 μ g/ml L-ascorbic acid, 10^{-8} M dexamethasone, and 10^{-2} M β -glycerophosphate then incubate at 37°C , 5% CO_2 . The medium was changed twice a week [74]. The osteogenic differentiation of MSC was determined by DNA assay, ALP activity assay, and calcium assay at 3-day, 1-week, 2-week, 3-week, 4-week, and 6-week time.

a) DNA assay

The hydrogel was minced and added with 1 ml sodium dodecyl sulfate lysis buffer (SDS) and incubated at 37°C , 5% CO_2 for 1 hour to break cell membrane. The obtained cell lysates were then centrifuged to separate supernatant. One hundred μ l of supernatant was pipetted into 96-well black plate, then Hoechst 33258 reagent (20 μ l Hoechst solution + 19 ml DI + 1 ml SSC) were added. The fluorescent intensity of the solution at 355 nm (Excitation) and 460 nm (Emission) were measured immediately using fluorescent microplate reader comparing to standard graph of cell numbers.

b) *Alkaline phosphatase (ALP) activity assay*

The minced hydrogel was added with 1 ml of SDS and incubated at 37°C, 5% CO₂ for 1 hour to break cell membrane, then pipetted 20 µl of samples into 96 well-plate. The cell lysates were added with 100 µl p-nitrophenyl phosphate into each well, then incubated at 37°C, 5% CO₂ for 15 min. The reaction was stopped by 80 µl of 0.02 N NaOH. P- nitrophenol, the product of hydrolysis of p-nitrophenol phosphate catalyzed by ALP enzyme, with an absorbance of yellow light at 405 nm was analyzed with micro plate reader [75].

c) *Calcium assay*

The minced hydrogel was added with 1 ml SDS and incubated at 37°C, 5% CO₂ for 1 hour to break cell membrane, then pipetted 100 µl of samples into 48-well plate. The cell lysates were added with 100 ml of 1 M HCl and incubated at 37°C, 5% CO₂ for 4 h to extract calcium, then pipette 10 µl of cell lysates to 48-well plate. One milliliter of 0.88 M ethanolamine buffer and 100 µl of 0.63 M O-cresolphthalein complex substrate (OCPC) were mixed together and added into each wells of plate. The reaction between OCPC and calcium yielded Calcium-O-cresolphthalein complex with an absorbance of purple light at 570 nm using micro plate reader [74].

3.4.7 *In vivo* osteogenesis in critical size bone defect induced by in situ-forming silk fibroin/collagen hydrogel

3.4.7.1 Preparation of Wistar rats

Thirty female Wistar rats (2 months old) were obtained from Animal research center, Mahidol University, Thailand. The animal use protocol was approved by the ethical committee of animal care and use protocol of Chulalongkorn University (Approval number 06/2560) (Appendix A). Animals were divided into 5 groups including 1 control group and 4 experiment groups (n=6 in each group). Four experiment groups included 1) Thai silk fibroin with collagen hydrogel (SF gel) group, 2) Thai silk fibroin with collagen hydrogel with PRP (SF gel + PRP) group, 3) Thai silk fibroin with collagen hydrogel with rat's MSC (SF gel + MSC) group,

and 4) Thai silk fibroin with collagen hydrogel with rat's MSC and PRP (SF gel + MSC + PRP) group.

3.4.7.2 Preparation of in situ-forming silk fibroin with collagen hydrogel \pm rat's MSC \pm PRP

a) *In situ-forming SF gel*

SFC/HLB3 hydrogel according to Table 3.3 was prepared and vortexed at 2500 rpm for 90 seconds. Then 200 ml of the vortexed solution was stored in an insulin syringe before injection into the bone defect.

b) *In situ-forming SF gel + PRP*

Platelet-rich plasma (PRP, anonymous male human donor through the National Blood Center, Thai Red Cross Society) was added at a concentration of 50 μ l/ml of vortexed solution of SFC/HLB3 hydrogel. Then 200 ml of the mixture was stored in an insulin syringe before injection into the bone defect.

c) *In situ-forming SF gel + MSC*

Rat's MSC were isolated and cultured according to 3.4.5.1. The second passage cells were used to obtain cell suspension with a density of 5×10^6 cell/ml. One hundred microliter of cell suspension was added and mixed with vortexed solution of SFC/HLB3 hydrogel to reach a final concentration of 5×10^5 cells/ml. Then 200 ml of the mixture was stored in an insulin syringe before injection into the bone defect.

d) *In situ-forming SF gel + MSC + PRP*

Rat's MSC from 3.4.7.2 c) and PRP from 3.4.7.2 b) were added to the vortexed solution of SFC/HLB3 hydrogel at a concentration of 5×10^5 cells/ml and 50 μ l/ml respectively. Then 200 ml of the mixture was stored in an insulin syringe before injection into the bone defect.

3.4.7.3 Surgical procedure

The rat was given 0.01 ml morphine (5 mg/kg) and 0.002 ml enrofloxacin (5 mg/kg). The induction of anesthesia was performed in an induction chamber with isoflurane 1-3% in oxygen, then anesthesia was maintained using a mask. (Figure 3.7) The rat's left forearm was shaved from wrist to elbow and the skin was disinfected with alcohol and povidone iodine. Surgery was performed using aseptic technique. The rat's ulnar

bone was approached from the caudolateral site of the forearm. Skin incision, 1-cm length, was made and subcutaneous tissue dissection was performed. Forearm muscles were separated to expose the ulnar bone. The 6-mm defect was created at the midshaft level with a mini-oscillating saw. (Figure 3.8) Radiograph in anteroposterior and lateral views was used to confirm size and location of bone defect.



Figure 3.7 Anesthesia of Wistar rat: Induction chamber (left), Under mask (right)



Figure 3.8 Creation of critical size defect in the ulnar bone

In control group, the bone defect was left without filling anything inside before layer-by layer wound closure.

In SF gel group, the bone defect was filled by the vortexed solution of SFC/HLB3 hydrogel (3.4.7.2 a) through 18G needle. In situ-formation of the hydrogel was observed, then wound closure was performed layer-by-layer.

In SF gel + PRP group, the bone defect was filled by the vortexed solution of SFC/HLB3 hydrogel added with PRP (3.4.7.2 b) through 18G needle. In situ-formation of the hydrogel was observed, then wound closure was performed layer-by-layer.

In SF gel + MSC group, the bone defect was filled by the vortexed solution of SFC/HLB3 hydrogel added with rat's MSC cell suspension (3.4.7.2 c) through 18G needle. In situ-formation of the hydrogel was observed, then wound closure was performed layer-by-layer.

In SF gel + MSC + PRP group, the bone defect was filled by the vortexed solution of SFC/HLB3 hydrogel added with PRP and rat's MSC cell suspension (3.4.7.2 d) through 18G needle. In situ-formation of the hydrogel was observed, then wound closure was performed layer-by-layer.



Figure 3.9 Injection of in situ-forming hydrogel into the bone defect

After the operation, the rats were given 0.002 ml of enrofloxacin (5 mg/kg) every 12 hours for 5 days and 0.01 ml of morphine (5 mg/kg) at 1, 6, and 24-h time, then once a day for 3 days.

3.4.7.4 Evaluation of *in vivo* bone formation

a) *Plain radiograph*

Plain radiograph of the left forearm in anteroposterior view and lateral view was performed in all animals at 4, 8, and 12 weeks after the operation. (Figure 3.10) The radiograph was performed under following settings : energy 60 kV, electrical current 30 MA, exposure time 0.1 sec, length from radiation source to specimen 10 cm, and x-ray window

100 cm². New bone formation and mineralization at the bone defect was evaluated.



Figure 3.10 Positions of Wistar rat during x-ray : Lateral view (left), Anteroposterior view (right)

b) *Micro-computed tomography (micro-CT)*

Three rats from each group were euthanized with 70% CO₂ at 4 weeks and the remaining 3 rats from each group were euthanized at 12 weeks after surgery. Then, the left forearms were taken out and dissected before being examined with micro-CT scanning machine. Each specimen was held with a 20-mm diameter × 75-mm height holder. Bone defect was scanned in high-resolution mode (energy 70 kV, 114 μA, 8 W, voxel size 15 μm, slice thickness 15 μm, and integration time 300 ms). Bone volume/total volume (BV/TV), trabecular thickness (Tb.Th), trabecular number (Tb.N), and trabecular spacing (Tb.Sp) of new bone formation were evaluated.

c) *Histology*

Tissue from bone defect from 3 rats in each group euthanized at 4 and 12 weeks after surgery were fixed in 10% neutral buffered formalin and embedded in paraffin. Specimens were sectioned and stained with Hematoxylin-Eosin (H&E), Alizarin Red S, and Masson Trichrome staining. Inflammatory reaction, new bone matrix and vessel formation were evaluated.

3.4.8 Statistical analysis

All experiments were done in triplicated. The results were reported as mean \pm SD. Comparison among hydrogels was analyzed using one-way ANOVA followed by post-hoc LSD test. The level of significance was set at $P < 0.05$.



CHAPTER 4

RESULTS AND DISCUSSION

4.1 Sterilization of SF solution

4.1.1 Autoclaving

Every concentration of SF solution transformed to gel after autoclaving. The turbidity and viscosity of gel increased with higher concentration of SF.

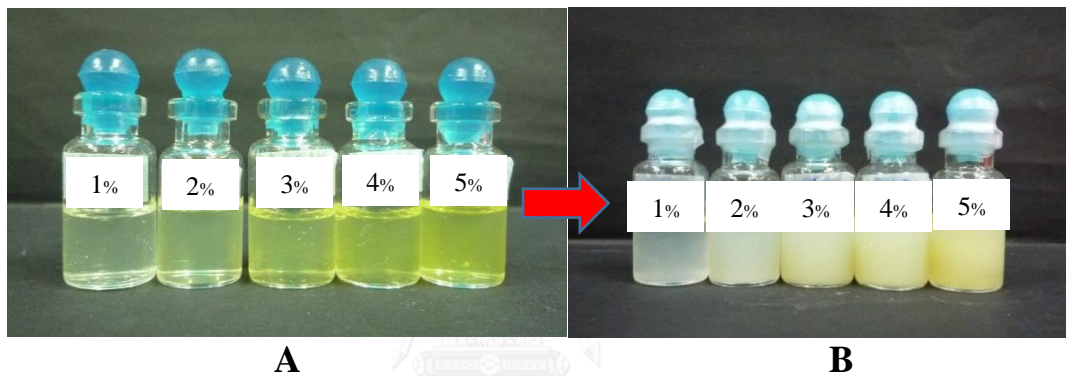


Figure 4.1 Sterilization of 1-5 wt% SF solution by autoclaving. (A) SF solution before autoclaving, (B) SF solution after autoclaving

4.1.2 Gamma radiation

SF solution with 2-5 wt% concentration turned to gel after irradiation. Only 1% SF was still in a liquid condition with altered appearance. The solution became more turbid and slightly more viscous.

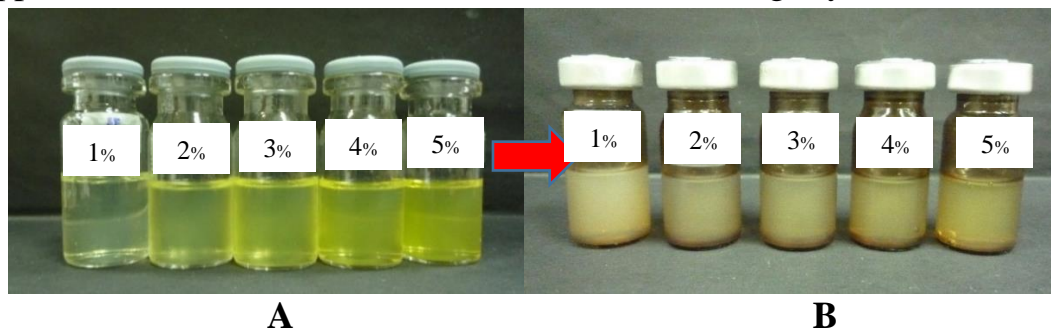


Figure 4.2 Sterilization of 1-5 wt% SF solution by gamma radiation. (A) SF solution before irradiation, (B) SF solution after irradiation

4.1.3 Sterile filtration

Due to the viscosity of the solution, the time used for filtration of 5 mL 1 wt% SF solution was 1 hour. This long period of filtration resulted in occlusion of the filter and gel formation. The resultant filtrate had appearance of mixed solution and white gel strips as in Figure 4.3.



Figure 4.3 Sterilization of 1 wt% SF solution by sterile filtration. The appearance of resultant filtrate demonstrated mixed solution and white gel strips

Among available sterilization methods, autoclaving, gamma radiation, and sterile filtration were chosen for sterilization of SF solution we prepared. We found that none of these methods can be used due to premature gelation of the solution. Although 1 wt% SF was still in a liquid condition after gamma radiation, it is too diluted to be developed further to be the desired hydrogel scaffold. The results we found are not corresponded with previous studies [53, 76, 77] which those methods could be used for sterilization. The results found in this study are possibly explained with the difference in strain with dissimilarity of structural properties between foreign and Thai silk. Nevertheless, it was reported in the literature that gamma radiation is capable of accelerating the sol-gel transition time of SF solution, and steam sterilization used for processing SF film increases beta-sheet contents of the film [78, 79]. Increase in temperature and humidity with autoclaving leads to structural transition of silk fibroin from random coil to beta-sheet and gamma irradiation can induce crosslinking

of silk fibroin, while sterile filtration through small pore size creates shearing force which accelerate formation of hydrogel network of silk fibroin. Hence, manufacturing under sterile condition is the method of choice in our study to prepare sterile aqueous SF solution to avoid alteration of structures or properties from any post-production sterilization procedures, even though the sterilization of silk fibers with autoclaving before dissolution in LiBr may have some effects on molecular weight of SF protein.

4.2 Sterile production of silk fibroin solution

The sterility was proved with microbiological attribution tests including total plate count and total yeast and molds (Table 4.1). This will be referred as SF solution used for the rest of all experiments in this dissertation.

Table 4.1 Microbiological attribution test results of sterilely produced SF solution

Testing	Result (cfu/ml)	Recommended microbial limit requirements for fluid extracts** (cfu/ml)
Total plate count*	<1	<1x10 ⁴
Total yeast and molds*	<1 est.	<1x10 ³

*Reference Methods, Total plate count (In house method TE-MI- 001 based on FDA BAM, 2001), Total yeast and molds (In house method TE-MI-017 based on AOAC (2016) 997.02)

**United State Pharmacopoeia 36 :<2023>Microbiological Attributes of Nonsterile Nutritional and Dietary Supplements

4.3 Induction of gelation of SF solution

4.3.1 Mechanical stimulation by vortex and homogenization

Table 4.2 Results of 4 wt% SF solution gelation induced by mechanical stimulation

Vortex (2500 rpm)	
1 minutes	turbid but not gel
3 minutes	turbid but not gel
5 minutes	inhomogeneous with partial gelation
Homogenization (6500 rpm)	
30 seconds	massive bubble formation but not gel
60 seconds	massive bubble formation but not gel

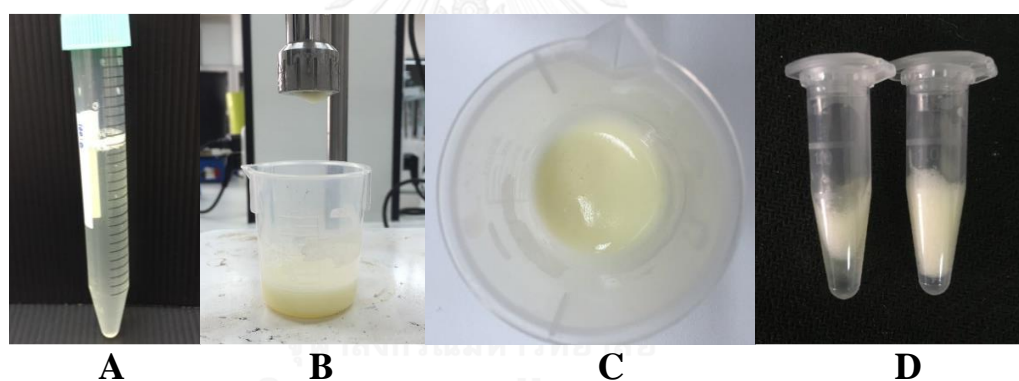


Figure 4.4 Mechanical stimulation for SF gelation induction. (A) 4 wt% SF solution being vortexed for 5 min. The solution became more turbid but no gel formation, (B, C and D) 4 wt% SF solution being homogenized for 60 min. Massive bubble formation occurred but no gel formation.

Shearing forces created by vortex increase the concentration fluctuations in the SF solution, leading to self-assembly into clusters and increased intercluster interaction and result in non-Gaussian stretching (unfolding) of SF molecular domains and formation of macromolecular network caused by increasing hydrophobic domain exposed to water. Gelation time of foreign *Bombyx mori* SF was reported to be decreased with increasing vortex time. However, the time required for formation of hydrogel consisting of permanent physical crosslinks after 7 minutes of

vortex was 1000 minutes which was still a very long time [52]. With 2500 rpm vortex of 4% SF solution for 1-3 minutes, no gelation occurred in 40 minutes. And from 5 minutes of vortex time, the 3% and 4% SF solution became inhomogeneous with gelation occurred partially making it difficult for further handling. Results from our study also indicated that vortex is not an appropriate way for facilitation of SF gelation for our work.

Even though it was reported that shearing force could decrease gelation time of SF solution, the effect was significant in SF solution from *A. pernyi* rather than SF solution from *B. mori*. Twenty-two to forty-eight hours were needed for SF gelation with shearing for 30-90 minutes at 280-480 rpm [80]. Not only the impractical long period of gelation time is needed, but also massive bubble formation within the solution found after shearing with homogenizer probe makes this method not a suitable way for induction of SF hydrogel for our work.

4.3.2 Surfactant-induced gelation

The gelation time of 4 wt% SF solution with and without 0.1 wt% collagen according to Table 3.1 and 3.2 mixed with surfactants made of a combination of oleic acid and poloxamer-188 with different HLB values from 1 to 20 was recorded. In SF/HLB1 and SFC/HLB1 sample, the solution precipitated almost immediately after surfactant addition becoming inhomogeneous gel. The rest of samples formed homogeneous gel in time period correlated to HLB values of surfactant added (Figure 4.5 and Table 4.3). The lower HLB value of surfactant resulted in shorter gelation time. The results indicated the effect of HLB value on gelation time of SF solution which will be discussed later in this chapter.

Table 4.3 Gelation time of 4 wt% SF hydrogels with and without 0.1 wt% collagen induced by oleic acid-poloxamer surfactants with different HLB values at 37°C

SF samples	Gelation time	SF + Collagen samples	Gelation time
SF/HLB1	N/A	SFC/HLB1	N/A
SF/HLB3	30 min	SFC/HLB3	30 min
SF/HLB5	50 min	SFC/HLB5	50 min
SF/HLB10	12 h	SFC/HLB10	12 h
SF/HLB15	24 h	SFC/HLB15	24 h
SF/HLB20	24 h	SFC/HLB20	24 h



Figure 4.5 Appearance of hydrogel of 4 wt% SF induced by oleic acid-poloxamer surfactants

4.4 Physicochemical characterization

4.4.1 Zeta potential of the solution

Zeta potential is the electric potential at the interface between the dispersed particle and the dispersion medium. It is used to indicate the relative surface charge of polymeric particle [81]. Surface charge of the material is the important basic character influential on protein adsorption and cell behavior that eventually affect the material biocompatibility [82, 83].

Zeta potentials of the surfactant mixture of oleic acid and poloxamer-188 with different HLB values were analyzed as shown in Table 4.4. At pH 4.0, 5.5, and 7.5, average surface charge of oleic acid-

poloxamer surfactants between HLB 3-20 showed totally negative charges. The surfactants with HLB 3 showed the most negative charge while the surfactants with HLB 5-20 revealed lower negative charges that were not different between them. Table 4.5 demonstrated the zeta potentials of SF and SF with collagen solutions. SF showed negative charge at pH 5.5, whereas collagen showed positive charge at both pH 5.5 (initial pH) and 7.5 (tissue comparable pH). When mixed with negatively charged surfactant, SF and SF with collagen solution displayed negative charge with added surfactant between HLB 1-20. The SF with collagen solution showed less negative charges compared with SF solution at pH 7.5 but no difference at pH 5.5. This result indicated that the addition of collagen does not alter surface charge of the solution at tissue-resemble pH. The effect of collagen addition, if there is, on properties and biocompatibility of the SF with collagen hydrogel may be resulted from other aspects in bioactivity, not from the surface charge.

Table 4.4 Zeta potentials of oleic acid-poloxamer surfactants with different HLB values at pH 4.0, 5.5, and 7.5 at 37°C (n = 4)

HLB of surfactant	Zeta potential (mV)		
	pH 4.0	pH 5.5	pH 7.5
1 (oleic acid)	-18.95 ± 1.69	-78.65 ± 3.04	-103.25 ± 2.06
3	-21.40 ± 1.35	-45.00 ± 0.96	-47.90 ± 0.94
5	-13.90 ± 0.59	-32.95 ± 0.58	-38.02 ± 0.37
10	-12.55 ± 0.49	-35.95 ± 1.67	-35.78 ± 1.23
15	-12.70 ± 0.62	-30.45 ± 0.48	-38.15 ± 0.62
20	-12.70 ± 0.18	-37.02 ± 1.67	-39.10 ± 1.06
29 (poloxamer)	10.78 ± 3.01	-19.95 ± 1.69	-18.95 ± 1.69

Table 4.5 Zeta potentials of 1 wt% SF with and without 0.1 wt% collagen mixed with oleic acid-poloxamer surfactants with HLB values and 0.05 wt% collagen at pH 5.5 and 7.5 at 37°C (n = 4)

SF samples	Zeta potential		SF + Collagen samples	Zeta potential	
	pH 5.5 (mV)	pH 7.5 (mV)		pH 5.5 (mV)	pH 7.5 (mV)
SF	-9.35 ± 0.96	-10.12 ± 0.43			
			Collagen	+8.56 ± 1.01	+8.87 ± 1.19
SF/HLB1	-11.42 ± 0.62	-14.08 ± 0.49	SFC/HLB1	-6.92 ± 0.47	-13.40 ± 0.65
SF/HLB3	-11.65 ± 0.54	-12.78 ± 0.25	SFC/HLB3	-7.24 ± 0.98	-12.30 ± 0.63
SF/HLB5	-12.82 ± 0.68	-14.50 ± 0.42	SFC/HLB5	-6.84 ± 0.41	-13.68 ± 0.26
SF/HLB10	-12.70 ± 0.32	-13.85 ± 0.61	SFC/HLB10	-7.59 ± 0.70	-14.82 ± 2.35
SF/HLB15	-14.22 ± 0.93	-14.00 ± 0.75	SFC/HLB15	-8.20 ± 0.50	-14.38 ± 0.58
SF/HLB20	-14.05 ± 0.44	-15.12 ± 0.62	SFC/HLB20	-8.89 ± 0.43	-13.32 ± 1.03

4.4.2 Gel fraction of the hydrogel

Gel fraction measured from the percentage of remained insoluble hydrogel parts after incubation in DI water (pH 7) at 37°C for 24 h was studied to determine the structural stability of hydrogel. The gel fractions of SF and SF with collagen hydrogels induced by oleic acid-poloxamer surfactants with HLB between 3-20 exhibited a trend of increased gel fraction in hydrogels induced with lower HLB (more lipophilic) surfactants. Presence of collagen in SF hydrogel had an effect in increased gel fraction when induced by surfactants with HLB 5-10. These results demonstrated that the stability of SF hydrogel decreased with induction by oleic acid-poloxamer surfactants with higher HLB values (more hydrophilicity). Addition of collagen can increase stability of the surfactant-induced SF hydrogel but only when the HLB values of surfactant was between 5-10. At lower HLB value of surfactant (HLB = 3), collagen may not provide additional stability to SF hydrogel that was already stable structurally. While at higher HLB value of surfactants (HLB = 15-20), the effect of hydrophilicity of surfactants may preclude the stabilization effect from collagen addition.

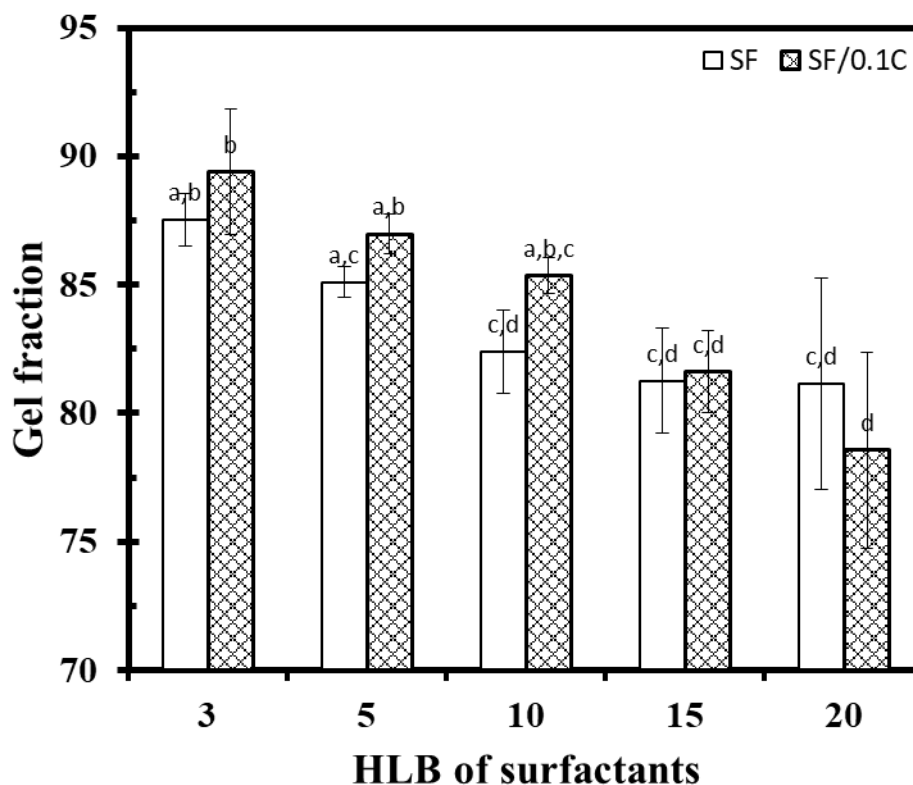


Figure 4.6 Gel fractions of 4 wt% lyophilized SF hydrogels with and without 0.1 wt% collagen induced by oleic acid-ploxamer surfactants with different HLB values after incubation in DI water at 37°C for 24 h. Small letters (a-d) indicate statistical differences at $P < 0.05$ between all samples ($n = 4$).

4.4.3 Water absorption of the hydrogel

The hydrogels revealed 3-12% water absorption capacity. There was a trend observed showing an increase in water absorption capacity of SF with collagen hydrogel induced by surfactants with higher HLB values (more hydrophilicity). There was no difference observed among SF hydrogels and between SF and SF with collagen hydrogels.

The capacity of water to be absorbed into the space between crosslinked networks of hydrogel depends on equilibrium of hydrogel swelling which is affected by polymer properties, crosslinked networks, and porosity of hydrogel. The result found in this study indicated effect of hydrophilicity of surfactants on this swelling equilibrium of the hydrogel

made of SF blended with collagen, which is corresponded with the morphologic findings from SEM images in section 4.4.5 that demonstrated increased pore sizes in SF with collagen hydrogels with higher HLB value of surfactants.

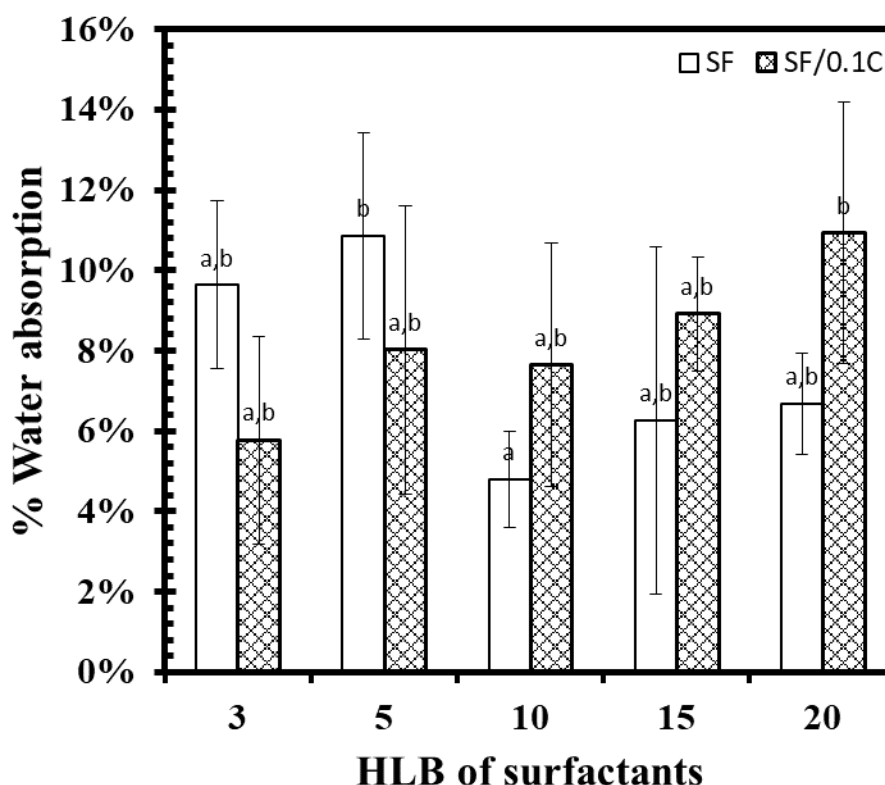


Figure 4.7 Water absorption capacity of 4 wt% SF hydrogels with and without 0.1 wt% collagen induced by oleic acid-poloxamer surfactants with different HLB values after incubation in DI water at 37°C for 24 h. Small letters (a-d) indicate statistical differences at $P < 0.05$ ($n = 4$).

4.4.4 Rheological property of the hydrogel

Behavior of viscoelastic materials that shows properties of both solid and liquid was determined by rheological study of the relationship between force, deformation, and time. For a purely elastic material, the stress and strain are in phase. For a purely viscous material, the stress and strain are out of phase by 90°. For a viscoelastic material, the phase difference between stress and strain is between 0-90°, while the phase angle (δ) at 45° represents the boundary between solid-like and liquid-like behavior. The

solid-like material has $\delta < 45^\circ$ ($\tan \delta < 1$) and the liquid-like material has $\delta > 45^\circ$ ($\tan \delta > 1$) (Figure 4.8). Total material stiffness (G^*) is geometrically divided to elastic contribution component as the storage modulus (G') and viscous contribution component as the loss modulus (G'') (Figure 4.9).

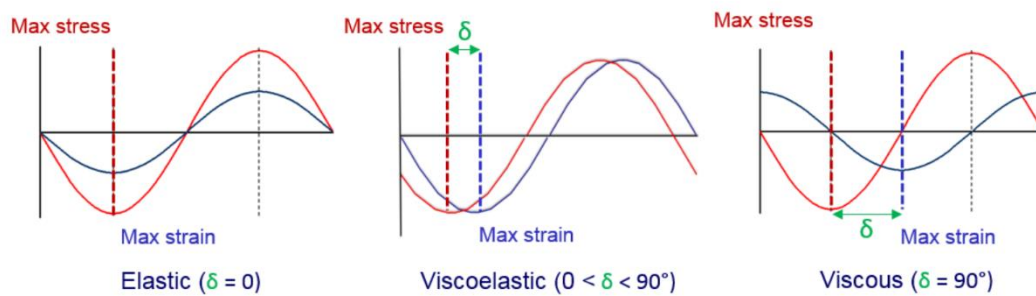


Figure 4.8 Stress and strain wave relationships for a purely elastic (ideal solid), purely viscous (ideal liquid) and a viscoelastic material (<https://cdn.technologynetworks.com/TN/Resources/PDF/WP160620BasicIntroRheology.pdf>)

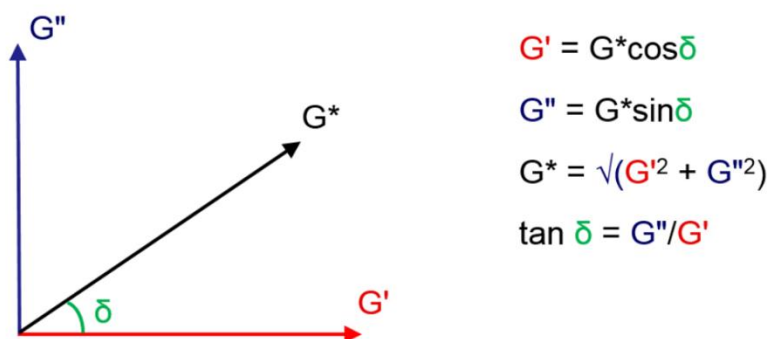


Figure 4.9 Geometric relationship between G^* and its components G' and G'' (<https://cdn.technologynetworks.com/TN/Resources/PDF/WP160620BasicIntroRheology.pdf>)

The amplitude oscillatory test was performed (Figure 4.10). The linear viscoelastic region (LVER), where the stress and strain are proportional and no structural breakdown occurs, was identified. When the yield point was reached, structural breakdown of the material began to occur and the stress and strain are not proportional anymore. The storage modulus (G') became stress or strain dependent. We calculated the ratio of

loss modulus/storage modulus (G''/G' or $\tan \delta$) and used the point where it started to increase as the yield point and the point where it equaled to 1 ($G' = G''$) as the failure point of the hydrogel. All SF and SF with collagen hydrogels induced by surfactants with different HLB values had similar LVER and comparable yield points but different failure patterns. In SF hydrogels, the failure point of gel induced by HLB 3 surfactants was higher than gels induced by surfactants with HLB 5, 10, 15, and 20 which their failure points were very close to each other (Figure 4.11). While in SF with collagen hydrogels, the gel induced by HLB15 surfactants was the first one to fail following by comparable HLB 3, 5, and 20 before the gel induced by HLB10 failed last (Figure 4.12). The direct relationship between HLB value of surfactants and failure points did not demonstrated, reflecting that there was an optimum of HLB value of surfactants for formation of intermolecular bonding to achieve maximum gel strength. The effect of collagen presented in the hydrogel on alteration the modulus was also demonstrated, probably due to cross-linking networks between collagen and SF.

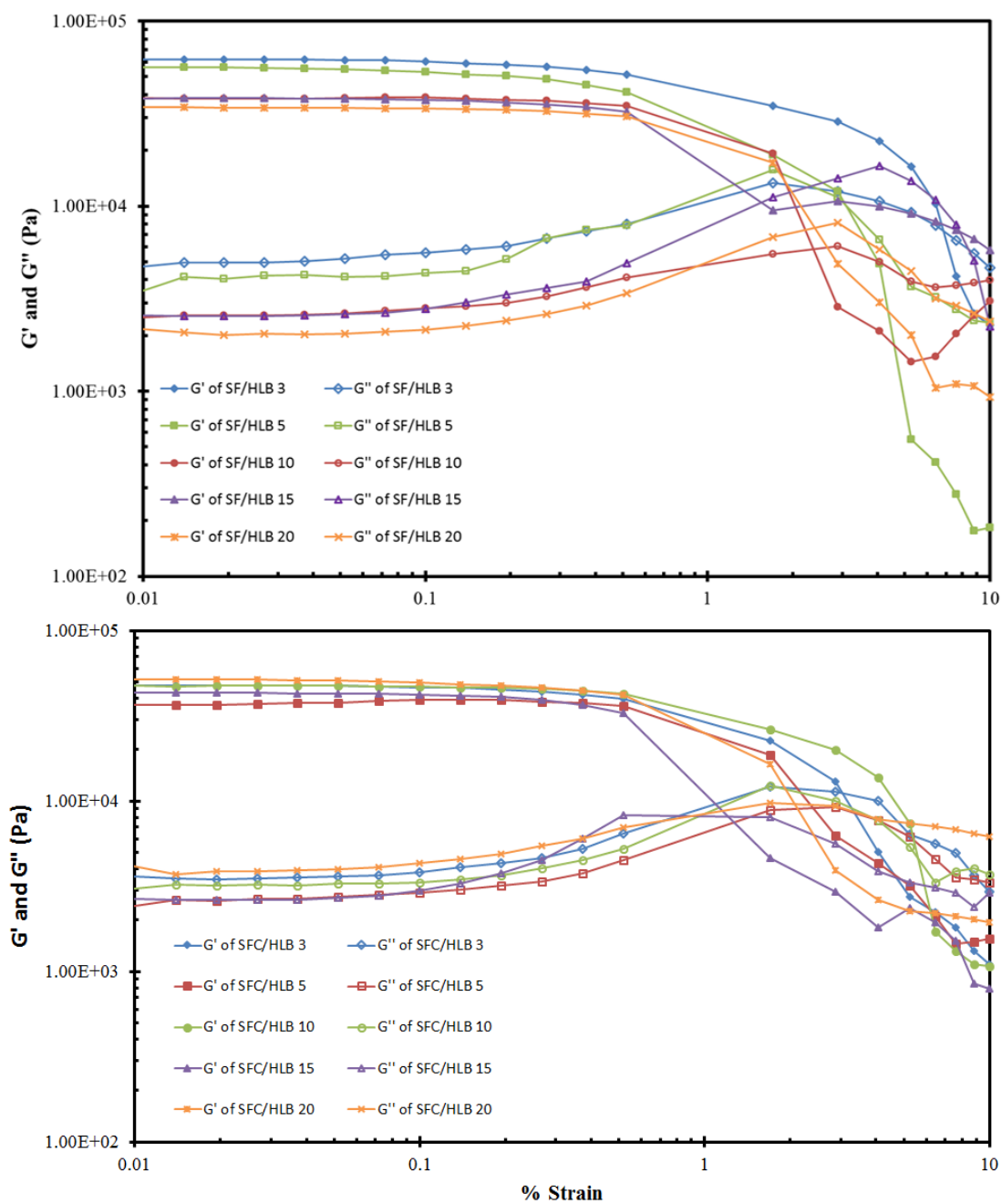


Figure 4.10 Amplitude sweep at 0.01 – 10% strain, 1 Hz of 4 wt% SF hydrogels (top) and SF hydrogels with collagen (bottom)

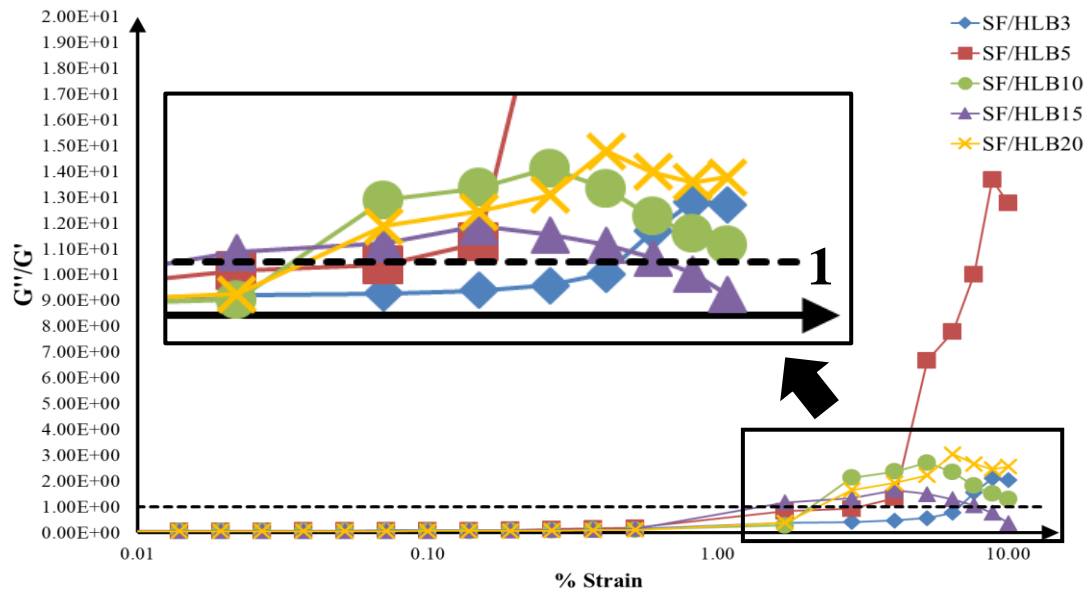


Figure 4.11 The ratio of loss modulus/storage modulus (G''/G') of 4 wt% SF hydrogels without 0.1 wt% collagen induced by oleic acid-poloxamer surfactants with different HLB values

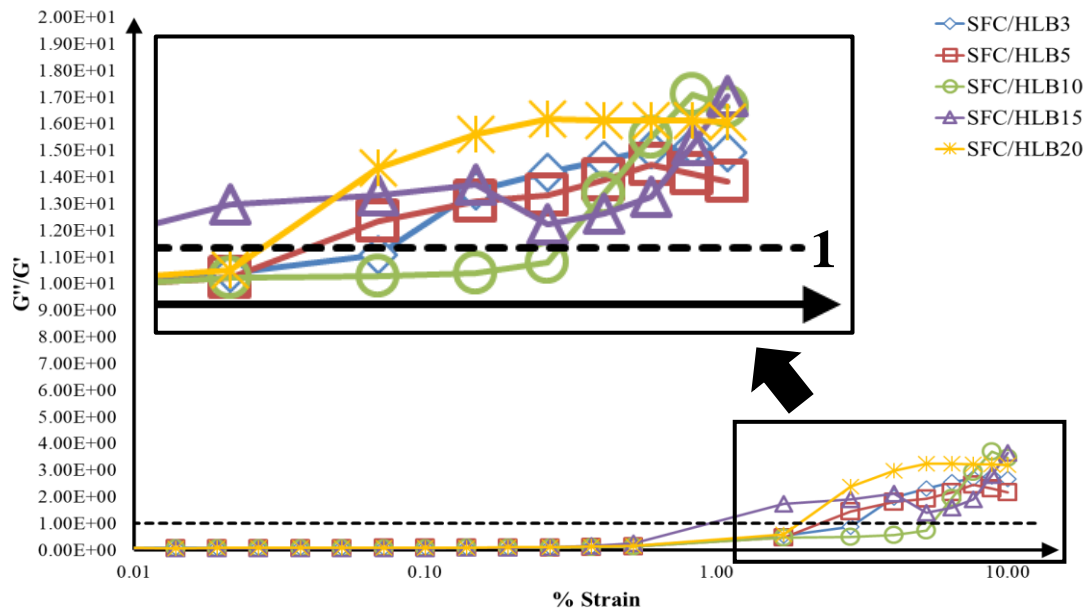


Figure 4.12 The ratio of loss modulus/storage modulus (G''/G') of 4 wt% SF hydrogels with 0.1 wt% collagen induced by oleic acid-poloxamer surfactants with different HLB values

The oscillatory frequency sweep was tested (Figure 4.13). It was found that during 0.1-10 Hz frequency the G' and G'' were parallel and independent of frequency. G'' was lower than G' implying more solid-like

behavior. In gel networks with imperfections, the response of the gel will depend on frequency. Ideal gels have properties of elastic response and independence of frequency [84]. These results showed that the SF and SF with collagen hydrogels induced by surfactants with HLB between 3-20 were ideal gels.

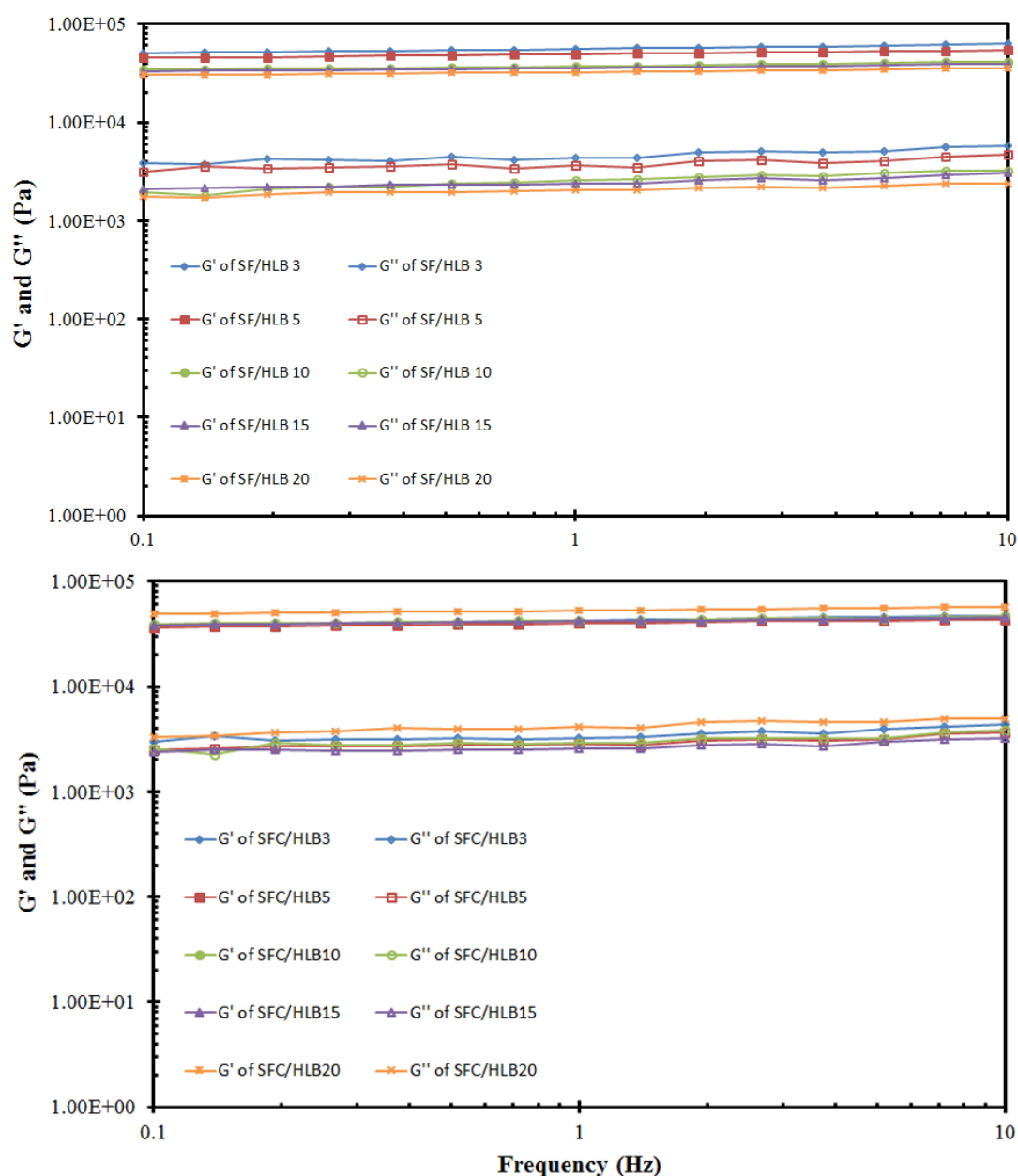
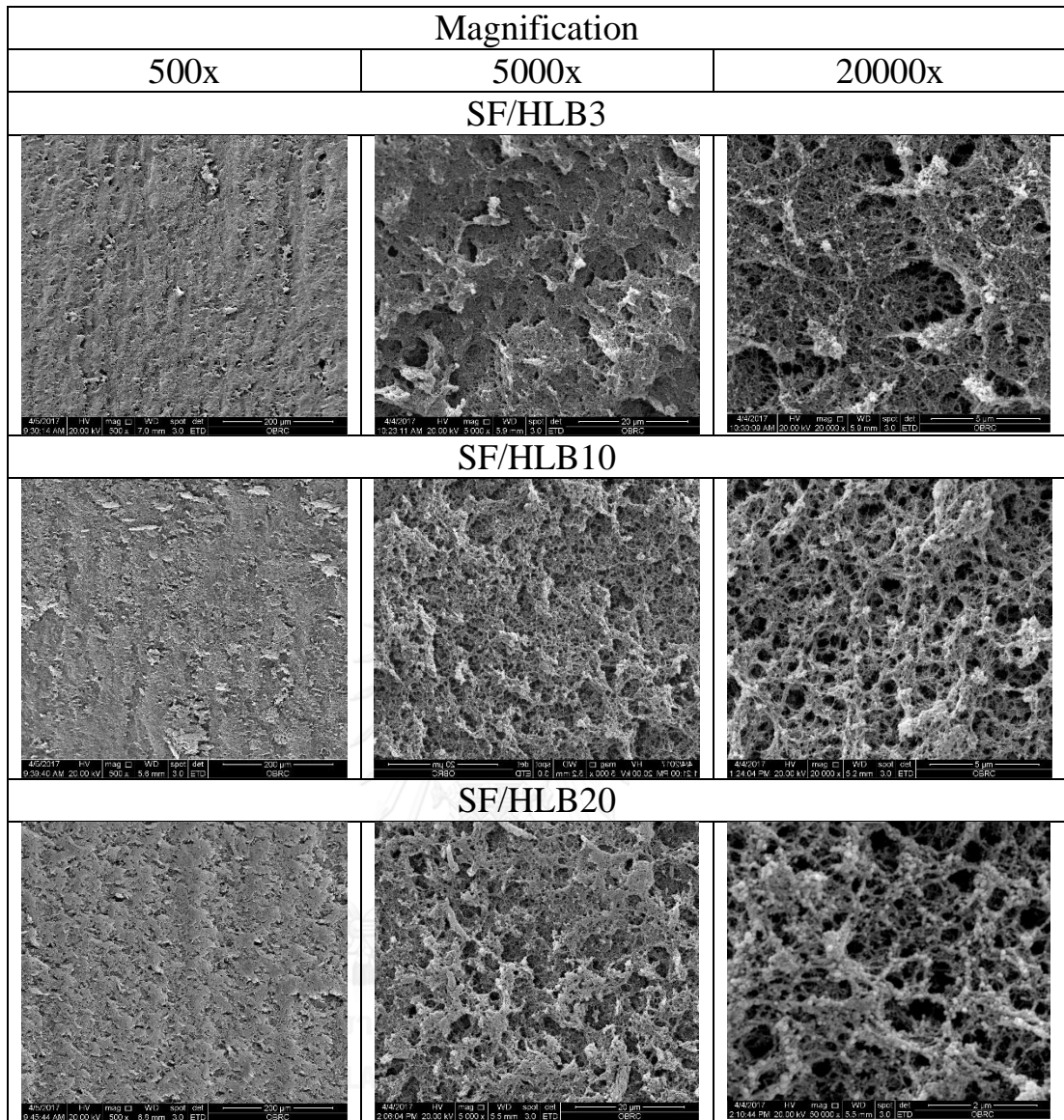


Figure 4.13 Frequency sweep at 1 – 10 Hz, 0.03% stain, 1 Hz of 4 wt% SF hydrogels (top) and SF hydrogels with collagen (bottom)

4.4.5 Morphology of the hydrogel

The morphology of the SF and SF with collagen hydrogels induced by oleic acid-poloxamer surfactants with different HLB values were observed using SEM after critical point drying. The SEM images of hydrogels were shown in Figure 4.14. Typical interconnected microporous morphology was observed in all hydrogels. The pore sizes were ranging from 2-4 μm in SF/HLB 3, SF/HLB 10, and SF/HLB 20, similarly. However, the pore sizes in SF with collagen hydrogels tended to increase with higher HLB value of surfactants used to induce hydrogel formation. The sizes of the pores were 4-6 μm in SFC/HLB 3 and SFC/HLB 10, whereas in SFC/HLB 20 the pore sizes were 8-12 μm . The thicker cross-linking networks were observed with an increase in HLB value of surfactants used to induce hydrogel formation. The SF with collagen hydrogels also exhibited thicker cross-linking networks compared with SF hydrogel induced by surfactants with similar HLB value. In SFC/HLB 20 hydrogel, SEM images revealed large pores with scant interporous connectivity and thick cross-linking networks.

The morphology of the SF hydrogels was reported to be affected by concentration of SF, processing methods, and blended materials [32, 85]. The result from our study indicates effect of HLB value of surfactants and collagen blending on morphology of SF hydrogel. An increase in HLB value of surfactants and addition of collagen resulted in larger pore size with less interporous connectivity and thicker cross-linking networks.



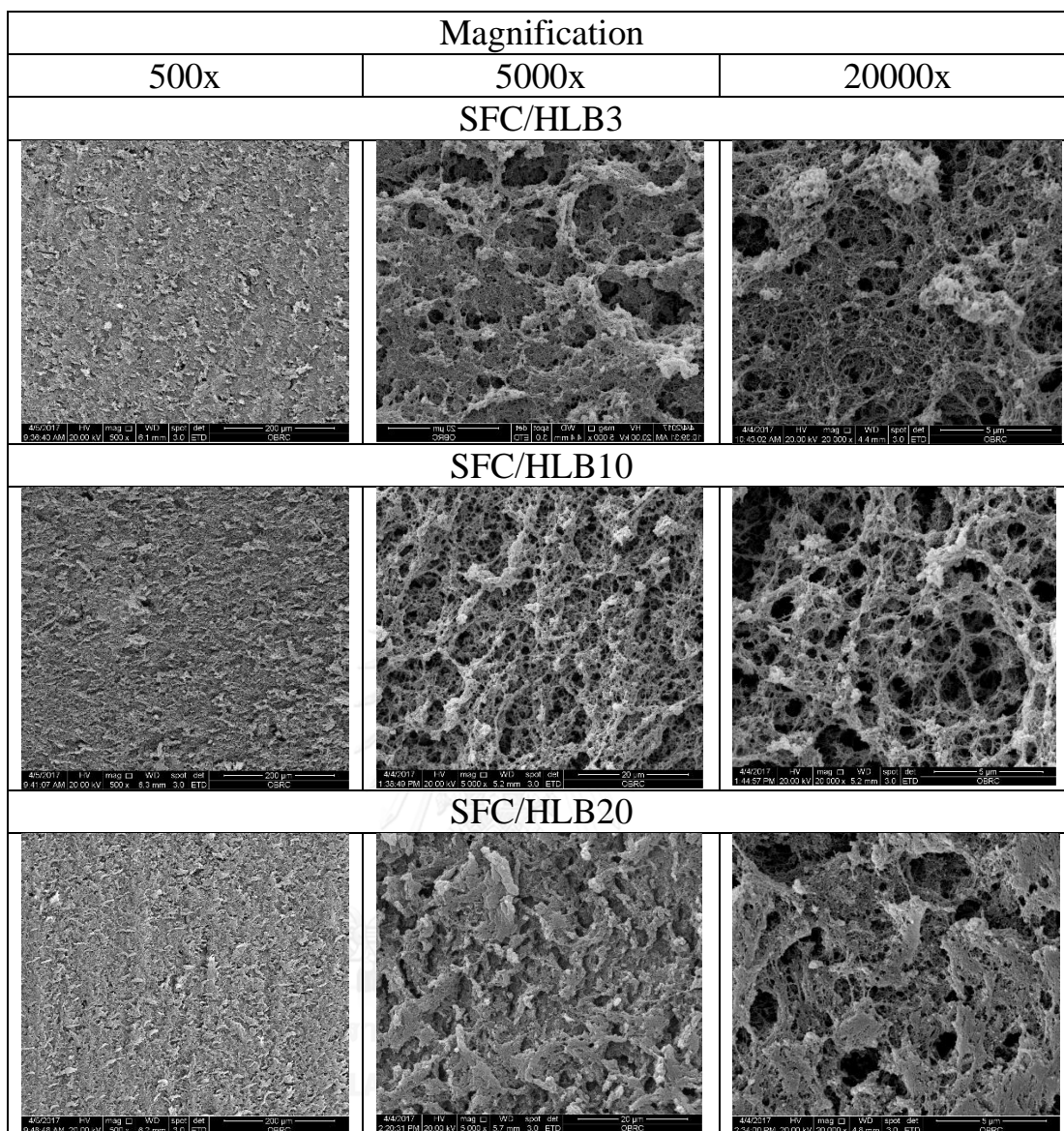


Figure 4.14 SEM images of 4 wt% SF hydrogels with and without 0.1 wt% collagen induced by oleic acid-poloxamer surfactants with HLB 3, 10, and 20

4.4.6 Thermal property of the hydrogel

Thermal properties of the SF and SF with collagen hydrogels were investigated using DSC. DSC curves of the SF and SF with collagen hydrogels were shown in Figure 4.15 and 4.16 respectively. Resulted thermal peaks were recorded and summarized in Table 4.6 and 4.7. All hydrogels showed endothermic peaks at around 100°C indicating dehydration. The SF and SFC hydrogels exhibited exothermic peaks at 225

and 230°C, respectively revealing the heat-induced beta-sheet crystallization, while the hydrogels induced with surfactants did not show this exothermic peak. The absence of this exothermic peaks reflected that the crystallization process of the hydrogels had already achieved its completion. This result is in consistent with the DSC curves finding in the regenerated SF membrane processed by dissolution in N-methyl morpholine N-oxide (MMNO) [86]. The endothermic peaks at 49°C of poloxamer [87, 88] found in SF/HLB 15, SF/HLB 20, SFC/HLB 15, and SFC/HLB 20 revealed the phase separation of poloxamer in hydrogels induced by surfactant with higher HLB values or higher proportion of poloxamer. The thermal decomposition peaks between 296-30°C were demonstrated in all hydrogels with a trend of higher temperature in hydrogels induced with surfactant with higher HLB values. This indicated the effect of HLB value of surfactants on thermal stability of the hydrogels. The different decomposition peaks of various forms of SF were reported. The well-orientated silk fibers exhibited decomposition peak at the temperature more than 300°C while the non-orientated silk materials with beta-sheet crystalline structure and amorphous SF showed their decomposition peaks between 290-295°C and less than 290°C respectively [86]. The double-peak degradation phenomenon was shown in SF and SFC hydrogels denoted the complicated degeneration involving thermal degradation of both alpha-helix and beta-sheet crystals in hydrogels [89]. This result corresponded with the deconvoluted data from FTIR spectra that there were higher percentage of alpha-helix structure in SF and SFC hydrogels than hydrogels induced by surfactants.

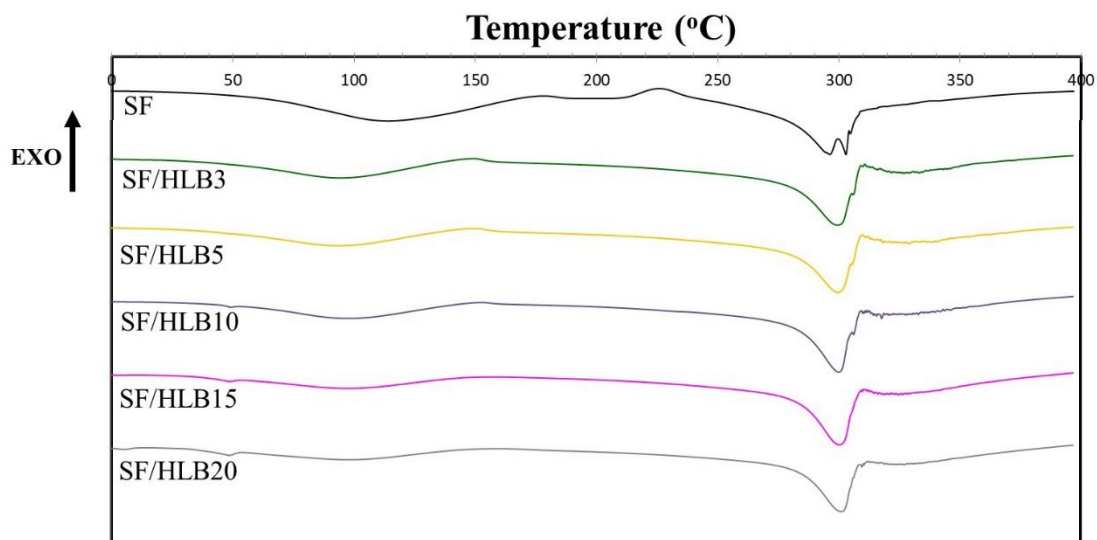


Figure 4.15 DSC curves of 4 wt% SF hydrogels without 0.1 wt% collagen induced by oleic acid-poloxamer surfactants with different HLB values

Table 4.6 Summary of thermal peaks from DSC of 4 wt% SF hydrogels without 0.1 wt% collagen induced by oleic acid-poloxamer surfactants with different HLB values

Samples	Thermal peak (°C)				
	SF	-	113.7	225.8	296.3
SF/HLB3	-	94.8	-	299.7	-
SF/HLB5	-	94	-	300	-
SF/HLB10	-	98.1	-	300.2	-
SF/HLB15	-	98.3	-	300.4	-
SF/HLB20	48.8	98.2	-	301.2	-

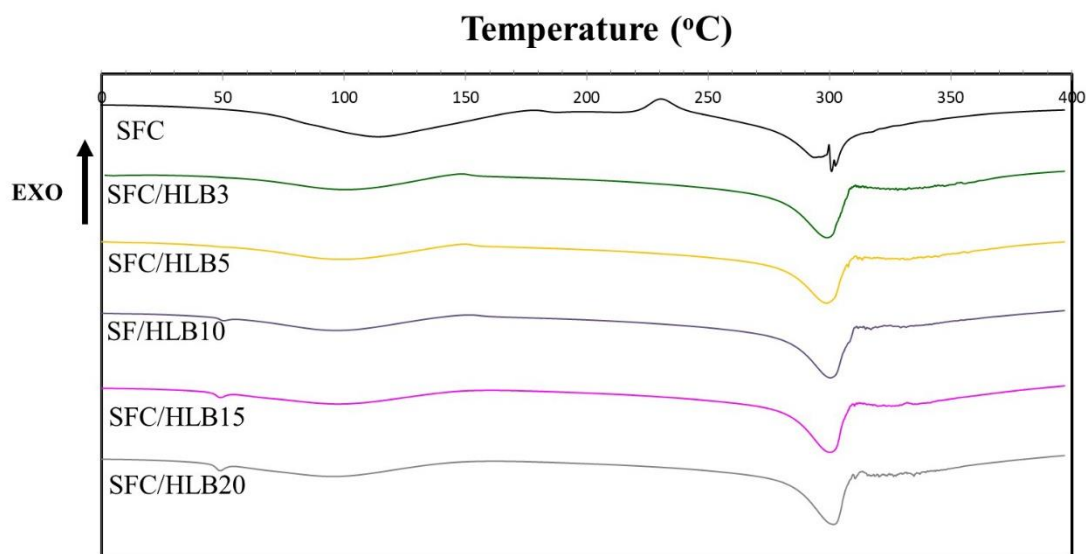


Figure 4.16 DSC curves of 4 wt% SF hydrogels with 0.1 wt% collagen induced by oleic acid-poloxamer surfactants with different HLB values

Table 4.7 Summary of thermal peaks from DSC of 4 wt% SF hydrogels with 0.1 wt% collagen induced by oleic acid-poloxamer surfactants with different HLB values

Samples	Thermal peak (°C)				
	SFC	-	114.4	230.6	-
SFC/HLB3	-	100.8	-	299	-
SFC/HLB5	-	99	-	298.8	-
SFC/HLB10	-	96.9	-	300.3	-
SFC/HLB15	49	97.2	-	300.2	-
SFC/HLB20	48.9	95.7	-	301.8	-

4.4.7 Secondary structure of the hydrogel

For determining the secondary structure of the SF and SF with collagen hydrogels induced by oleic acid-poloxamer surfactants with different HLB values, FTIR was studied. The result of FTIR spectra are shown in Figure 4.17 and 4.18.

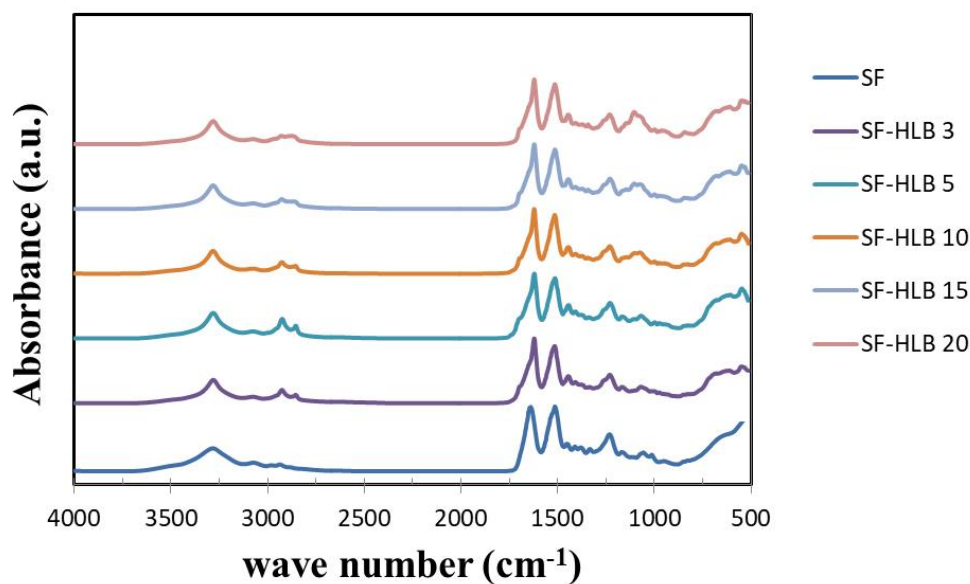


Figure 4.17 FTIR spectra of 4 wt% SF hydrogels induced by oleic acid-poloxamer surfactants with different HLB values

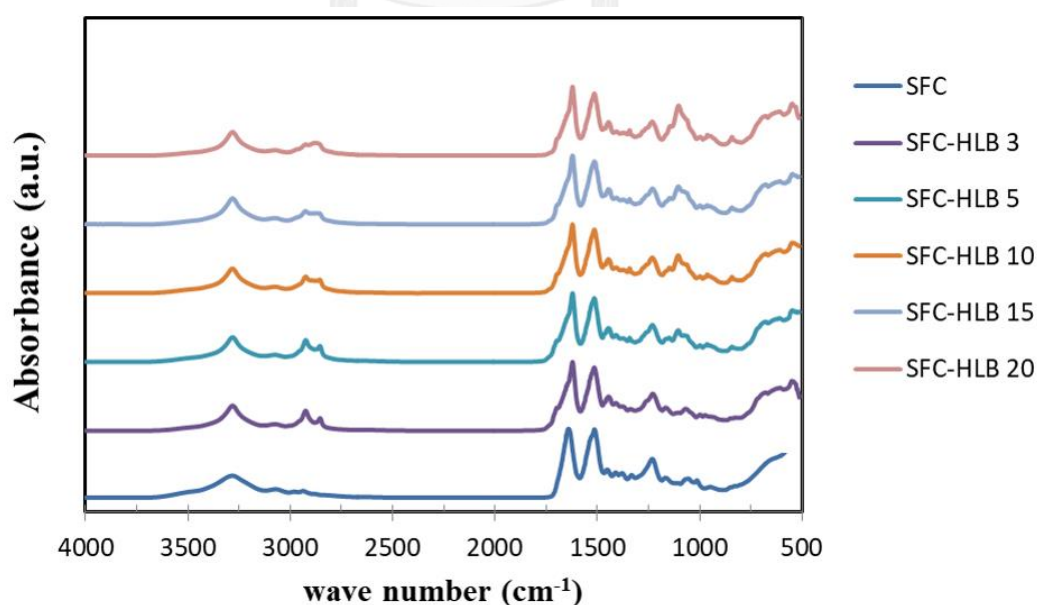


Figure 4.18 FTIR spectra of 4 wt% SF hydrogels with 0.1 wt% collagen induced by oleic acid-poloxamer surfactants with different HLB values

All hydrogels exhibited high intensities in their Amide I (between 1600-1700 cm^{-1}), Amide II (between 1500-1600 cm^{-1}), Amide III (between 1200-1300 cm^{-1}), and O-H stretching region (3282 cm^{-1}) (Table 4.8). SF/HLB 3, SF/HLB 5, SFC/HLB 3, SFC/HLB 5, SF/HLB 10 hydrogels showed the other peak intensity and 2925 cm^{-1} which was corresponded to the peak intensity found in FTIR spectra of oleic acid [90, 91]. Amide I bands were deconvoluted and curve-fitted to quantitatively analyze their secondary structures.

Table 4.8 Summary of peak intensities from FTIR spectra of 4 wt% SF hydrogels with and without 0.1 wt% collagen induced by oleic acid-poloxamer surfactants with different HLB values

Samples	Amide I	Amide II	Amide III		
	C=O stretch	N-H bend C-N stretch	N-H deform C-N stretch	CH ₂ stretch	O-H stretch
SF	1642	1515	1232		3283
SF/HLB3	1622	1516	1231	2926	3282
SF/HLB5	1621	1515	1230	2925	3282
SF/HLB10	1622	1516	1231		3282
SF/HLB15	1622	1515	1231		3282
SF/HLB20	1622	1515	1231		3282
SFC	1641	1515	1232		3283
SFC/HLB3	1622	1515	1230	2925	3282
SFC/HLB5	1622	1515	1232	2925	3282
SFC/HLB10	1622	1515	1232	2925	3283
SFC/HLB15	1622	1515	1232		3282
SFC/HLB20	1622	1515	1232		3282

Figure 4.19 and 4.20 present the relative contents in molecular structures of the SF and SF with collagen hydrogels. Among the SF hydrogels, SF hydrogel formed without induction by surfactant had the lowest amount of beta-sheet structure (about 35%) and the highest amount of random coil structure (31%). While the SF hydrogels induced by oleic acid-poloxamer surfactants had relatively higher percentage of beta-sheet structure (more than 50%) with highest percentage in SF/HLB 15 and

SF/HLB 20 hydrogels (60% approximately). The random coil structure of the SF hydrogels induced by oleic-acid surfactants was found around 18%. In SF with collagen hydrogels, the SFC hydrogel had similar contents of secondary structures as the SF hydrogel. The SFC induced by oleic acid-poloxamer surfactants also showed relatively higher percentage of beta-sheet structure than SFC hydrogel without induction by surfactant. There was no difference of beta-sheet structure content among SFC hydrogels induced by surfactant with different HLB values.

The results found in our study demonstrated the effect of HLB value of the surfactants on the secondary structure of the SF hydrogel. SF hydrogel induced by higher HLB (HLB 15 and 20) of surfactants revealed higher percentage of beta-sheet structure (60%) which is comparable to the maximum percentage of beta-sheet structure of SF scaffolds reported in the literature including the scaffolds prepared by 90-100°C water vapor annealing and 121°C steam autoclaving [89]. The content of beta-sheet structure was varied in SF hydrogels prepared by different methods e.g. 15-16% in SF electrogel, 24-35% in vortex-induced SF hydrogel, and 41-15% in spontaneously-formed SF hydrogel [92]. Native silk monofilament was reported to have beta-sheet structure content around 50% [93]. However, the effect of HLB value of the surfactants was not demonstrated on the SF with collagen hydrogels. The presence of collagen in the hydrogel precluded the effect of HLB value of the surfactants on the crystallinity of SF hydrogel, therefore the maximum crystallinity of the SF hydrogel at 60% could not be achieved.

According to the gelation time in Table 4.3, the SF hydrogels induced by lower HLB surfactants exhibited shorter gelation time. This means that the gelation of SF hydrogels induced by lower HLB surfactant was resulted from interaction between SF and surfactants rather than conformational change to beta-sheet of the hydrogels.

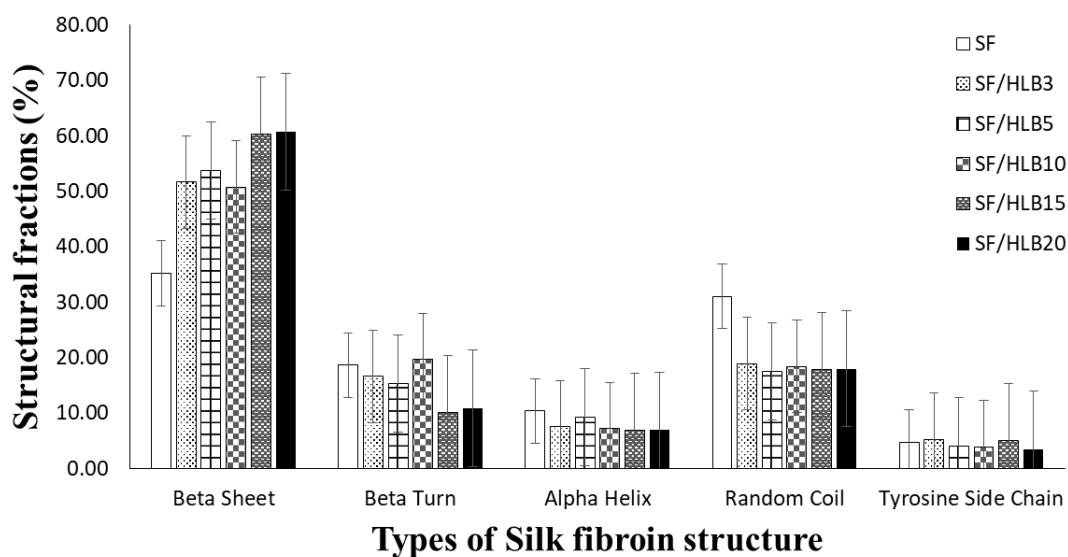


Figure 4.19 Relative contents of secondary structures of 4 wt% SF hydrogels without 0.1 wt% collagen induced by oleic acid-poloxamer surfactants with different HLB values

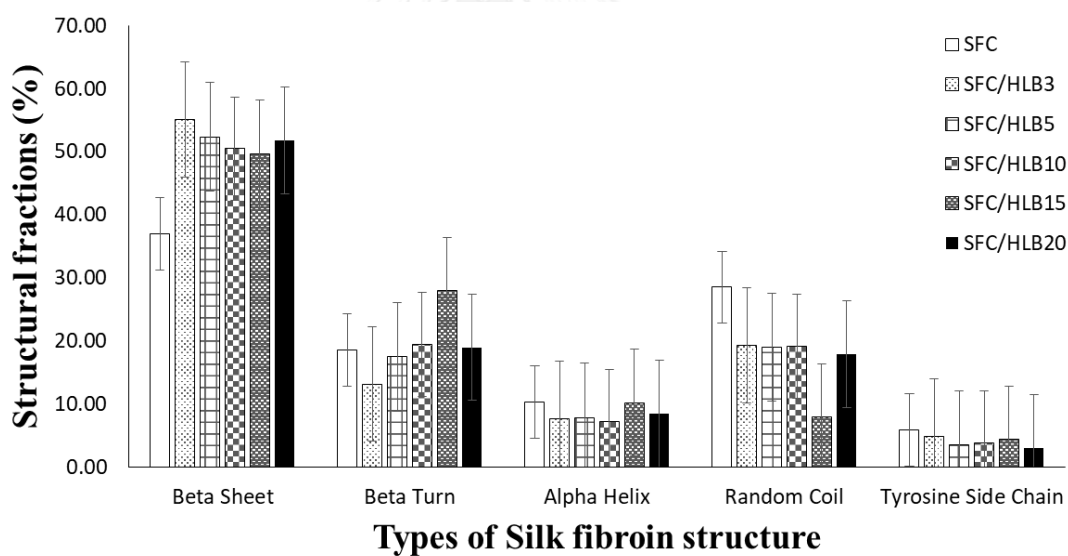


Figure 4.20 Relative contents of secondary structures of 4 wt% SF hydrogels with 0.1 wt% collagen induced by oleic acid-poloxamer surfactants with different HLB values

4.5 *In vitro* cell culture

4.5.1 Viability and proliferation

Rat's MSC proliferated on all hydrogels in the first 24 hours, then cell numbers declined continually before reaching plateau phase at 5-day time-point. After that, the number of cells was maintained during day 7-14 of culture (Figure 4.21). The MSC cultured on SF/0.1C hydrogel exhibited the lowest encapsulation efficiency (Table 4.9) and cell numbers during day 3-5 but when the cultured cells reach plateau phase during day 7-14, there were no statistical significance of cell numbers among all hydrogels. The low encapsulation efficiency with collagen blended in the hydrogel may be resulted from a decrease of surface area for cell attachment due to increased pore size as demonstrated in SEM images.

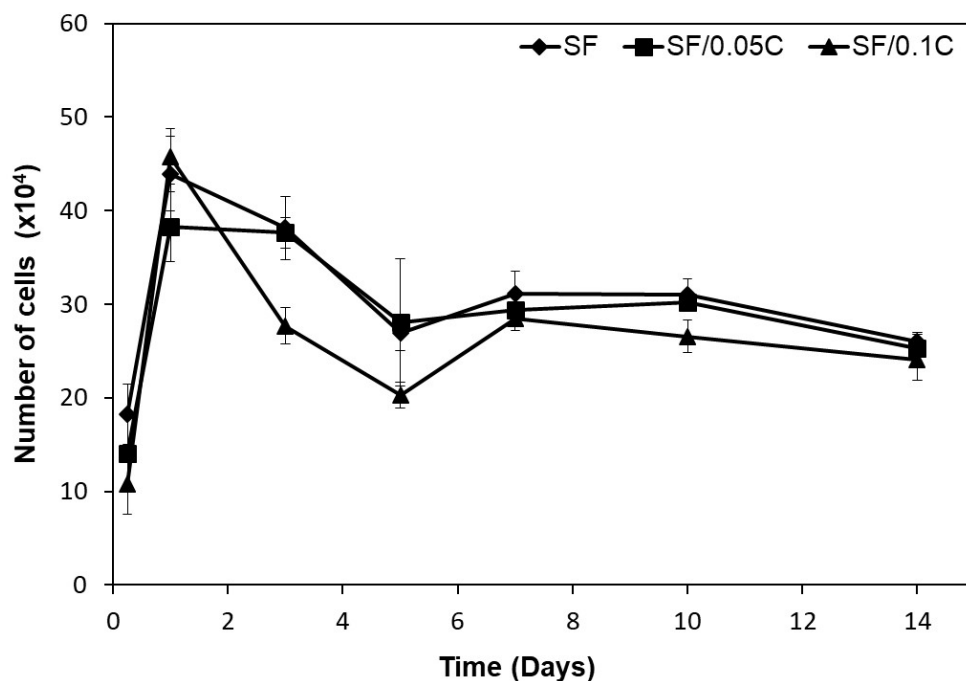


Figure 4.21 Growth kinetics of rat's MSC cultured on SF, SF/0.05C, and SF/0.1C hydrogels for 14 days

Table 4.9 Encapsulation efficiency of rat's MSC cultured on hydrogels at 6 hours. * indicate statistical differences at $P < 0.05$

Hydrogels	Encapsulation efficiency (cells/mm ³)
SF	364.07±64.30 (72.81±12.86%)
SF/0.05C	280.70±1.25 (56.14±0.25%)
SF/0.1C	214.81±64.75* (37.73±9.36%)*



4.5.2 Osteogenic differentiation

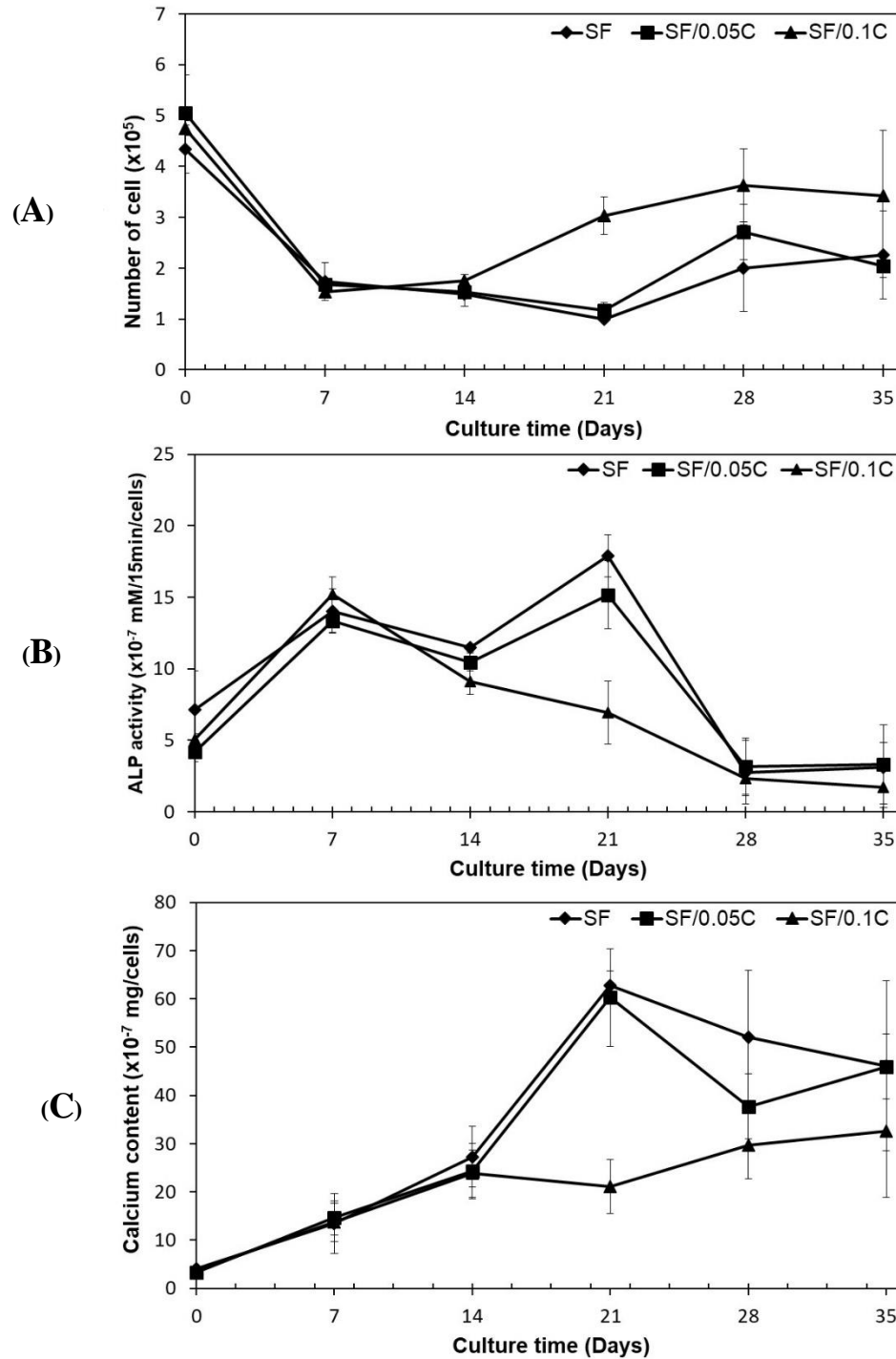


Figure 4.22 DNA assay (A), ALP activity (B), and calcium content (C) of rat's MSC cultured on SF, SF/0.05C, and SF/0.1C hydrogels in osteogenic induction medium for 14 days

At the 21-day time-point, the cells proliferation on SF/0.1C hydrogel was significantly greater than SF hydrogel. There were no significant differences identified between three groups in other time-points (Figure 4.22A).

After one week of culture, ALP was found increased in MSC cultured on all hydrogels. Then ALP level in SF/0.1C hydrogel declined, whereas in SF and SF/0.05C hydrogels the activity continued rising to the highest level at 3-week time-point (Figure 4.22B).

Calcium level in SF and SF/0.05C hydrogels were significantly higher than in SF/0.1C hydrogel at 21-day time-point but no differences in other time-points (Figure 4.22C).

SEM analysis revealed random distribution of polygonal osteoblast-like cells within the pores with deposited calcium in dense matrix of scaffold in all hydrogels. The culture in SF/0.1C hydrogel demonstrated most abundant fibril-like matrix while the SF hydrogel exhibited least matrix amount (Figure 4.23). EDS analysis (Table 4.9 and Figure 4.24) showed the presented amount of calcium level in following order -: SF/0.05C > SF > SF/0.1C. The Ca/P ratios of SF, SF/0.05C, and SF/0.1C were 4.28 ± 2.38 , 2.91 ± 1.09 , and 3.61 ± 1.75 respectively.

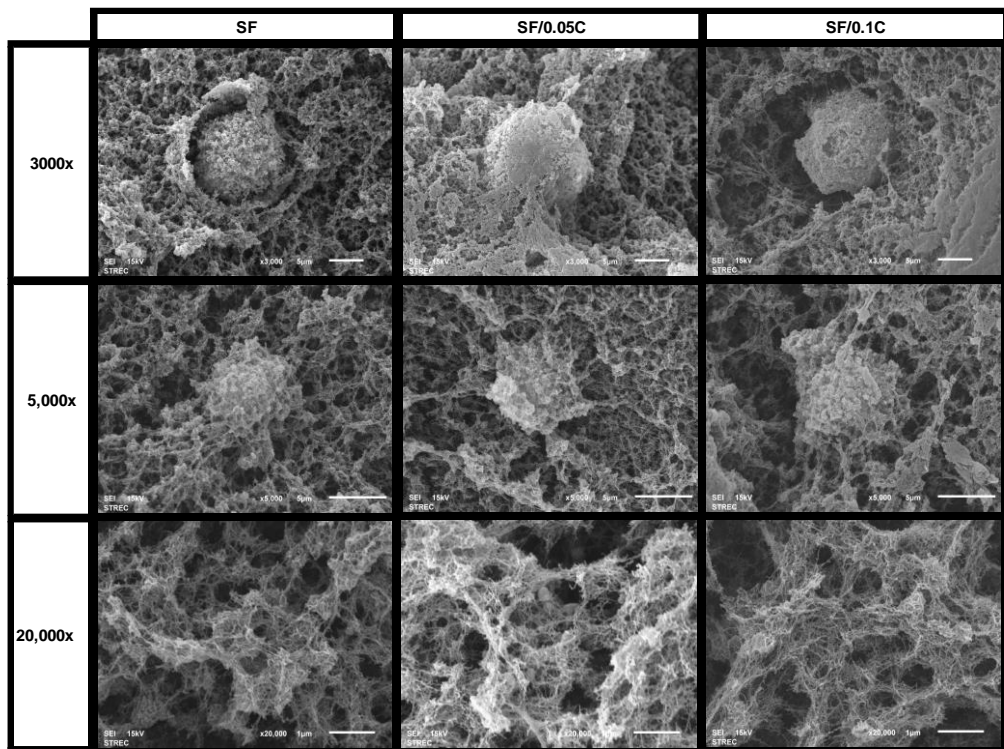


Figure 4.23 SEM images of rat's MSC cultured on SF, SF/0.05C, and SF/0.1C hydrogels under different magnifications

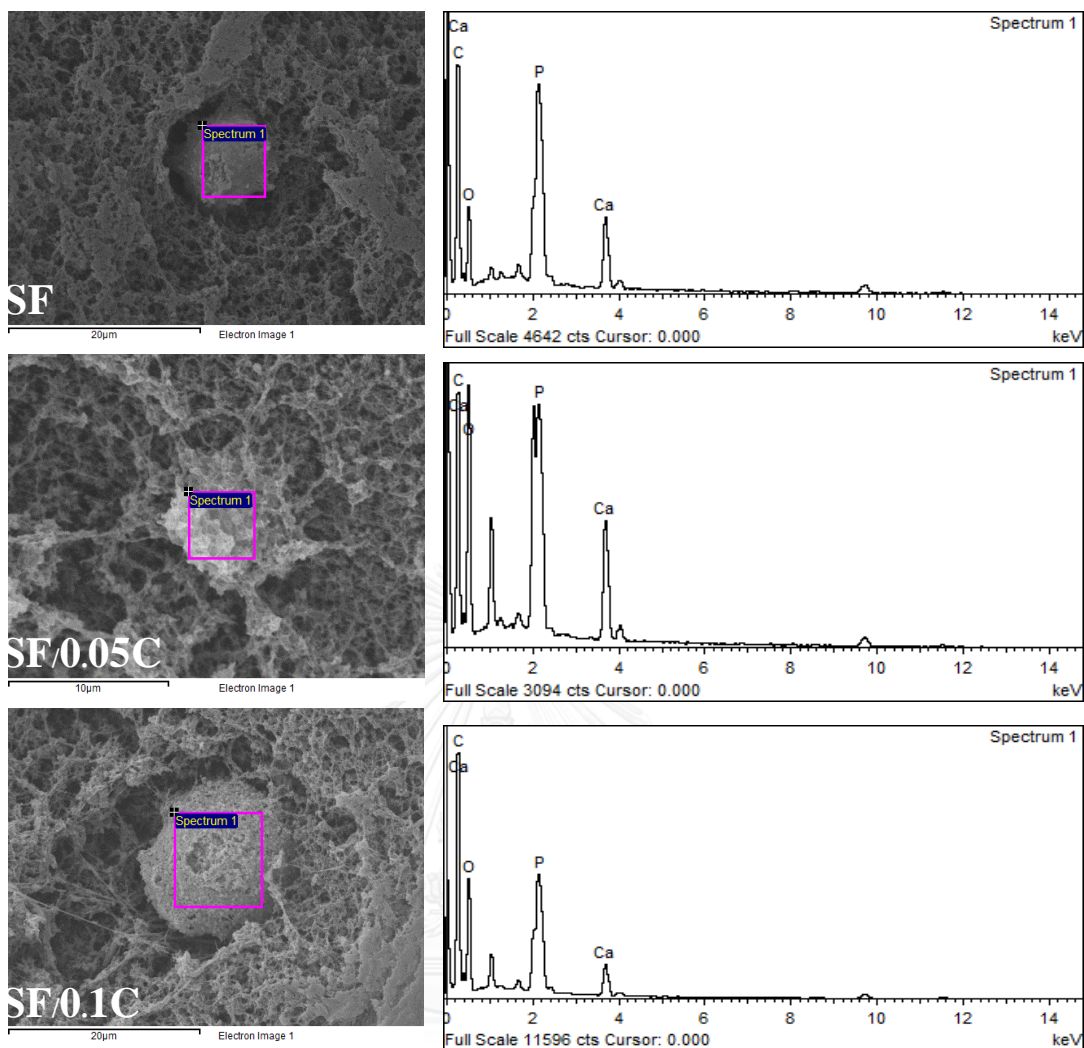


Figure 4.24 Elemental analysis of SF, SF/0.05C, and SF/0.1C hydrogels cultured with rat's MSC by EDS

Table 4.9 Weight percent of C, O, Ca, and P, and Ca/P ratio of SF, SF/0.05C, and SF/0.1C hydrogels cultured with rat's MSC from elemental analysis results (without blank deduction)

Hydrogels	C (wt%)	O (wt%)	Ca (wt%)	P (wt%)	Ca/P
SF	45.03±5.56	37.61±3.75	13.99±1.68	4.03±1.81	4.28±2.38
SF/0.05C	39.36±2.96	33.99±10.56	19.27±7.13	7.38±3.37	2.91±1.09
SF/0.1C	45.92±10.00	38.96±3.11	10.86±6.04	4.27±4.37	3.61±1.75

The viability and proliferation of encapsulated rat's MSC demonstrated in this study verified the biocompatibility of SF and SF

blended with collagen hydrogel scaffolds. Even though the SF with collagen hydrogel seemed to have less encapsulation efficiency of rat's MSC, the growth at the plateau phase of all hydrogels were comparable. Inability to maintain cell viability as cell populations declined during day 1-5 period was observed. Cell numbers then plateaued and maintained until day 14 of culture. This indicated balance between apoptotic cell death and proliferation which is similar to the result found in in vitro culture of human MSC in a chitosan-hyaluronan-based hydrogel reported previously [94]. The cell density at plateau phase was approximately 20-30% of loaded cells. The viability of rat MSCs in SF and SF with collagen hydrogels presented in this study was lower than other hydrogels reported in the literature [95-97]. The contributing factors for loss of viability of rat's MSC in SF and SF with collagen hydrogels may include cell damage from surfactants, limited cell distribution in hydrogel, inadequate mass transport, or partial degradation of hydrogel. Cytotoxicity introduced to the system by hydrogel and surfactants is unlikely according to the previous reports in biocompatibility of hydrogel of silk fibroin with collagen and of poloxamer [98].

Regarding the osteogenic differentiation, significantly highest ALP activity and calcium content were detected in rat's MSC cultured on all hydrogels demonstrated their potential to induce osteogenic differentiation of encapsulated rat's MSC in induction medium even with the apparent initial cell loss and the low proliferation. The rat's MSC growth kinetics in the induction medium revealed the same characters as in the growth medium. The cell numbers decreased in the first week before maintaining their level in the second week. From the third week, rat's MSC in SF/0.1C proliferated greater than in SF and SF/0.05C hydrogels. On the other hand, SF/0.1C showed less ALP activity and calcium content, indicating less osteogenic differentiation. According to these results, SF/0.1C appeared to express promotional effect more on proliferation rather than differentiation compared with SF and SF/0.05C hydrogels. This finding does not support the postulation of enhanced biomineralization with combined SF and collagen in hydrogel. We think that, in blended SF and collagen hydrogels, not only the biological activity of collagen that resulted in varied expression of osteogenic differentiation of each hydrogel, but

physicochemical properties of the hydrogels e.g. density, stiffness, hydrophobicity, gel stability, and water absorption, that were altered due to addition of collagen, must also be taken into account.

Comparable distribution of osteoblast-like cells within the pores of scaffold was observed from SEM analysis among each hydrogel groups. However, greater amount of matrix was noted in SF hydrogel supplemented with collagen. This finding indicated beneficial effect of collagen in matrix formation induction.

Calcium content analyzed by EDS was highest in SF/0.05C hydrogel, following by SF hydrogel, and lowest in SF/0.1C. This observation appeared to be correlated with the results of ALP activity and calcium assay, which does not meet the expectation of facilitated mineralization in combined SF and collagen hydrogel. Comparing with Ca/P ratio of hydroxyapatite and calcium phosphate (1.67-2.0) [99], the Ca/P ratio found in this study was around 2.9-4.3 suggesting that other forms of calcium compounds presented in the hydrogels during osteogenic stimulation.

4.6 *In vivo* osteogenesis in critical size bone defect induced by in situ-forming SF with collagen hydrogel

4.6.1 Gross observation

The injection of all hydrogels into the segmental bone defect through 18G needle performed immediately after vortex mixing was convenient. Within 20 minutes, the injected pre-gelled solution turned into soft white gel steadily contained in the bone defect with no leakage (Figure 4.25). Soft tissue edema was generally observed during the first week after the operation. No wound infections occurred in any rats. All animals were in good health during the time of experiment.



Figure 4.25 In situ gelling of the hydrogel injected into the segmental bone defect of ulnar bone of Wistar rat.

4.6.2 Plain radiograph

The plain radiographs taken immediately after the operation confirmed created 6-mm segmental defect in the diaphysis of the ulnar bone. The injected hydrogel was radiolucent. In control group, the bone defect showed no signs of bone formation in radiographs obtained at any time points. Whereas in the other groups, there was radiopaque shadow detected in the bone defect at 8 weeks and the density was higher at 12 weeks postoperatively, however, the bone defect was not fully bridged (Figure 4.26). There was no obvious difference among the four experiment groups.



Figure 4.26 Plain radiographic images obtained at 12 weeks. (A) Control group showed no signs of bone regeneration. (B) SF gel + MSC + PRP group showed radiopaque shadow (black arrow) with focal calcification (open arrow) in the bone defect.

4.6.3 Micro CT imaging

Micro-CT analysis revealed bone regeneration within the defect site in four experiment groups with hydrogel injection but only minor bone formation was seen in the control group (Figure 4.27). Nevertheless, full defect bridging was not reached in all groups. The morphometric parameters are shown in Table 4.10. No significant differences in any outcomes among groups were detected at both at 4 and 12 weeks. However, there was a superior tendency in bone volume density (bone volume/tissue volume, BV/TV) and trabecular thickness (Tb.Th) in four experiment groups with hydrogel injection compared with the control group.

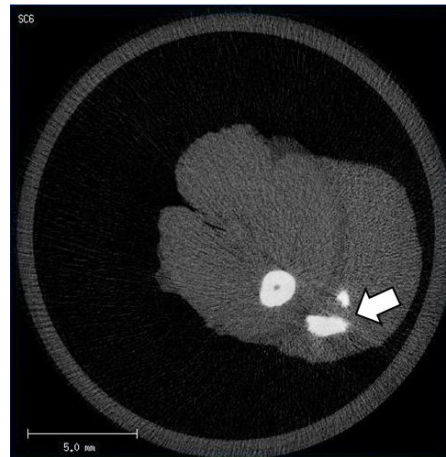


Figure 4.27 Image in axial view from micro-CT scan of SF gel + MSC group at 12 weeks revealed new bone formation (open arrow) in the ulnar bone defect.

Table 4.10 Morphometric parameters on newly formed bone in the segmental bone defect at 4 and 12 weeks in control and experiment groups presented as Mean \pm SD.

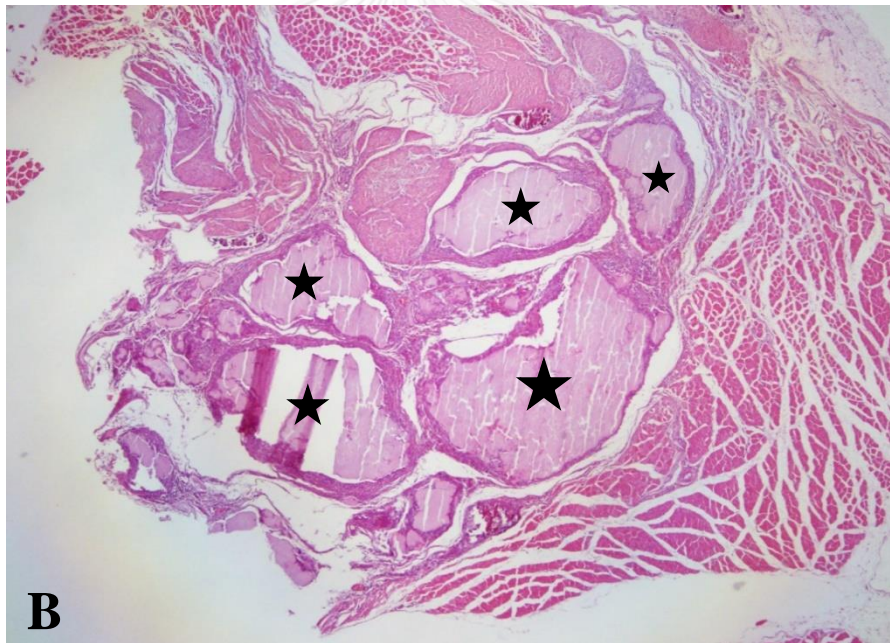
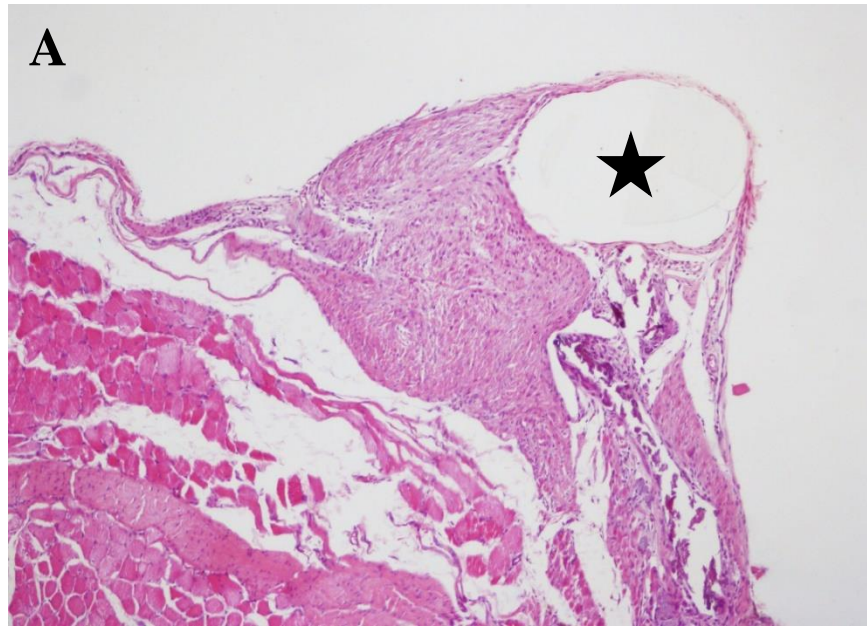
Samples	BV/TV (%)	Tb.Th (μm)	Tb.N (mm^{-1})	Tb.Sp (μm)
4 weeks				
- Control	0.003 \pm 0.002	0.049 \pm 0.003	0.719 \pm 0.120	1.418 \pm 0.245
- SF gel	0.002 \pm 0.002	0.048 \pm 0.012	0.738 \pm 0.178	1.401 \pm 0.342
- SF gel + MSC	0.002 \pm 0.002	0.047 \pm 0.007	0.505 \pm 0.040	1.988 \pm 0.157
- SF gel + PRP	0.001 \pm 0.001	0.054 \pm 0.016	0.615 \pm 0.198	1.719 \pm 0.553
- SF gel + MSC + PRP	0.001 \pm 0.000	0.045 \pm 0.007	0.583 \pm 0.137	1.757 \pm 0.424
12 weeks				
- Control	0.002 \pm 0.002	0.146 \pm 0.121	0.316 \pm 0.153	3.599 \pm 1.710
- SF gel	0.008 \pm 0.004	0.333 \pm 0.085	0.324 \pm 0.092	3.305 \pm 1.092
- SF gel + MSC	0.007 \pm 0.005	0.252 \pm 0.072	0.389 \pm 0.192	2.949 \pm 1.186
- SF gel + PRP	0.009 \pm 0.007	0.193 \pm 0.224	0.534 \pm 0.365	2.526 \pm 1.463
- SF gel + MSC + PRP	0.010 \pm 0.006	0.330 \pm 0.127	0.302 \pm 0.033	3.381 \pm 0.317

BV/TV: bone volume/total volume, Tb.Th: trabecular thickness, Tb.N: trabecular number, Tb.Sp: trabecular spacing

4.6.4 Histological evaluation

At 4 weeks after the operation, the defect area in the control group showed an empty hole with fibrous encapsulation around (Figure 4.28A). No signs of new bone or vessel formation were detected. In the other four experiment groups, the defect areas were filled with gel appeared as irregular shaped eosinophilic material surrounded by inflammatory cells and fibrous capsule (Figure 4.28B). The amounts of inflammatory cells were relatively higher in SF gel + PRP and SF gel + MSC + PRP groups compared with SF gel and SF gel + MSC groups (Figure 4.28C). Formation of new capillaries was noted in all four experiment groups (Figure 4.28D). There was scant new bone formation observed in SF gel and SF gel + MSC groups.

Compared with 4 weeks, the control group still showed no signs of new bone or vessel formation. In the other four experiment groups, the histologic findings showed relatively similar patterns. There was an increase in newly formed bone in the defect area. The fragments of residual nondegraded gel surrounded by fibrosis were noticed adjacent to the area of bone formation but the amount was substantially decreased from the gel observed at 4 weeks. There were little inflammatory cells observed but less than at 4 weeks (Figure 4.29).



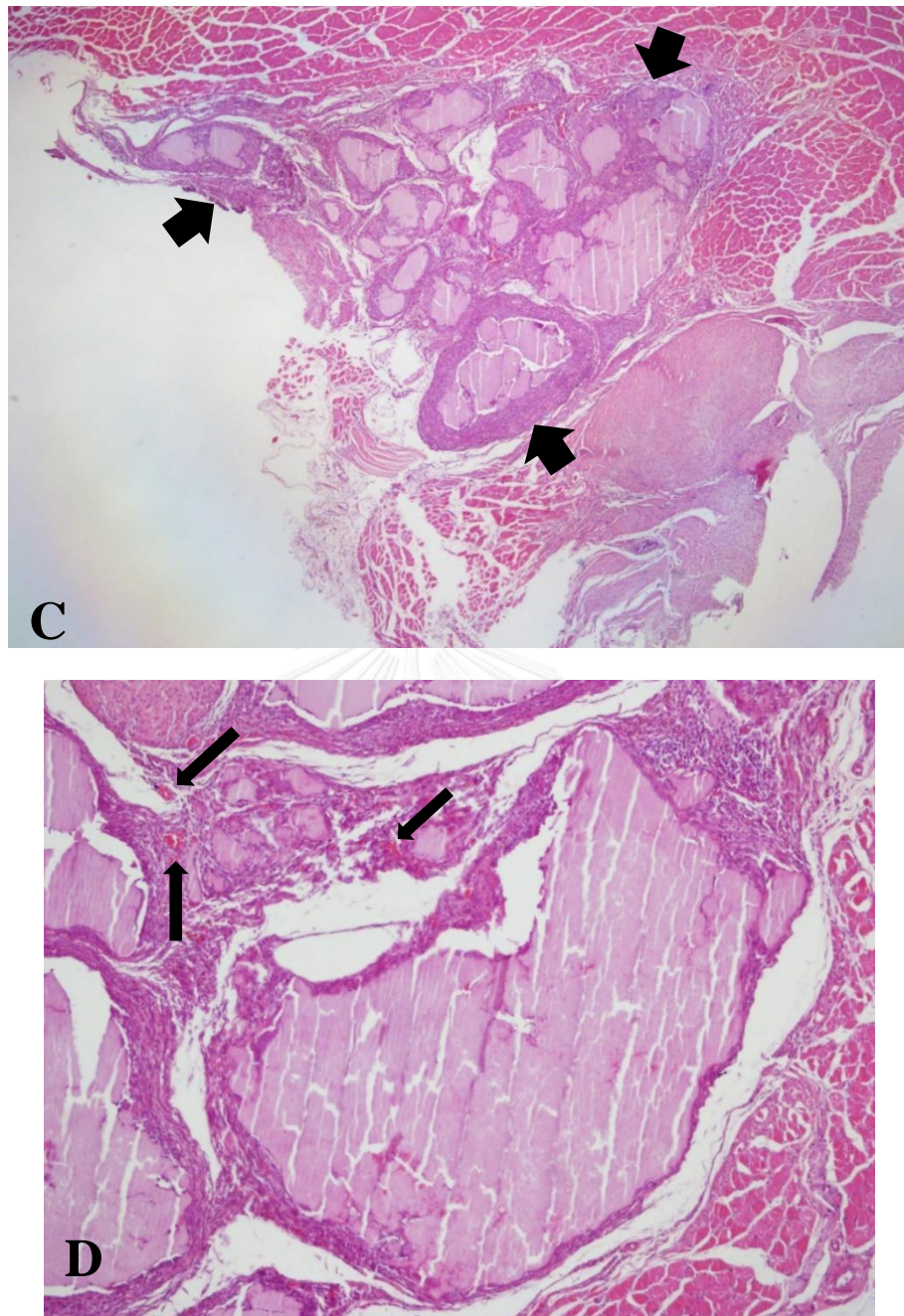


Figure 4.28 H&E staining of decalcified sections at 4 weeks, (A) an empty defect surrounded by fibrosis (black star) in the control group, (B) Collection of hydrogel appeared as eosinophilic irregular-shaped material surrounded by inflammatory cells (black star) in SF gel group, (C) Higher amount of inflammatory cells surrounding gel material (black arrow) in SF gel + PRP group compared with hydrogel without PRP groups, (D) New vessel formation (black arrow) in SF gel group showed in high power view.

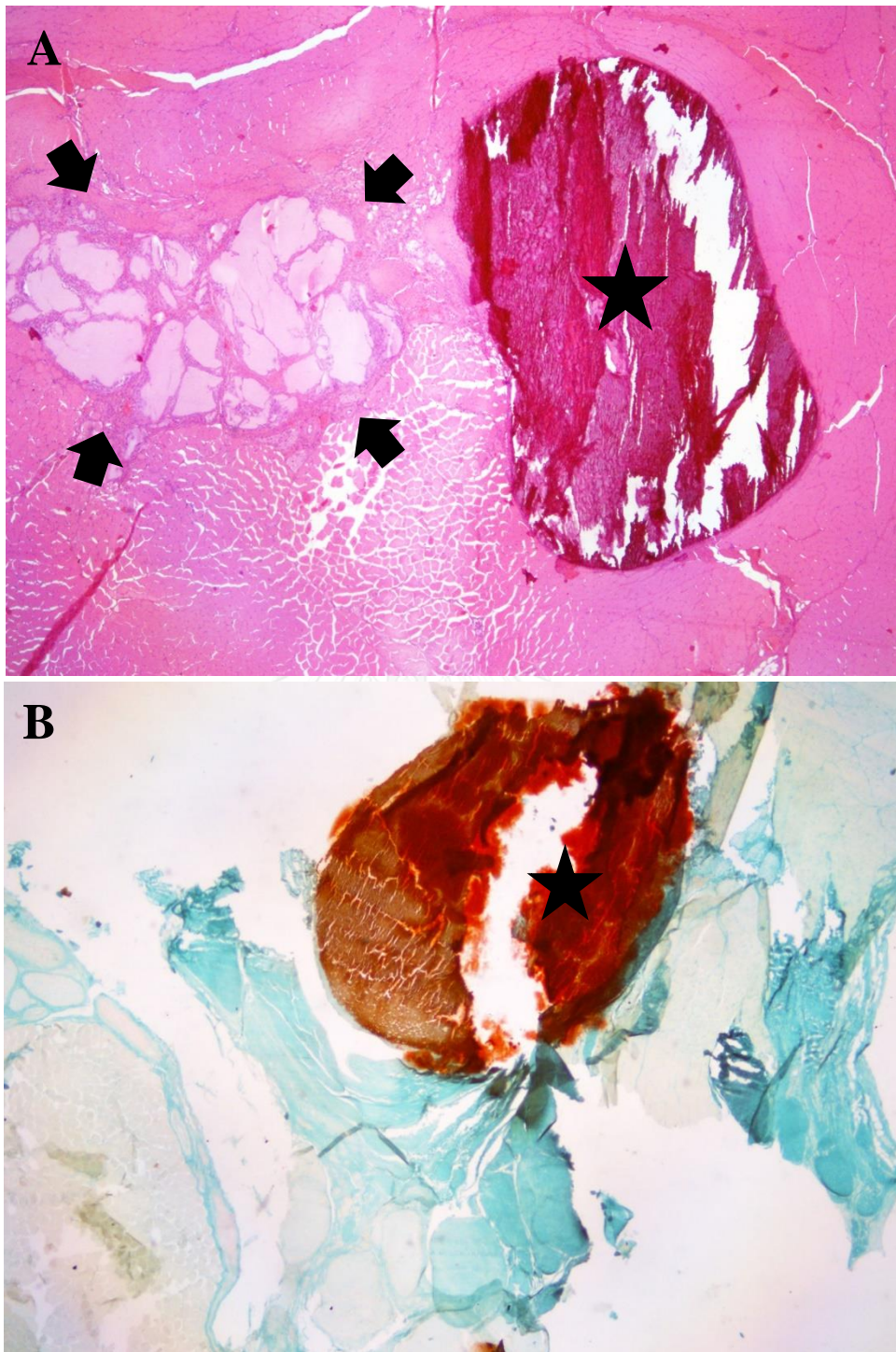


Figure 4.29 Histological section at 12 weeks of SF gel + MSC group, (A) H&E staining showed new bone formation (black star) and residual hydrogel fragments (black arrow) in SF gel + MSC group, (B) Alizarin Red S staining showed new bone formation appeared as collected reddish orange material in pale green background (black star).

All four experiment groups showed a trend indicating more new bone formation at 12 weeks compared with the control group from micro-CT analysis, although not statistically significant. Among the experiment groups with hydrogel, the morphometric parameters of newly formed bone were comparable. The histological results were in agreement with micro-CT result. No new bone or vessel formation was observed in the control group, whereas newly formed bone was found in the other four experiment groups with hydrogel. The histological patterns of all four experiment groups were relatively similar except the inflammatory reaction that was noticed more in hydrogel with PRP added group. However, the foreign body reaction was generally limited, indicating biocompatibility of the silk fibroin/collagen hydrogel *in vivo*. The hydrogel fragments were still noticeable at 12 weeks histologically but the amount was much less than the gel observed initially at 4 weeks which was similar to findings by Fini et al. and Zhang et al [53, 100].

Although beneficial effect on promotion of bone formation from silk fibroin/collagen hydrogel was demonstrated, comparable morphometric parameters and relatively similar histological patterns observed reflected that encapsulation of MSCs and growth factor in the hydrogel did not yield more positive effect on bone regeneration. This may be resulted from the use of xenogenic PRP from human donor which may not be compatible with the animal host causing foreign body reaction instead of enhancing the bone formation, as shown in histological results with appearing of more inflammatory cells in hydrogel with PRP added groups. The reason that the advantage from in encapsulation of MSC in the hydrogel could not be demonstrated was yet unclear. The biocompatibility of hydrogel with MSCs in proliferation and differentiation was possibly one factor to concern and further study is suggested.

CHAPTER 5

CONCLUSIONS

This study aimed to develop bone scaffold from in situ-forming hydrogel of Thai silk fibroin (SF) and collagen. Thai SF was prepared from Thai domestic silk cocoons, *Bombyx mori*, Nangnoi Sisaket 1.

In order to manufacture SF hydrogel from regenerated SF solution for medical purpose, sterility of SF is essential. In the present study, autoclaving, gamma radiation, and sterile filtration were experimented for sterilization of SF solution. However, premature gelation of SF solution precluded these method from being used. Even though gamma irradiated 1% SF solution survived from premature gelation, its dilution was unfavorable to be developed further. Manufacturing of SF under sterile condition was the method of choice in our study.

Appropriate gelation time is also one important factor for practical use in medical field. Hence, appropriate processing method was searched in our current work to achieve desired gelling time. Physical manners including vortex and homogenization did not result in fine gel formation in appropriate time. Surfactant addition was found effective for induction of gelation and was chosen for the later part of this work. Varying ratio of oleic acid and poloxamer-188 yielded surfactant combinations with different HLB values. The effect of different HLB values of surfactants on gelation time and physicochemical properties of induced 4 wt% SF with and without 0.1 wt% collagen was studied.

Regarding the gelation time of SF and SF with collagen hydrogel, lower HLB value of surfactant resulted in shorter gelation time of hydrogel. Results from zeta potential measurement revealed SF and SF with collagen solution displayed negative charge with added surfactant between HLB1-20. The SF with collagen solution showed less negative charges compared with SF solution at pH7.5 but no difference at pH5.5. This indicated that the addition of collagen does not alter surface charge of SF and SF with collagen solution at tissue-resemble pH.

To determine the solubility of hydrogel, gel fraction measurement was performed. The results demonstrated the inverse relationship between higher HLB value of surfactants and stability of SF hydrogels (decreased

SF hydrogel stability with induction by surfactants with higher HLB value). Presence of collagen increased stability of surfactant-induced SF hydrogel in HLB range of surfactants between 5-10. The 4 wt% SF hydrogels with and without 0.1 wt% collagen revealed 3-12% water absorption capacity with a trend showing an increase in water absorption capacity of SF with collagen hydrogel induced by surfactants with higher HLB values. There was no difference observed among SF hydrogels and between SF and SF with collagen hydrogels.

Results from amplitude oscillatory test revealed that there was an optimum of HLB value of surfactants for formation of intermolecular bonding to achieve maximum gel strength. The effect of collagen presented in the hydrogel on alteration the modulus of the SFC/HLB10 hydrogel was also demonstrated, probably due to cross-linking networks between collagen and SF. The oscillatory frequency sweep demonstrated that 4 wt% SF hydrogels with and without 0.1 wt% collagen induced by surfactants with HLB value between 3-20 were ideal gels with more solid-like behavior.

Observation from SEM found typical interconnected microporous morphology in all hydrogels. The effect of HLB value of surfactants and collagen blending on morphology of SF hydrogel were shown. An increase in HLB value of surfactants and addition of collagen resulted in larger pore size with less interporous connectivity and thicker cross-linking networks.

Thermal properties studied by DSC demonstrated more complete crystallization achieved in SF and SFC hydrogels induced by surfactants compared with SF and SFC hydrogels without induction. There was a trend of higher temperature of thermal decomposition peaks in hydrogels induced with surfactant with higher HLB values indicating the effect of HLB value of surfactants on thermal stability of the hydrogels.

The study of secondary structure of hydrogels using FTIR demonstrated the effect of HLB value of the surfactants on the secondary structure of the SF hydrogel. SF hydrogel induced by higher HLB (HLB 15 and 20) of surfactants revealed higher percentage of beta-sheet structure (60%). However, the effect of HLB value of the surfactants was not demonstrated on the SF with collagen hydrogels. The presence of collagen in the hydrogel precluded the effect of HLB value of the surfactants on the

crystallinity of SF hydrogel, therefore the maximum crystallinity of the SF hydrogel could not be achieved. The gelation of SF hydrogels induced by lower HLB surfactant was resulted from interaction between SF and surfactants rather than conformational change to beta-sheet of the hydrogels.

In vitro experiment verified the biocompatibility of SF and SF with collagen hydrogel scaffolds. Rat's MSC proliferated in the first 24 hours, then cell numbers declined continually before reaching plateau phase at 5-day time-point. After that, the number of cells was maintained during day 7-14 of culture. Even though the SF with collagen hydrogel seems to have less encapsulation efficiency of rat MSCs, the growth at the plateau phase of all hydrogels were comparable. SF and SF with collagen hydrogels demonstrated their potential to induce osteogenic differentiation of encapsulated rat's MSC in induction medium. However, 4 wt% SF with 0.1 wt% collagen expressed promotional effect more on proliferation rather than differentiation. Beneficial effect of collagen in matrix formation induction was also indicated from SEM analysis. The resulted Ca/P ratio from EDS suggested that other forms of calcium compounds presented in the hydrogels during osteogenic stimulation.

In vivo study of osteogenesis in segmental defect of rat's ulnar bone demonstrated biocompatibility and potential of the silk fibroin/collagen hydrogel as a scaffold and carrier for cell and growth factor for bone regeneration. Implantation of in situ-forming hydrogel of 4 wt% SF with 0.1 wt% collagen, with or without MSC and PRP showed a trend indicating more new bone formation at 12 weeks compared with the control group from micro-CT analysis, although not statistically significant. The foreign body reaction was generally limited. Nevertheless, hydrogel fragments were still noticeable at 12 weeks histologically.

Further study is recommended to identify more detailed effects and relationship between HLB value of surfactants and rheological properties of hydrogel. In vitro cell viability and differentiation study of the hydrogel should also be reviewed further for optimization of hydrogel properties to achieve the highest osteogenic potential as possible. Data regarding hydrogel degradation is an essential property needed to be explored.

Moreover, in vivo immune response is also another major concern that ought to be investigated prior to clinical use.



REFERENCES

1. Wiese A, Pape HC. Bone defects caused by high-energy injuries, bone loss, infected nonunions, and nonunions. *Orthop Clin North Am.* 2010;41:1-4.
2. Ashman O, Phillips AM. Treatment of non-unions with bone defects: which option and why? *Injury.* 2013;44 Suppl 1:S43-5.
3. Buckwalter JA, Einhorn TA, Marsh J, Gulotta L, Ranawat A, Lane J. Bone and joint healing. In: Bucholz R, Heckman J, Court-Brown C, Tornetta P, editors. *Rockwood and Green's Fractures in Adults* 7th ed. Baltimore: Lippincott Williams & Wilkins; 2010. p. 85-13.
4. Einhorn T, Kakar S. Tissue Engineering of Bone. *Bone Tissue Engineering: CRC Press;* 2004. p. 277-302.
5. Luo Y, Engelmayer G, Auguste DT, Ferreira LdS, Karp JM, Saigal R, et al. Three-Dimensional Scaffolds. *Principles of Tissue Engineering.* 3rd ed. Burlington: Academic Press; 2007. p. 359-73.
6. Omidian H, Park K. Introduction to hydrogels. In: Peppas N, Ottenbrite R, Park K, Okano T, editors. *Biomedical applications of hydrogels handbook: Springer;* 2010. p. 1-16.
7. Jin R, Dijkstra PJ. Hydrogels for Tissue Engineering Applications. In: Ottenbrite RM, Park K, Okano T, editors. *Biomedical Applications of Hydrogels Handbook.* New York: Springer; 2010. p. 203-25.
8. Nicodemus GD, Bryant SJ. Cell encapsulation in biodegradable hydrogels for tissue engineering applications. *Tissue Eng Part B Rev.* 2008;14:149-65.
9. Kasoju N, Bora U. Silk fibroin in tissue engineering. *Adv Healthc Mater.* 2012;1:393-412.
10. Kundu B, Rajkhowa R, Kundu SC, Wang X. Silk fibroin biomaterials for tissue regenerations. *Adv Drug Deliv Rev.* 2013;65:457-70.
11. Ghezzi CE, Marelli B, Donelli I, Alessandrino A, Freddi G, Nazhat SN. The role of physiological mechanical cues on mesenchymal stem cell differentiation in an airway tract-like dense collagen-silk fibroin construct. *Biomaterials.* 2014;35:6236-47.
12. Ghezzi CE, Marelli B, Donelli I, Alessandrino A, Freddi G, Nazhat SN. Multilayered dense collagen-silk fibroin hybrid: a platform for mesenchymal stem cell differentiation towards chondrogenic and osteogenic lineages. *J Tissue Eng Regen Med.* 2015;11:2046-59.
13. Long K, Liu Y, Li W, Wang L, Liu S, Wang Y, et al. Improving the mechanical properties of collagen-based membranes using silk fibroin for corneal tissue engineering. *J Biomed Mater Res A.* 2015;103:1159-68.
14. Shen Y, Redmond SL, Papadimitriou JM, Teh BM, Yan S, Wang Y, et al. The biocompatibility of silk fibroin and acellular collagen scaffolds for tissue engineering in the ear. *Biomed Mater.* 2014;9:015015.

15. Wang G, Hu X, Lin W, Dong C, Wu H. Electrospun PLGA-silk fibroin-collagen nanofibrous scaffolds for nerve tissue engineering. *In Vitro Cell Dev Biol Anim.* 2011;47:234-40.
16. Wang J, Zhou W, Hu W, Zhou L, Wang S, Zhang S. Collagen/silk fibroin bi-template induced biomimetic bone-like substitutes. *J Biomed Mater Res A.* 2011;99:327-34.
17. Wei G, Li C, Fu Q, Xu Y, Li H. Preparation of PCL/silk fibroin/collagen electrospun fiber for urethral reconstruction. *Int Urol Nephrol.* 2015;47:95-9.
18. Zhou J, Cao C, Ma X, Lin J. Electrospinning of silk fibroin and collagen for vascular tissue engineering. *Int J Biol Macromol.* 2010;47:514-9.
19. Lv Q, Hu K, Feng Q, Cui F. Fibroin/collagen hybrid hydrogels with crosslinking method: preparation, properties, and cytocompatibility. *J Biomed Mater Res A.* 2008;84:198-207.
20. Marelli B, Ghezzi CE, Alessandrino A, Barralet JE, Freddi G, Nazhat SN. Silk fibroin derived polypeptide-induced biomineralization of collagen. *Biomaterials.* 2012;33:102-8.
21. Eroschenko VP, Di Fiore MS. DiFiore's atlas of histology with functional correlations. 11th ed. Baltimore: Lippincott Williams & Wilkins; 2008. p. 79-97.
22. Reichert JC, Berner A, Saifzadeh S, Hutmacher DW. Preclinical Animal Models for Segmental Bone Defect Research and Tissue Engineering. In: Steinhoff G, editor. *Regenerative Medicine: From Protocol to Patient.* 2nd ed. Dordrecht: Springer; 2013. p. 1023-64.
23. Cameron JA, Milner DJ, Lee JS, Cheng J, Fang NX, Jasiuk IM. Employing the biology of successful fracture repair to heal critical size bone defects. *Curr Top Microbiol Immunol.* 2013;367:113-32.
24. Gulrez SK, Al-Assaf S, Phillips GO. Hydrogels: methods of preparation, characterisation and applications. In: Carpi A, editor. *Progress in Molecular and Environmental Bioengineering-From Analysis and Modeling to Technology Applications: InTech;* 2011. p. 117-41.
25. Omidian H, Park K. Hydrogels. In: Siepmann J, Siegel R, Rathbone M, editors. *Fundamentals and applications of controlled release drug delivery.* New York: Springer; 2012. p. 75-105.
26. Drury JL, Mooney DJ. Hydrogels for tissue engineering: scaffold design variables and applications. *Biomaterials.* 2003;24:4337-51.
27. Altman GH, Diaz F, Jakuba C, Calabro T, Horan RL, Chen J, et al. Silk-based biomaterials. *Biomaterials.* 2003;24:401-16.
28. Vepari C, Kaplan DL. Silk as a biomaterial. *Prog Polym Sci.* 2007;32:991-1007.
29. Wang Y, Kim HJ, Vunjak-Novakovic G, Kaplan DL. Stem cell-based tissue engineering with silk biomaterials. *Biomaterials.* 2006;27:6064-82.
30. Hardy JG, Römer LM, Scheibel TR. Polymeric materials based on silk proteins. *Polymer.* 2008;49:4309-27.

31. McPherson A. Introduction to protein crystallization. *Methods*. 2004;34:254-65.
32. Kim UJ, Park J, Li C, Jin HJ, Valluzzi R, Kaplan DL. Structure and properties of silk hydrogels. *Biomacromolecules*. 2004;5:786-92.
33. Numata K, Katashima T, Sakai T. State of water, molecular structure, and cytotoxicity of silk hydrogels. *Biomacromolecules*. 2011;12:2137-44.
34. Rammensee S, Huemmerich D, Hermanson K, Scheibel T, Bausch A. Rheological characterization of hydrogels formed by recombinantly produced spider silk. *Appl Phys A*. 2006;82:261-4.
35. Stevenson CL. Characterization of protein and peptide stability and solubility in non-aqueous solvents. *Curr Pharm Biotechnol*. 2000;1:165-82.
36. Wang W, Nema S, Teagarden D. Protein aggregation--pathways and influencing factors. *Int J Pharm*. 2010;390:89-99.
37. Wu X, Hou J, Li M, Wang J, Kaplan DL, Lu S. Sodium dodecyl sulfate-induced rapid gelation of silk fibroin. *Acta Biomater*. 2012;8:2185-92.
38. Hanawa T, Watanabe A, Tsuchiya T, Ikoma R, Hidaka M, Sugihara M. New oral dosage form for elderly patients: preparation and characterization of silk fibroin gel. *Chem Pharm Bull (Tokyo)*. 1995;43:284-8.
39. Kang GD, Nahm JH, Park JS, Moon JY, Cho CS, Yeo JH. Effects of poloxamer on the gelation of silk fibroin. *Macromol Rapid Commun*. 2000;21:788-91.
40. Motta A, Migliaresi C, Faccioni F, Torricelli P, Fini M, Giardino R. Fibroin hydrogels for biomedical applications: preparation, characterization and in vitro cell culture studies. *J Biomater Sci Polym Ed*. 2004;15:851-64.
41. Chen X, Li W, Zhong W, Lu Y, Yu T. pH sensitivity and ion sensitivity of hydrogels based on complex-forming chitosan/silk fibroin interpenetrating polymer network. *J Appl Polym Sci*. 1997;65:2257-62.
42. Haider ZA, Arai M, Hirabayashi K. Mechanism of the gelation of fibroin solution. *Biosci Biotechnol Biochem*. 1993;57:1910-2.
43. Matsumoto A, Chen J, Collette AL, Kim UJ, Altman GH, Cebe P, et al. Mechanisms of silk fibroin sol-gel transitions. *J Phys Chem B*. 2006;110:21630-8.
44. Terry AE, Knight DP, Porter D, Vollrath F. pH induced changes in the rheology of silk fibroin solution from the middle division of *Bombyx mori* silkworm. *Biomacromolecules*. 2004;5:768-72.
45. Floren M, Migliaresi C, Motta A. Processing Techniques and Applications of Silk Hydrogels in Bioengineering. *J Funct Biomater*. 2016;7:26.
46. Murphy AR, John PS, Kaplan DL. Modification of silk fibroin using diazonium coupling chemistry and the effects on hMSC proliferation and differentiation. *Biomaterials*. 2008;29:2829-38.
47. Murphy AR, Kaplan DL. Biomedical applications of chemically-modified silk fibroin. *J Mater Chem*. 2009;19:6443-50.
48. Nagarkar S, Nicolai T, Chassenieux C, Lele A. Structure and gelation mechanism of silk hydrogels. *Phys Chem Chem Phys*. 2010;12:3834-44.

49. Davis NE, Beenken-Rothkopf LN, Mirsoian A, Kojic N, Kaplan DL, Barron AE, et al. Enhanced function of pancreatic islets co-encapsulated with ECM proteins and mesenchymal stromal cells in a silk hydrogel. *Biomaterials*. 2012;33:6691-7.
50. Ji H, Helfand E. Concentration fluctuations in sheared polymer solutions. *Macromolecules*. 1995;28:3869-80.
51. Rangel-Nafaile C, Metzner AB, Wissbrun KF. Analysis of stress-induced phase separations in polymer solutions. *Macromolecules*. 1984;17:1187-95.
52. Yucel T, Cebe P, Kaplan DL. Vortex-induced injectable silk fibroin hydrogels. *Biophys J*. 2009;97:2044-50.
53. Zhang W, Wang X, Wang S, Zhao J, Xu L, Zhu C, et al. The use of injectable sonication-induced silk hydrogel for VEGF 165 and BMP-2 delivery for elevation of the maxillary sinus floor. *Biomaterials*. 2011;32:9415-24.
54. Paulusse MJ, Sijbesma RP. Ultrasound in polymer chemistry: Revival of an established technique. *J Polym Sci, Part A: Polym Chem*. 2006;44:5445-53.
55. Wang X, Kluge JA, Leisk GG, Kaplan DL. Sonication-induced gelation of silk fibroin for cell encapsulation. *Biomaterials*. 2008;29:1054-64.
56. Kojic N, Panzer MJ, Leisk GG, Raja WK, Kojic M, Kaplan DL. Ion Electrodiffusion Governs Silk Electrogelation. *Soft Matter*. 2012;8:2897-905.
57. Leisk GG, Lo TJ, Yucel T, Lu Q, Kaplan DL. Electrogelation for protein adhesives. *Adv Mater*. 2010;22:711-5.
58. Friess W. Collagen--biomaterial for drug delivery. *Eur J Pharm Biopharm*. 1998;45:113-36.
59. Olsen D, Yang C, Bodo M, Chang R, Leigh S, Baez J, et al. Recombinant collagen and gelatin for drug delivery. *Adv Drug Deliv Rev*. 2003;55:1547-67.
60. Cartmell SH, Porter BD, Garcia AJ, Guldberg RE. Effects of medium perfusion rate on cell-seeded three-dimensional bone constructs in vitro. *Tissue Eng*. 2003;9:1197-203.
61. Dominici M, Le Blanc K, Mueller I, Slaper-Cortenbach I, Marini F, Krause D, et al. Minimal criteria for defining multipotent mesenchymal stromal cells. The International Society for Cellular Therapy position statement. *Cytotherapy*. 2006;8:315-7.
62. Komori T, Kishimoto T. Cbfa1 in bone development. *Curr Opin Genet Dev*. 1998;8:494-9.
63. Lian JB, Stein GS. Concepts of osteoblast growth and differentiation: basis for modulation of bone cell development and tissue formation. *Crit Rev Oral Biol Med*. 1992;3:269-305.
64. Devi DR, Sandhya P, Hari BV. Poloxamer: a novel functional molecule for drug delivery and gene therapy. *J Pharm Sci Res*. 2013;5:159-65.
65. Torcello-Gómez A, Wulff-Pérez M, Gálvez-Ruiz MJ, Martín-Rodríguez A, Cabrerizo-Vílchez M, Maldonado-Valderrama J. Block copolymers at interfaces: Interactions with physiological media. *Adv Colloid Interface Sci*. 2014;206:414-27.

66. Kabanov AV, Batrakova EV, Alakhov VY. Pluronic® block copolymers as novel polymer therapeutics for drug and gene delivery. *J Control Release*. 2002;82:189-212.
67. Gadhawe A. Determination of hydrophilic-lipophilic balance value. *Int J Sci Res*. 2014;3:573-5.
68. Holmberg K, Jönsson B, Kronberg B, Lindman B. *Surfactants and polymers in aqueous solution*. 2nd ed. Chichester: John Wiley & Sons; 2003.
69. Schott H. Hydrophilic-lipophilic balance, solubility parameter, and oil-water partition coefficient as universal parameters of nonionic surfactants. *J Pharm Sci*. 1995;84:1215-22.
70. Tadros TF. *Emulsion Formation, Stability, and Rheology*. In: Tadros T, editor. *Emulsion Formation and Stability*. 1st ed. Weinheim: Wiley-VCH Verlag; 2013. p. 1-75.
71. Tungtasana H, Shuangshoti S, Shuangshoti S, Kanokpanont S, Kaplan DL, Bunaprasert T, et al. Tissue response and biodegradation of composite scaffolds prepared from Thai silk fibroin, gelatin and hydroxyapatite. *J Mater Sci Mater Med*. 2010;21:3151-62.
72. Kasoju N, Hawkins N, Pop-Georgievski O, Kubies D, Vollrath F. Silk fibroin gelation via non-solvent induced phase separation. *Biomater Sci*. 2016;4:460-73.
73. Takahashi Y, Tabata Y. Homogeneous seeding of mesenchymal stem cells into nonwoven fabric for tissue engineering. *Tissue Eng*. 2003;9:931-8.
74. Takahashi Y, Yamamoto M, Tabata Y. Osteogenic differentiation of mesenchymal stem cells in biodegradable sponges composed of gelatin and beta-tricalcium phosphate. *Biomaterials*. 2005;26:3587-96.
75. Ginis I, Weinreb M, Abramov N, Shinar D, Merchav S, Schwartz A, et al. Bone progenitors produced by direct osteogenic differentiation of the unprocessed bone marrow demonstrate high osteogenic potential in vitro and in vivo. *Biores Open Access*. 2012;1:69-78.
76. Diab T, Pritchard EM, Uhrig BA, Boerckel JD, Kaplan DL, Guldborg RE. A silk hydrogel-based delivery system of bone morphogenetic protein for the treatment of large bone defects. *J Mech Behav Biomed Mater*. 2012;11:123-31.
77. Rockwood DN, Preda RC, Yucel T, Wang X, Lovett ML, Kaplan DL. Materials fabrication from *Bombyx mori* silk fibroin. *Nat Protoc*. 2011;6:1612-31.
78. Lawrence BD, Omenetto F, Chui K, Kaplan DL. Processing methods to control silk fibroin film biomaterial features. *J Mater Sci*. 2008;43:6967.
79. Wu X, Mao L, Qin D, Lu S. Impact of Sterilization Methods on the Stability of Silk Fibroin Solution. *Adv Mat Res*. 2011;311-313:1755-9.
80. Liu Y, Xiong S, You R, Li M. Gelation of *Antheraea pernyi* Silk Fibroin Accelerated by Shearing. *Mater Sci Appl*. 2013;4:365-73.
81. Childress AE, Elimelech M. Effect of solution chemistry on the surface charge of polymeric reverse osmosis and nanofiltration membranes. *J Membr Sci*. 1996;119:253-68.

82. Chang H-I, Wang Y. Cell responses to surface and architecture of tissue engineering scaffolds. *Regenerative medicine and tissue engineering- cells and biomaterials: InTech*; 2011. p. 571-88.
83. Hehrlein C, Zimmermann M, Metz J, Ensinger W, Kubler W. Influence of surface texture and charge on the biocompatibility of endovascular stents. *Coron Artery Dis.* 1995;6:581-6.
84. Grillet AM, Wyatt NB, Gloe LM. Polymer gel rheology and adhesion. *Rheology: InTech*; 2012. p. 59-80.
85. Hu X, Lu Q, Sun L, Cebe P, Wang X, Zhang X, et al. Biomaterials from ultrasonication-induced silk fibroin-hyaluronic acid hydrogels. *Biomacromolecules.* 2010;11:3178-88.
86. Freddi G, Pessina G, Tsukada M. Swelling and dissolution of silk fibroin (*Bombyx mori*) in N-methyl morpholine N-oxide. *Int J Biol Macromol.* 1999;24:251-63.
87. Shah TJ, Amin AF, Parikh JR, Parikh RH. Process optimization and characterization of poloxamer solid dispersions of a poorly water-soluble drug. *AAPS PharmSciTech.* 2007;8:18-24.
88. Xie Y, Li G, Yuan X, Cai Z, Rong R. Preparation and in vitro evaluation of solid dispersions of total flavones of *Hippophae rhamnoides L.* *AAPS PharmSciTech.* 2009;10:631-40.
89. Hu X, Shmelev K, Sun L, Gil E-S, Park S-H, Cebe P, et al. Regulation of silk material structure by temperature-controlled water vapor annealing. *Biomacromolecules.* 2011;12:1686-96.
90. Labidi NS, Iddou A. Adsorption of oleic acid on quartz/water interface. *J Saudi Chem Soc.* 2007;11:221-34.
91. Premaratne W, Priyadarshana W, Gunawardena S, De Alwis A. Synthesis of Nanosilica from Paddy Husk Ash and Their Surface Functionalization. *J Sci Univ Kelaniya.* 2013;8:33-48.
92. Lin Y, Xia X, Shang K, Elia R, Huang W, Cebe P, et al. Tuning chemical and physical cross-links in silk electrogels for morphological analysis and mechanical reinforcement. *Biomacromolecules.* 2013;14:2629-35.
93. Lefèvre T, Rousseau M-E, Pézolet M. Protein secondary structure and orientation in silk as revealed by Raman spectromicroscopy. *Biophys J.* 2007;92:2885-95.
94. Lindborg BA, Brekke JH, Scott CM, Chai YW, Ulrich C, Sandquist L, et al. A chitosan-hyaluronan-based hydrogel-hydrocolloid supports in vitro culture and differentiation of human mesenchymal stem/stromal cells. *Tissue Eng Part A.* 2015;21:1952-62.
95. Moshaverinia A, Chen C, Akiyama K, Xu X, Chee WW, Schricker SR, et al. Encapsulated dental-derived mesenchymal stem cells in an injectable and biodegradable scaffold for applications in bone tissue engineering. *J Biomed Mater Res A.* 2013;101:3285-94.

96. Raucci MG, Alvarez-Perez MA, Demitri C, Sannino A, Ambrosio L. Proliferation and osteoblastic differentiation of hMSCs on cellulose-based hydrogels. *J Appl Biomater Funct Mater*. 2012;10:302-7.
97. Sanchez-Ferrero A, Mata A, Mateos-Timoneda MA, Rodriguez-Cabello JC, Alonso M, Planell J, et al. Development of tailored and self-mineralizing citric acid-crosslinked hydrogels for in situ bone regeneration. *Biomaterials*. 2015;68:42-53.
98. Lee JH, Baek H-R, Lee KM, Lee H-K, Im SB, Kim YS, et al. The Effect of Poloxamer 407 - Based Hydrogel on the Osteoinductivity of Demineralized Bone Matrix. *Clin Orthop Surg*. 2014;6:455-61.
99. Burguera EF, Guitian F, Chow LC. Effect of the calcium to phosphate ratio of tetracalcium phosphate on the properties of calcium phosphate bone cement. *J Biomed Mater Res A*. 2008;85:674-83.
100. Fini M, Motta A, Torricelli P, Giavaresi G, Nicoli Aldini N, Tschon M, et al. The healing of confined critical size cancellous defects in the presence of silk fibroin hydrogel. *Biomaterials*. 2005;26:3527-36.

APPENDIX



จุฬาลงกรณ์มหาวิทยาลัย
CHULALONGKORN UNIVERSITY

APPENDIX A
THE APPROVED OF ANIMAL USE PROTOCOL



เลขที่ใบรับรอง 06/2560 เลขที่โครงการวิจัย 022/2559

คณะกรรมการกำกับดูแลการเลี้ยงและใช้สัตว์
คณะแพทยศาสตร์ จุฬาลงกรณ์มหาวิทยาลัย

ใบรับรองการอนุมัติให้ดำเนินการเลี้ยงและใช้สัตว์เพื่องานทางวิทยาศาสตร์
ณ คณะแพทยศาสตร์ จุฬาลงกรณ์มหาวิทยาลัย

ชื่อข้อเสนอการวิจัย


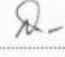
(ภาษาไทย) การศึกษาการสร้างเนื้อเยื่อกระดูกจากไฮโดรเจลก่อตัวได้ของไฟโบรอินไหมไทยและคอลลาเจนในสัตว์ทดลอง

(ภาษาอังกฤษ) Animal study of osteogenesis in in situ-forming hydrogel of Thai silk fibroin and collagen

ผู้เสนอโครงการใช้สัตว์ทดลอง นายแพทย์จิรันดร อภินันท์

หน่วยงานที่สังกัด ภาควิชาออร์โธปิดิกส์ คณะแพทยศาสตร์ จุฬาลงกรณ์มหาวิทยาลัย

ขอเสนอโครงการใช้สัตว์ทดลองนี้ผ่านการรับรองจากคณะกรรมการกำกับดูแลการเลี้ยงและใช้สัตว์แล้ว เห็นว่ามีความสอดคล้องกับจรรยาบรรณการใช้สัตว์เพื่องานทางวิทยาศาสตร์สภากวิจัยแห่งชาติ จึงเห็นสมควรให้ดำเนินการเลี้ยงและใช้สัตว์ตามข้อเสนอโครงการใช้สัตว์ทดลองนี้ได้

<p>ลงนาม..... </p> <p>(รองศาสตราจารย์ นายแพทย์สมพล สงวนรังศิริกุล)</p> <p>ประธานคณะกรรมการกำกับดูแลการเลี้ยงและใช้สัตว์</p>	<p>ลงนาม..... </p> <p>(ศาสตราจารย์ นายแพทย์สุทธิพงศ์ วีระสินธุ)</p> <p>คณบดี คณะแพทยศาสตร์ จุฬาลงกรณ์มหาวิทยาลัย</p>
----------------------------------------------------------------------------------------------------------------------------------------------------------------------------------------------------------------	-----------------------------------------------------------------------------------------------------------------------------------------------------------------------------------------------------------

วันที่รับรอง : พฤษภาคม พ.ศ.2560
วันหมดอายุ : พฤษภาคม พ.ศ.2561

Figure A.1 Certificate approval for animal use protocol number 06/2560
by the ethical committee of animal care and use protocol of
Chulalongkorn University

APPENDIX B
SERIAL PLAIN RADIOGRAPHS IN *IN VIVO* STUDY



Figure B.1 Serial radiographs at 0, 4, 8, and 12 wks of the control group, SF/Col hydrogel group, SF/Col hydrogel + MSC group, SF/Col hydrogel + PRP group, and SF/Col hydrogel + MSC + PRP group

VITA

Jirun Apinun was born in Thailand on October 24, 1978. He graduated Doctor of Medicine degree (1st Class honors) at Chulalongkorn University Medical School, Bangkok, Thailand. After graduated he worked as general practitioner for 4 years before attending the residency and fellowship program at Orthopaedic Division, King Chulalongkorn Memorial Hospital. He received the Diploma of Clinical Sciences (Surgery), Diploma in Orthopaedic Surgery and Certificate in Sports Medicine & Arthroscopy.

After received the diploma, he has worked at King Chulalongkorn Memorial Hospital as full time consultant. During 2012-2-14, he did his fellowship in Foot and ankle surgery at Universitatlinikum "Carl Gustav Carus", Germany; Schulthess Klinik, Switzerland; Groupe Chirurgical Republique & Clinique des Alpes, France; Instituto Clinico Humanitas, Italy; Instituto Ortopedico Rizzoli of Bologna, Italy; Avon Orthopaedic Centre, North Bristol NHS Trust, UK.

Apart from full-time working at King Chulalongkorn Memorial Hospital, he also works as part-time consultant at BNH Hospital, Bumrungrad Hospital, and Bangpakok9 International Hospital. He also contributes to work as a board committee of Thai Foot and Ankle Society and the deputy head of accounting department of Thai Orthopaedic Society of Sports Medicine. The researches and books that he conducted or co-worked are listed below.

- Apinun J, Krittayakeeron K. New instruments in hemostasis. In : Pak-at R (editor), Surgical Reviews. Bangkok, Thailand: Parbpim Publishing; 2005.
- Apinun J. Haglund's syndrome. In : Tanthawichian T, Suankratat C, Jirasiritham S, et al. (editors), Contemporary medicine. Bangkok, Thailand: Chulalongkorn publishing; 2011.
- Apinun J, Kuptniratsaikul S. Impingement syndrome of the shoulder. *Chula Med J* 2012; 56(3); 343-58.
- Apinun J, Kuptniratsaikul S. Arthroscopic PCL reconstruction - Transtibial, single-bundle technique. In : Sudhassanee V (editor), TOSSM Advances in Cruciate Ligaments. Bangkok, Thailand: Concept Medicus; 2012.
- Charoenlap C, Hongsaprabhas C, Apinun J, Kuptniratsaikul S. Novel arthroscopic technique for solitary enchondroma of distal femur. Poster presentation in 9th Asia Pacific musculoskeletal tumor society meeting 2012. Kuala Lumpur, Malaysia.
- Apinun J, Sengprasert P, Yuktanandana P, Ngarmukos S, Tanavalee A, Reantragoon R. Immune Mediators in Osteoarthritis: Infrapatellar fat pad-infiltrating CD8+ T cells are increased in osteoarthritic patients with higher clinical radiographic grading. *Int J Rheumatol* 2016; 2016:9525724. doi: 10.1155/2016/9525724.
- Apinun J, Damrongsakkul S, Yamdech R, Jamkratoke J, Kanokpanont S. Viability of rat's bone marrow-derived mesenchymal stem cells in a surfactant-induced Thai silk fibroin hydrogel. *BMEiCON 2017* : Proceedings of the 10th Biomedical Engineering International Conference; 2017; Hokkaido, Japan.
- Apinun J, Honsawek S, Kuptniratsaikul S, Jamkratoke J, Kanokpanont S. In vitro osteogenic differentiation of rat bone marrow-derived mesenchymal stem cells encapsulated in an injectable surfactant-induced Thai silk fibroin/collagen hydrogel. *Asian Biomed* (under reviewing).
- Apinun J, Chaisuparat R, Wangdee C, Kuptniratsaikul S, Kanokpanont S. Evaluation of bone regeneration in segmental bone defects of rat using injectable surfactant-induced Thai silk fibroin/collagen in situ-forming hydrogel. *J Med*